Click here to return to the Appendixes Menu

Appendix I

Environmental Consequences of Long-Term Repository Performance

TABLE OF CONTENTS

LIST OF TABLES

LIST OF FIGURES

APPENDIX I. ENVIRONMENTAL CONSEQUENCES OF LONG-TERM REPOSITORY PERFORMANCE

This appendix provides detailed supporting information on the calculation of the environmental consequences of long-term (postclosure, up to 1 million years) repository performance. Chapter 5 summarizes these consequences for the Proposed Action, and Section 8.3 summarizes the cumulative impacts of Inventory Modules 1 and 2.

Section I.1 introduces the bases for long-term performance assessment calculations. Section I.2 provides an overview of the use of computational models developed for the Total System Performance Assessment – Viability Assessment used for this environmental impact statement (EIS). Section I.3 identifies and quantifies the inventory of waste constituents of concern for long-term performance assessment. Section I.4 details the modeling extensions to the Viability Assessment *base case* (high thermal load scenario with the Proposed Action inventory) developed to estimate potential impacts for other thermal load scenarios and expanded inventories. Section I.5 provides detailed results for waterborne radioactive material impacts, while Section I.6 provides the same for waterborne chemically toxic material impacts. Section I.7 describes atmospheric radioactive material impacts. To aid readability, all the figures have been placed at the end of the appendix.

I.1 Long-Term Repository Performance Assessment Calculations

HOW ARE THE VIABILITY ASSESSMENT AND THIS EIS PERFORMANCE ASSESSMENT RELATED?

The long-term performance assessment for this EIS builds incrementally on the Viability Assessment (DOE 1998a, Volume 3, all; TRW 1998a,b,c,d,e,f,g,h,i,j,k, all).

This appendix reports only those aspects of the EIS long-term performance assessment that are incremental over the Viability Assessment. Only those parts of the analysis unique to the EIS are reported here, and the text refers to the appropriate Viability Assessment documents for information on the bases of the analyses.

This EIS analysis of postclosure impacts used and extended the modeling work done for the Total System Performance Assessment – Viability Assessment, as reported in the U.S. Department of Energy's (DOE's) *Viability Assessment of A Repository at Yucca Mountain, Volume 3* (DOE 1998a, Volume 3, all) and in the *Total System Performance Assessment – Viability Assessment (TSPA-VA) Analyses Technical Basis Document* (TRW 1998a,b,c,d,e,f,g,h,i,j,k, all). The Proposed Action inventory under the high thermal load scenario is identical to the Viability Assessment base case, except that the Viability Assessment only considered 20 kilometers (12 miles) from the repository, while the EIS considers impacts of radiological dose to maximally exposed individuals through the groundwater pathway at 5, 20, 30, and 80 kilometers (3, 12, 19, and 50 miles) from the repository. The EIS analysis used a repository integrated program computer model (Golder 1998, all) that DOE used for the total-system model to calculate radiological doses through the groundwater pathway. This performance assessment model and supporting Viability Assessment process models were extended to predict waterborne chemically toxic material impacts. Additional calculations provided estimates of atmospheric radiological doses to local and global populations.

The process of performing performance assessment analyses for this EIS required several steps. The EIS analysis was designed to incorporate the Total System Performance Assessment – Viability Assessment model of the base case repository configuration. Additional modeling (described in this appendix) was performed to evaluate the impacts of alternative thermal load scenarios and expanded waste inventories. The performance assessment model used for the Viability Assessment was expanded to accommodate calculations of the radiological dose to people at distances other than those used in the Viability

Assessment. Other adaptations to the model were made to calculate impacts from nonradiological materials not considered in the Viability Assessment.

The performance assessment model simulates the transport of radionuclides away from the repository into the unsaturated zone, through the unsaturated zone, and ultimately through the saturated zone to the accessible environment. Performance assessment analyses depend greatly on the underlying process models necessary to provide thermal-hydrologic conditions, near-field geochemical conditions, unsaturated zone flow fields, and saturated zone flow fields as a function of time. Using these underlying process models involves multiple steps that must be performed sequentially before performance assessment modeling can begin.

Figure I-1 shows the general flow of information between data sources, process models, and the total system performance assessment model. (Note: Figures are on pages I-67 to I-110.) Several computer models are identified in Figure I-1; these models are introduced in Section I.2. The general purpose of each of these computer models is described below its name in the figure. For example, TOUGH-2 is used for the mountain-scale thermohydrology model and the drift-scale and mountain-scale unsaturated zone flow model. The dashed box in the figure encompasses those portions of the performance assessment model that are modeled within the repository integration program. Other functions are run externally as "process models" to provide information to the repository integration program model. The ultimate result sought from performance assessment modeling is a characterization of radiological dose to humans with respect to time, which is depicted as the "Final Performance Measure" in the figure (the depiction is for illustrative purposes only).

I.2 Total System Performance Assessment Methods and Models

DOE conducted analyses for this EIS to evaluate potential long-term impacts to human health from the release of radioactive materials from the Yucca Mountain Repository. The analyses were conducted in parallel with, but distinct from, the Total System Performance Assessment calculations for the Viability Assessment (DOE 1998a, Volume 3, all). The methodologies and assumptions are detailed in the Total System Performance Assessment – Viability Assessment Technical Bases Document (TRW 1998a,b,c,d,e,f,g,h,i,j,k, all). Extensions of the Viability Assessment analyses to meet distinct EIS requirements were made using the same overall methodology.

The Total System Performance Assessment is a comprehensive systems analysis in which models of appropriate levels of complexity represent all important features, events, and processes to predict the behavior of the system being analyzed and to compare this behavior to specified performance standards. In the case of the potential Yucca Mountain Repository system, a Total System Performance Assessment must capture all of the important components of both the engineered and the natural barriers. In addition, the Yucca Mountain Total System Performance Assessment must evaluate the overall uncertainty in the prediction of waste containment and isolation, and the risks caused by the uncertainty in the individual component models and corresponding parameters.

The components of the Yucca Mountain Repository system include five major elements that the Total System Performance Assessment must evaluate:

- The natural environment unperturbed by the presence of underground openings or emplaced wastes
- Perturbations to the natural system caused by construction of the underground facilities and waste emplacement
- The long-term degradation of the engineered components designed to contain the radioactive wastes

- The release of the radionuclides from the engineered containment system

- The migration of these radionuclides through the engineered and natural barriers to the biosphere and their potential uptake by people, leading to a radiation dose consequence

The processes that operate within these five elements are interrelated. To model the complexity of the system efficiently, however, the following distinct process models were used in Total System Performance Assessment – Viability Assessment and in performance assessment calculations for this EIS:

- The unsaturated-zone flow was modeled directly with a three-dimensional, site-scale, unsaturated zone flow model, using the TOUGH2 program (Pruess 1991, all). Total System Performance Assessment calculations modeled *climate change* by assuming a series of step changes in climatic boundary conditions.

- Drift-scale unsaturated zone thermal-hydrology was modeled with the NUFT program (Nitao 1998, all) in three dimensions using a model domain that contains discrete waste packages and extends vertically from the water table to the ground surface.

- Waste package degradation was modeled using the WAPDEG program (TRW 1998l, all), which includes both individual package variability and package-to-package variability.

- Waste-form and cladding degradation was modeled in the repository integration program model using empirical degradation-rate formulas developed from available data. The model analyses used for the Total System Performance Assessment – Viability Assessment and for this EIS included representation of the protective benefits of fuel cladding for commercial spent nuclear fuel. The cladding failure model is described in detail in DOE (1998a, Volume 3, Section 3.5.2, pages 3-100 to 3-103).

CLIMATE CHANGE

The EIS performance assessment considered three climate scenarios: (1) a *present-day climate*, (2) a *long-term average* climate (wetter than the present-day climate) scenario, and (3) a scenario in which *superpluvial* conditions (much wetter than the present-day climate) are added at a short-duration fixed interval on a periodic basis 100,000 years after waste emplacement. The climate changes are step changes for the duration of the climate periods, and the lengths of the sequences are 10,000 years for the present-day dry climate and the superpluvial climate, and 90,000 years for the long-term average climate (DOE 1998a, Volume 3, Section 5.1.1, page 5-1).

- Engineered barrier-system transport was modeled in the repository integration program model (Golder 1998, all), using the program's cells algorithm. The transport modeling was based on an idealized representation consisting of a linked series of equilibrium batch reactors, including the waste form, waste package, corrosion products, and invert, and radionuclide transport through these reactors (TRW 1998e, all).

- Unsaturated zone radionuclide transport was modeled directly with a three-dimensional site-scale unsaturated zone-transport model using the FEHM model (Zyvoloski et al. 1995, all).

- Saturated zone flow and transport were modeled using a convolution method, in which the three-dimensional, site-scale, saturated zone, flow-and-transport FEHM model (Zyvoloski et al. 1995, all; TRW 1998g, all) was used to generate a library of solutions for translating time-varying mass inputs to the saturated zone into water concentrations at exposure locations downgradient.

- The biosphere was modeled using biosphere dose-conversion factors that convert saturated zone radionuclide concentrations to total radiological dose to an individual. The biosphere dose-conversion factors were developed using the GENII-S program (Leigh et al. 1993, all). The total radiological doses would be the final product of the Total System Performance Assessment calculations.

The performance assessment calculations for both the Total System Performance Assessment – Viability Assessment and this EIS were performed within a probabilistic framework combining the most likely ranges of behavior for the various component models, processes, and related parameters. This appendix presents the results in three main forms: (1) as probability distributions (for example, *complementary cumulative distribution functions*) for peak radiological dose to a maximally exposed individual during the 10,000 and 1 million years following repository closure; (2) as time histories of peak radiological dose to a maximally exposed individual over 10,000 and 1 million years following repository closure; and (3) in the case of this EIS only, as peak population radiological dose during 10,000 years for the local population using contaminated groundwater. For maximally exposed individuals, the Viability Assessment considered only a person 20 kilometers (12 miles) downgradient of the repository, while this EIS considers individuals 5, 20, 30, and 80 kilometers (3, 12, 19, and 50 miles) downgradient from the repository.

As noted above, the repository integration program model implements some of the individual process models directly, while other process models run outside the repository integration program model to produce *abstractions* in the form of data tables, response surfaces, or unit-response functions. The repository integration program model provides a framework for incorporating these abstractions, integrating them with other subsystem models. This is done in a *Monte Carlo* simulation-based methodology to create multiple random combinations of the likely ranges of the parameter values related to the process models. Probabilistic performance of the entire waste-disposal system is computed in terms of radiological dose to individuals at selected distances from the repository.

The EIS performance assessment methodology draws on the extensive analyses performed in support of the Total System Performance Assessment – Viability Assessment. Most of the process models (and their

THE COMPLEMENTARY CUMULATIVE DISTRIBUTION FUNCTION

Example application for individual radiological dose

The value of many variables such as individual radiological dose in the performance assessment models cannot be known precisely, but they can be described in a statistical sense. One of the statistical descriptions used is a complementary cumulative distribution function. The function for individual radiological dose is a curve that represents the probability of exceeding various levels of radiological dose. Although the complementary cumulative distribution function is a curve, one can make probability statements for points on the curve. For example, the stylized function for total radiological dose to an individual shown here indicates that there is a probability of 1 that radiological dose exceeds 0 millirem per year, a probability of 0.6 that radiological dose exceeds 10 millirem per year, a probability of 0.1 that radiological dose exceeds 20 millirem per year, and a probability of 0 that radiological dose exceeds 39 millirem per year.

Stylized Complementary Cumulative Distribution Function of Individual Dose

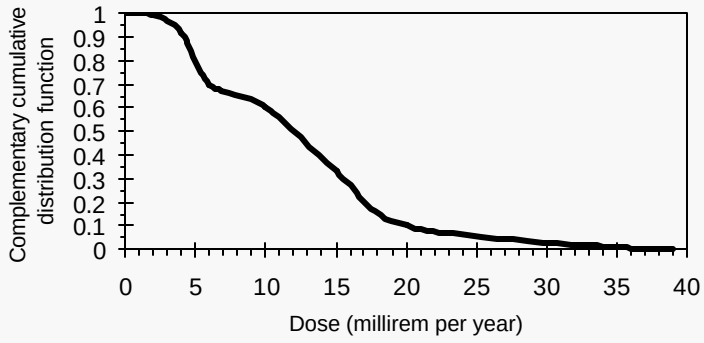

ABSTRACTION

Abstraction is the distillation of the essential components of a process model into a suitable form for use in a total system performance assessment. The distillation must retain the basic intrinsic form of the process model but does not usually require its original complexity. Model abstraction is usually necessary to maximize the use of limited computational resources while allowing a sufficient range of sensitivity and uncertainty analyses (DOE 1998a, Volume 3, page A-1).

MONTE CARLO METHOD: UNCERTAINTY

An analytical method that uses random sampling of parameter values available for input into numerical models as a means of approximating the uncertainty in the process being modeled. A Monte Carlo simulation comprises many individual runs of the complete calculation using different values for the parameters of interest as sampled from a probability distribution. A different final outcome for each individual calculation and each individual run of the calculation is called a *realization* (DOE 1998a, Volume 3, page A-48).

abstractions) developed for the Viability Assessment were used directly in the analyses described in this appendix. Only components that were modified to account for the additional analyses considered in this EIS (but not the Viability Assessment) are described in this appendix.

I.3 Inventory

The analyses of long-term performance considered the following waste categories for radioactive materials:

- Commercial spent nuclear fuel comprised of both conventional enriched uranium fuel and mixed-oxide fuel using treated surplus fissile material that was reprocessed (consisting primarily of plutonium)
- DOE spent nuclear fuel
- High-level radioactive waste (some of which contains immobilized surplus weapons-usable plutonium)
- Greater-Than-Class-C waste and Special-Performance-Assessment-Required waste

The analysis assumed the waste would be in dual-shell waste packages. The outer shell would be comprised of corrosion-allowance material (carbon steel) with an inner shell of corrosion-resistance material (Alloy-22, a nickel-chromium alloy) (DOE 1998a, Volume 3, Figure 3-40, page 3-74). As described in TRW (1997a, Section 2.6), it was assumed that the waste packages would contain fuel assemblies from boiling-water reactors or pressurized-water reactors, naval ship or submarine reactors, DOE research reactors, foreign research reactors, or vitrified high-level radioactive waste in canisters. In addition, surplus plutonium not suitable for use in mixed-oxide fuel would be immobilized into 6.7-centimeter (2.6-inch)-diameter ceramic disks that would be packed in cylindrical *cans*, each containing approximately 1.0 kilogram (2.2 pounds) of plutonium (see Appendix A). Twenty-eight of these cans would be placed in a high-level radioactive waste canister and would occupy about 12 percent of the volume of the canister. The remainder of each canister would be filled with vitrified high-level radioactive waste. The plutonium encased in the high-level radioactive waste glass would then be incorporated in standard waste packages. This analysis assumed that the high-level radioactive waste would be in five-pack waste packages, each containing five high-level radioactive waste canisters and disposed of with or without a canister of DOE spent nuclear fuel. The inventory used for this EIS

assessment was the same as that used in the Viability Assessment (TRW 1998m, all), which also considered more detailed sensitivity studies concerned with ceramic waste forms, alternative waste package configurations, individual fuel assembly configurations, and mixed waste forms (DOE 1998a, Volume 3, Section 5.5).

Thirty-nine radionuclides were included in the initial estimates of total inventories using the ORIGEN2 program (Croff 1980, all). In the Viability Assessment and the EIS performance assessment model, the list of 39 radionuclides was reduced to nine, based on the screening criteria discussed in this section and observing the nuclides that contributed most to total radiological dose as calculated in the performance assessment models. These nine radionuclides are carbon-14, iodine-129, neptunium-237, protactinium-231, plutonium-239, plutonium-242, selenium-79, technetium-99, and uranium-234.

This section discusses the inventories of waterborne radioactive materials used to model impacts and of some nonradioactive, chemically toxic waterborne materials used in the repository environment that could present health hazards. This section also discusses the inventory of atmospheric radioactive materials.

I.3.1 WATERBORNE RADIOACTIVE MATERIALS

There would be more than 200 radionuclides in the materials to be placed in the repository (see Appendix A). Because some of the radionuclides have a small inventory and some have short half-lives, this analysis did not need to consider all of these radionuclides when estimating long-term repository performance. Therefore, a screening analysis was performed to choose a subset of these radionuclides for further analysis.

I.3.1.1 Reduction of the List of Radionuclides for Performance Assessment Modeling

This evaluation of postclosure performance reduced the number of radionuclides considered by eliminating any radionuclides that:

- Have short half-lives and are not decay products of long-lived radionuclides
- Have high chemical sorption such that long travel times to a human exposure location would result in extremely low concentrations due to radioactive decay (unless the radionuclide has a large inventory and the potential for colloidal transport)
- Have low biosphere dose-conversion factors

Any one or any combination of these factors would result in a diminished contribution by the radionuclide to the total radiological dose; thus, eliminating that radionuclide from consideration would not reduce estimates of radioactive material impacts. Based on these considerations and previous performance analysis results (TRW 1995, all), DOE selected nine dominant radionuclides for analysis and focused on those radionuclides that would have the most impact on human health, thereby enhancing modeling efforts.

Two other factors were a part of the decision to reduce the list of radionuclides explicitly modeled in performance assessment calculations. First, there was a need to reduce the number of radionuclides in order to focus on only those radionuclides with the greatest impact on human health. Large multidimensional flow-and-transport models such as the unsaturated zone and saturated zone particle-tracking and transport models that are part of the repository integration program model require extensive computer time (days or weeks). Hence, it was necessary to focus on those radionuclides that would have the most impact on human health. The reduced list of radionuclides adequately characterized the impacts without requiring an unnecessary computer modeling effort. Second, knowledge and experience gained from earlier assessments (Wilson et al. 1994, all; TRW 1995, all), as well as the experience of other

organizations (Wescott et al. 1995, all), were incorporated into the choice of radionuclides included for analysis. To be included for the Total System Performance Assessment – Viability Assessment, a radionuclide had to pass the elimination process performed under the basic criteria described above. It also had to have an overall larger inventory than a similar radionuclide with similar performance importance, or it had to have been identified as important in earlier studies.

The following is a discussion of the further rationale for the final selection of the specific radionuclides to model.

Selected Radionuclides

- *Carbon-14, technetium-99, and iodine-129.* These radionuclides are highly soluble and exhibit little or no chemical sorption. Technetium-99 and iodine-129 were major radiological dose contributors in previous Total System Performance Assessments (Barnard et al. 1992, all; Wilson et al. 1994, all). Carbon-14 and iodine-129 could be liberated from the waste packages as gases and subsequently dissolved in water.

- *Selenium-79, protactinium-231, uranium-234, and neptunium-237.* These radionuclides are relatively soluble and have relatively low chemical sorption. Selenium-79 is the major radiological dose contributor through a cow's liver pathway. Protactinium-231 has a relatively high sorption coefficient, but because it is a decay product of uranium-235, it should be transported relatively quickly and have a long residence time. Uranium-234 has a large inventory, is a decay product of uranium-238, and has a high biosphere dose conversion factor. Neptunium-237 has been the most important radionuclide in previous Total System Performance Assessments for exposure periods between 20,000 and 1,000,000 years after repository closure.

- *Plutonium-239 and plutonium-242.* Although these plutonium isotopes are highly sorbing, they were included on the list because of their large inventory and the possibility that they might migrate by colloidal transport. These radionuclides would be among the most important radionuclides involved in colloid-facilitated transport, if colloidal transport of plutonium were determined to be important. Plutonium-242 was selected over plutonium-240 because of its longer half-life, thus making it more likely to reach the accessible environment (especially via colloidal transport).

Radionuclides Not Selected

- *Curium-246, curium-245, americium-241, americium-243, plutonium-240, uranium-238, thorium-230, radium-226, lead-210, cesium-137, cesium-135, niobium-94, and nickel-59.* These radionuclides were among those selected by the U.S. Nuclear Regulatory Commission for its Iterative Performance Assessment (Wescott et al. 1995, page 5-5). The Viability Assessment did not include curium isotopes because of their similarity to plutonium. Americium isotopes were not included directly because they have short half-lives, americium-243 was included in the plutonium-239 inventory, and the activity of americium-241 was included in the neptunium-237 inventory. Plutonium-240 was not selected because it is highly sorbing (although plutonium-242 was selected to address colloidal transport). Uranium-238 was not selected because its decay product uranium-234 was chosen. Ingrowth of uranium-238 was compensated for by increasing the uranium-234 inventory. Thorium, radium, lead, cesium, niobium, and nickel were generally not included because they are highly sorbing. In addition, lead-210, cesium-137, and radium-226 have relatively short half-lives, while cesium-135, nickel-59, and niobium-94 have low inventories. For these reasons, none of these radionuclides would contribute significantly to radiological dose (that is, including these radionuclides in the calculations would not change the estimates of dose within the number of significant figures reported for results).

Using only a subset of the radionuclides leads to potential underestimates of impacts to humans. The modeling results reported in Chapters 5 and 8 show that in the first 10,000 years, the radiological dose is

dominated by technetium-99, iodine-129, and carbon-14. These radionuclides all have relatively high solubility and little chemical sorption. There are no other radionuclides with a meaningful inventory in the proposed repository that share these characteristics. Thus, the error introduced by excluding other radionuclides is very small in the first 10,000 years after repository closure.

The potential for underestimating impacts increases with time periods greater than 10,000 years after repository closure. The possible error is largely due to the modeling of a few nuclides without modeling the entire decay chain for the nuclide. Based on decay equilibrium calculations for the first 1,000,000 years after repository closure, the error from neglecting all other nuclides is about 5 percent of the total radiological dose rate (DOE 1998a, Appendix C, page C6-2 and Figure C6-1).

The inventories for the categories of spent nuclear fuel and high-level radioactive waste described in the following paragraphs include these nine radionuclides. The inventories of these radionuclides were used in the performance assessment model to estimate the impacts to people.

The Viability Assessment and these EIS performance assessment calculations included only certain nuclides of prominent decay chains. To account for the lack of ingrowth of decay products, modifications were made to the nine radionuclide inventories for commercial spent nuclear fuel, DOE spent nuclear fuel, and high-level radioactive waste. These modifications helped produce conservative estimates of the activities of these nuclides (that is, estimates of the inventory would be equal to or greater than the real inventory, so that any uncertainty would tend to overpredict impacts), which were then used by the performance assessment model to determine impacts to individuals at specific exposure locations. Three of the radionuclide inventories were modified as follows:

- The amount of protactinium-231 was entered in the repository integration program model as grams per waste package of protactinium-231 rather than as curies per waste package, which allowed the inventory of protactinium-231 to be modeled in secular equilibrium with its parent nuclide uranium-235.

- The estimated activities of neptunium-237 and uranium-234 were increased by 58 percent and 13 percent, respectively. The increase in the activity of neptunium included the activity of the precursors californium-249, curium-245, plutonium-241, and americium-241 in the performance assessment model. Neptunium-237 transports faster than the precursor radionuclides, so putting the entire inventory in neptunium-237 would not underestimate the radiological dose. The increase of activity in uranium-234 included the activity of precursors such as californium-250, curium-246, plutonium-242, americium-242, curium-242, uranium-238, and plutonium-238.

I.3.1.2 Radionuclide Inventory Used in the Performance Assessment Model

Radioactive material inventories were included in the performance assessment model for Total System Performance Assessment calculations by the following waste categories: commercial spent nuclear fuel, high-level radioactive waste, and DOE spent nuclear fuel. For each waste category, an *abstracted waste package* was represented with an average radionuclide inventory for the nine radionuclides selected in the screening analysis (see Section I.3.1.1).

The quantity of abstracted packages was determined, in part, by averaging the characteristics of the several different types of actual waste packages planned for each waste category and, in part, by demands for a symmetrical, replicating arrangement of waste packages necessary for efficient thermal-hydrologic modeling. Therefore, the quantity of abstracted packages in the performance assessment model differed slightly from the actual quantity of waste packages identified in Appendix A and elsewhere. Other inventory differences between the performance assessment model and Appendix A, and the associated implications, are discussed in this section.

ABSTRACTED WASTE PACKAGES

The number of waste packages used in the performance assessment simulations do not exactly match the number of actual waste packages specified in TRW (1998n, all).

The performance assessment model uses three types of *abstracted waste packages,* representing the averaged inventory of all the actual waste packages used for a particular waste category (commercial spent nuclear fuel, DOE spent nuclear fuel, or high-level radioactive waste).

While the number of abstracted waste packages might vary from TRW (1998n, all), the total radionuclide inventory (activity) represented by all of the abstracted waste packages collectively is equivalent to the total inventory given in Appendix A, unless otherwise noted.

I.3.1.2.1 *Commercial Spent Nuclear Fuel*

The commercial spent nuclear fuel inventory is discussed in detail in Appendix A. The quantities and activities were weighted according to the contributors and the expected waste package configurations. Using these data, the analysis established an abstracted waste package commercial spent nuclear fuel radionuclide inventory for the Total System Performance Assessment – Viability Assessment and EIS performance assessment modeling (TRW 1998m, page 5-10). Table I-1 lists the radionuclide inventory for commercial spent nuclear fuel used for both the EIS and Viability Assessment analyses.

Table I-1. Performance assessment model radionuclide inventory (curies per waste package) for commercial spent nuclear fuel.[a]

Nuclide	Inventory
Carbon-14	12
Iodine-129	0.29
Neptunium-237	11
Protactinium-231[b]	5.1
Plutonium-239	3,100
Plutonium-242	17
Selenium-79	3.7
Technetium-99	120
Uranium-234	21

a. Source: DOE (1998a, Volume 3, page 3-96).
b. Protactinium-231 is listed in grams per package to facilitate modeling as an equilibrium decay product of uranium-235. The specific activity of protactinium-231 is 0.0000022 curies per gram.

I.3.1.2.2 *DOE Spent Nuclear Fuel*

The DOE spent nuclear fuel inventory is discussed in detail in Appendix A. Table I-2 lists the abstracted waste package radionuclide inventory for DOE spent nuclear fuel used for the Viability Assessment and the EIS analyses for the Proposed Action.

I.3.1.2.3 *High-Level Radioactive Waste*

High-level radioactive waste is the highly radioactive material resulting from the reprocessing of spent nuclear fuel, and the inventory for its disposal is presented in Appendix A. The high-level radioactive waste inventory assembled for Total System Performance Assessment – Viability Assessment and EIS performance assessment modeling was derived from the inventories of high-level radioactive waste at the Hanford Site, Savannah River Site, Idaho National Engineering and Environmental Laboratory, and West

Table I-2. Performance assessment model radionuclide inventory (curies per waste package) for DOE spent nuclear fuel.[a]

Nuclide	Inventory
Carbon-14	0.31
Iodine-129	0.0057
Neptunium-237	0.15
Protactinium-231[b]	0.66
Plutonium-239[c]	155
Plutonium-242	0.11
Selenium-79	0.089
Technetium-99	2.6
Uranium-234	0.54

a. Source: DOE (1998a, Volume 3, page 3-96).
b. Protactinium-231 is listed in grams per package to facilitate modeling as an equilibrium decay product of uranium-235. The specific activity of protactinium-231 is 0.0000022 curies per gram.
c. Inventory for plutonium-239 is correct; DOE (1998a, Volume 3, page 3-96) contains a typographical error.

Valley Demonstration Project. This inventory was established from the National Low-Level Waste Database and weighted for the expected contributions from the four principal high-level radioactive waste sites listed above using quantities calculated in the *Waste Quantity, Mix and Throughput Report* (TRW 1997a, all). This inventory is listed in Table I-3 for the nine modeled radionuclides.

Table I-3. High-level radioactive waste mass and volume summary.

Parameter	EIS analyses	Appendix A
Mass (metric tons)	NA[a]	58,000
Volume (cubic meters)	18,000	21,000
Number of canisters	19,234	22,280
Waste packages (5-packs)	3,848	4,456[b]

a. NA = not applicable.
b. Derived from data presented in Appendix A.

These data were included in the high-level radioactive waste inventory for the Viability Assessment base case (TRW 1998o, all); long-term performance assessment analyses for this EIS used this same inventory.

Recent updates of the waste inventories from the DOE sites are in Appendix A. The most recent estimates from these sites indicated a higher total volume of high-level radioactive waste but with an overall lower activity. Appendix A provides a 1998 summary of the potential total mass, volume, and number of canisters of high-level radioactive waste that would be available to the Yucca Mountain Repository from the principal waste sites.

These performance assessment analyses did not use the most recent information reported in Appendix A, because the more recent estimates of high-level radioactive waste activity were received too late for inclusion in the Viability Assessment and EIS performance assessment calculations (see TRW 1998f, page 6-16). A sensitivity analysis of high-level radioactive waste was performed by comparing the high-level radioactive waste inventory used in EIS analyses to the inventory in Appendix A. The results of the analysis showed that the estimate of total radiological dose to maximally exposed individuals at 20 kilometers (12 miles) from the Yucca Mountain Repository, using the high-level radioactive waste base case inventory for the Viability Assessment, led to higher amounts of radionuclides contributing to radiological dose than those calculated using the revised data from Appendix A. Therefore, actual impacts would be lower than estimated if the more recent information were used. Table I-4 compares the nine radionuclide inventories used in the Viability Assessment and EIS analyses with those used in the Appendix A inventory. Note that the nine modeled radionuclides do not contribute equally to radiological

Table I-4. Comparison of high-level radioactive waste inventories (curies per package).

Nuclide	TSPA-VA inventory [a] (3,848 packages)	Appendix A inventory (4,456 packages)
Carbon-14	0	0.032
Iodine-129	0.000042	0.0085
Neptunium-237	0.74	0.13
Protactinium-231[b]	0.036	0.82
Plutonium-239	24	68
Plutonium-242	0.02	0.014
Selenium-79	0.29	0.49
Technetium-99	30	13
Uranium-234	0.9	0.15

a. Source: TSPA-VA = (Total Systems Performance Assessment – Viability Assessment); DOE (1998a, Volume 3, page 3-96).

b. Protactinium-231 is listed in grams per package to facilitate modeling as an equilibrium decay product of uranium-235. The specific activity of protactinium-231 is 0.0000022 curies per gram.

dose, so a comparison of the inventories in Table I-4 can be misleading. For example, neptunium-237 typically contributes more than 90 percent of the dose in the 1-million-year period, so the larger inventory of neptunium-237 in the Total Systems Performance Assessment – Viability Assessment inventory column is more important that the smaller inventory of other radionuclides relative to the Appendix A inventory column. Similarly, iodine-129 and technetium-99 inventories contribute most of the dose in the 10,000-year period, so difference in those inventories are most important in that case.

The source used for the Viability Assessment to establish the inventory of high-level radioactive waste was the Characteristics Database (DOE 1992, all). Appendix A contains data submitted by the individual sites in response to an EIS data call. The differences in the data from each source are listed below by site.

Discussion of differences is limited to the nine radionuclides modeled in the performance assessment analyses.

Hanford Site

- The Characteristics Database (DOE 1992, all) assumes 1,650 kilograms (3,630 pounds) of glass per canister.

- Appendix A reports the mass of glass per canister as 3,040 kilograms (6,700 pounds). Values in Appendix A are generally higher than those presented in the Characteristics Database (DOE 1992, all); these values are listed in Table I-5. Nuclide values which are generally lower in Appendix A than the Characteristics Database are presented in Table I-6.

Table I-5. Nuclides at the Hanford Site for which Appendix A presents values greater than those in the Characteristics Database.[a]

Nuclide	Factor
Iodine-129	100
Protactinium-231	100,000
Plutonium-239	2.5
Selenium-79	8
Uranium-234	5

a. Source: DOE (1992, all).

Table I-6. Nuclides for which Appendix A presents values lower than those in the Characteristics Database.[a]

Nuclide	Factor
Neptunium-237	100
Technetium-99	3

a. Source: DOE (1992, all).

Idaho National Environmental and Engineering Laboratory

- The Characteristics Database (DOE 1992, all) inventory numbers do not include the projected high-level radioactive waste inventory from the Argonne National Laboratory-West ceramic and metal waste matrices (approximately 102 canisters).

- Appendix A reported values for carbon-14 and iodine-129 (0.000083 and 0.017 curie per canister, respectively), while the Characteristics Database (DOE 1992, all) reported no values for these nuclides.

- The Characteristics Database (DOE 1992, all) reported 0.08 curie per canister for selenium-79; however, no value is reported for use in Appendix A.

- For the other nuclides, the values reported in Appendix A are greater by a variety of factors, as listed in Table I-7.

Table I-7. Nuclides at the Idaho National Engineering and Environmental Laboratory for which Appendix A presents values greater than those in the Characteristics Database.[a]

Nuclide	Factor
Neptunium-237	270
Plutonium-239	2.25
Plutonium-242	1.65
Technetium-99	3.7
Uranium-234	200,000

a. Source: DOE (1992, all).

Savannah River Site

- In general, the Appendix A values for the other nuclides are slightly smaller (generally less than 1 percent) than those presented in the Characteristics Database (DOE 1992, all). The uranium-234 value reported in Appendix A is 77 percent less; however, most of the other nuclides are within 1 percent of the values in the Characteristics Database.

West Valley Demonstration Project

- The Characteristics Database (DOE 1992, all) does not include data for carbon-14 or iodine-129; Appendix A uses approximately 0.53 and 0.00081 curie per canister, respectively, for these nuclides.

- Neptunium-237, plutonium-239, plutonium-242, and protactinium-231 differ slightly in Appendix A (by about 1 percent) due largely to the difference in reporting accuracy (Appendix A reports two significant figures; the Characteristics Database reports three).

- Uranium-234 is increased by about 15 percent in Appendix A.

- Technetium-99 and selenium-79 are both higher in Appendix A by a factor of approximately 15.

I.3.1.2.4 *Greater-Than-Class-C and Special-Performance-Assessment-Required Wastes*

Wastes with concentrations above Class-C limits (shown in 10 CFR Part 61.55, Tables 1 and 2 for long and short half-life radionuclides, respectively) are called Greater-Than-Class-C low-level waste. These wastes generally are not suitable for near-surface disposal. The Greater-Than-Class-C waste inventory is discussed in detail in Appendix A.

DOE Special-Performance-Assessment-Required low-level radioactive waste could include production reactor operating wastes, production and research reactor decommissioning wastes, non-fuel-bearing components of naval reactors, sealed radioisotope sources that exceed Class-C limits for waste classification, DOE isotope production related wastes, and research reactor fuel assembly hardware. The Special-Performance-Assessment-Required waste inventory is discussed in detail in Appendix A.

The final disposition method for Greater-Than-Class-C and Special-Performance-Assessment-Required low-level radioactive waste is not known. If these wastes were to be placed in a repository, they would be placed in canisters before shipment. This appendix assumes the use of a canister similar to the naval dual-purpose canister described in Section A.2.2.5.6.

Table I-8 lists existing and projected volumes through 2055 for the three Greater-Than-Class-C waste sources. DOE conservatively assumes 2055 because that year would include all Greater-Than-Class-C low-level waste resulting from the decontamination and decommissioning of commercial nuclear reactors. The projected volumes conservatively reflect the highest potential volume and activity expected based on inventories, surveys, and industry production rates.

Table I-8. Greater-Than-Class-C low-level waste volumes (cubic meters)[a] by source.[b]

Source	1993	2055
Nuclear electric utility	26	1,300
Sealed sources	40	240
Other	74	470
Totals	**140**	**2,010**

a. To convert cubic meters to cubic feet, multiply by 35.314.
b. Source: DOE (1994, Tables 6-1 and 6-3).

The data concerning the volumes and projections of Greater-Than-Class-C low-level waste are from Appendix A-1 of the *Greater-Than-Class-C Low-Level Radioactive Waste Characterization: Estimated Volumes, Radionuclide Activities, and Other Characteristics* (DOE 1994, all). This appendix provides detailed radioactivity reports for such waste currently stored at nuclear utilities. Table I-9 summarizes the radioactivity data for the nine radionuclides modeled in performance assessment calculations, decayed to 2055.

I.3.2 WATERBORNE CHEMICALLY TOXIC MATERIALS

Waterborne chemically toxic materials that could present a human health risk would be present in materials disposed of in the repository. The most abundant of these chemically toxic materials would be nickel, chromium, and molybdenum, which would be used in the waste package, and uranium in the disposed waste. Uranium is both a chemically toxic and radiological material. Screening studies were conducted to determine which, if any, of these or other materials could be released in sufficient quantities to have a meaningful impact on groundwater quality.

Table I-9. Performance assessment model radionuclide inventory (curies per waste package) for Greater-Than-Class-C and Special-Performance-Assessment-Required waste.[a]

Nuclide	Inventory
Carbon-14	38
Iodine-129	0.000000012
Neptunium-237	0.000000052
Protactinium-231[b]	0.0000015
Plutonium-239	48
Plutonium-242	0.0000040
Selenium-79	0.0000010
Technetium-99	2.6
Uranium-234	0.00000062

a. Source: TRW (1999a, Table 2.2-6, page 2-10).

b. Protactinium-231 is listed in grams per package to facilitate modeling as an equilibrium decay product of uranium-235. The specific activity of protactinium-231 is 0.0000022 curies per gram.

I.3.2.1 Identification of Waterborne Chemically Toxic Materials

An inventory of chemical materials to be placed in the repository under the Proposed Action was prepared. The inventories of the chemical components in the repository were combined into four groups:

- Materials outside the waste packages (concrete, copper bus bars, structural members, emplacement tracks and supports, etc.)
- Carbon steel in the outer layer of the waste packages
- Alloy-22 in the inner layer of the waste packages
- Materials internal to the waste packages

These materials were organized into groups with similar release times for use in the screening study. Table I-10 lists the chemical inventories. Plutonium is not listed in Table I-10 because, while it is a heavy metal and therefore could have toxic effects, its radiological toxicity far exceeds its chemical toxicity (DOE 1998b, Section 2.6.1) (see Section I.5 for more information). Also, while there are radiological limits set for exposure to plutonium, no chemical toxicity benchmarks have been developed. Therefore, because of this lack of data to analyze chemical toxicity, plutonium was not analyzed for the chemical screening.

I.3.2.2 Screening Criteria

Only those chemicals likely to be toxic to humans were carried forward in the screening study. Uranium was an exception; it was carried forward due to its high inventory and also to serve as a check on the screening study. Chemicals included in the substance list for the U.S. Environmental Protection Agency's Integrated Risk Information System (EPA 1999, all) were evaluated further to determine a concentration that would be found in drinking water in a well downgradient from the repository. The chemicals on the Integrated Risk Information System substance list that would be in the repository are barium, boron, cadmium, chromium, copper, lead, manganese, mercury, molybdenum, nickel, selenium, uranium, vanadium, and zinc.

Table I-10. Inventory (kilograms)[a] of chemical materials placed in the repository under the Proposed Action.

	Inventory					
Element	Outside package	Carbon steel	Alloy-22	Internal	High-level radioactive waste	Totals
Aluminum	0	0	0	1,205,000	0	1,205,000
Barium	0	0	0	0	19,000	19,000
Boron	0	0	0	223,000	0	223,000
Cadmium	0	0	0	0	43,000	43,000
Carbon	286,000	796,000	8,000	5,000	0	1,096,000
Chromium	0	0	9,670,000	3,903,000	0	13,573,000
Cobalt	0	0	1,357,000	27,000	0	1,384,000
Copper	1,135,000	0	0	3,000	0	1,139,000
Iron	91,482,000	320,089,000	2,171,000	9,000	0	413,751,000
Lead	0	0	0	0	2,000	2,000
Magnesium	0	0	0	12,000	0	12,000
Manganese	234,000	3,007,000	271,000	2,000	0	3,514,000
Mercury	0	0	0	0	200	200
Molybdenum	0	0	5,934,000	302,000	0	6,236,000
Nickel	0	0	29,727,000	5,563,000	0	35,290,000
Phosphorus	37,000	114,000	11,000	0	0	161,000
Selenium	0	0	0	0	300	300
Silicon	361,000	943,000	43,000	7,000	0	1,354,000
Sulfur	46,000	114,000	11,000	0	0	170,000
Titanium	0	0	0	2,000	0	2,000
Tungsten	0	0	1,628,000	0	0	1,628,000
Uranium	0	0	0	70,000,000	0	70,000,000
Vanadium	0	0	190,000	0	0	190,000
Zinc	0	0	0	3,000	0	3,000

a. To convert kilograms to pounds, multiply by 2.2046.

I.3.2.3 Screening Application

The screening calculations for chemically toxic materials assume that groundwater would move through the repository, dissolving and transporting the potentially chemically toxic materials. This analysis treated the repository materials and the carbon-steel layer of the waste package as simultaneously degrading in the groundwater. After the carbon-steel layer of the waste degraded, the Alloy-22 corrosion-resistant material would start degrading. Finally, once the waste package was breached, the materials inside the waste packages would become available for dissolution and transport.

I.3.2.3.1 *Solubility of Chemically Toxic Materials in the Repository*

The release of chemically toxic materials to the accessible environment depends on the solubility of the materials in water. Table I-11 lists the solubility values used for the screening study.

Maximum source concentrations for materials in the repository that are not a part of the waste package materials were calculated as solubilities of an element in repository water. This calculation would provide the maximum possible concentration of that element in water entering the unsaturated zone if it dissolved at a sufficiently high rate. The solubilities were obtained by modeling with the EQ3 code (Wolery 1992, all). The simulations were started with water from well J-13 near the Yucca Mountain site (Harrar et al. 1990, all). EQ3 calculates chemical equilibrium of a system so that by making successive runs with gradually increasing aqueous concentrations of an element, eventually a result will show the saturation of a mineral in that element. That concentration at which the first mineral saturates is said to be

SCREENING ANALYSIS

A *screening analysis* is a method applied to avoid unnecessary calculations and focus on potentially large impacts.

The repository would contain many materials that could result in impacts to human health. However, most of these materials would either not be present in large enough quantities or not dissolve readily enough in water to pose a risk.

To evaluate the potential risk posed by so many materials, an analysis could either rigorously evaluate every material at great cost, or could apply a screening analysis to identify those materials with too little inventory or too little solubility to be of concern. The screening analysis applied for the EIS was a simplified scoping calculation which resulted in a short list of materials that merited further consideration. Any preliminary concentrations predicted under the simplified assumptions of the screening analysis were treated as conservative estimates used only to determine if the material should be rigorously modeled again using the performance assessment model. For those materials that the screening analysis indicated must be evaluated further, more realistic concentrations and impacts were computed with the performance assessment model and are reported in Sections I.5 and I.6.

Table I-11. Source concentrations[a] (milligrams per liter)[b] of waterborne chemically toxic materials for screening purposes.

Element	Concentration	Aqueous species	Reference
Boron	6,400	B(OH)3aq	Solubility in repository water by EQ3[c] simulation
Chromium	300	CrO_4^{--}	EQ6 [d] simulation of Alloy 22 corrosion
Copper	0.018	$CuOH^+$, $Cu(CO_3)$aq, Cu^{++}	Solubility in repository water by EQ3 [c] simulation
Manganese	4.40×10^{-11}	Mn^{++}	EQ6 [d] simulation of Alloy 22 corrosion
Molybdenum	218	MoO_4^{--}	EQ6 [d] simulation of Alloy 22 corrosion
Nickel	1.00×10^{-6}	Ni^{++}	EQ6 [d] simulation of Alloy 22 corrosion
Uranium	0.6	$UO_2(OH)_2$aq	Derived from TRW (1997b), Figure C-3, page C-8[e]
Vanadium	4.8	VO_3OH^{--}, HVO_4^{--}	EQ6[d] simulation of Alloy 22 corrosion
Zinc	63	Zn++	Solubility in repository water by EQ3 [c] simulation

a. Concentration at the point where the chemical enters unsaturated zone water, controlled by solubility or local chemistry of dissolution and interaction with tuff. Note that these concentrations are not used for transport modeling (which is discussed in Section I.6) but are used only for screening analysis purposes. Refer to Section I.6 for groundwater concentrations of chemically toxic materials that were selected for further consideration based on the screening analysis.
b. To convert milligrams per liter to pounds per cubic foot, multiply by 0.00000624.
c. EQ6 code, Version 7.2b (Wolery and Daveler 1992, all).
d. EQ3 code, Version 7.2b (Wolery 1992, all).
e. For ph=8 and $Co_2=10^{-3}$ atmospheric partial pressure.

the "solubility." For example, the solubility of copper (from the bus bars left in the tunnels) would be obtained by increasing copper concentrations in successive runs of EQ3. At a concentration of 0.01811 milligram per liter, tenorite (CuO) would be saturated. This mineral would then be in equilibrium with dissolved copper existing in approximately equal molar parts as $CuOH^+$, $Cu(CO_3)$aq, and Cu^{++}. The aqueous concentration was then reported in Table I-11 as a "solubility" of copper for the purposes of screening the potentially toxic chemicals.

The largest quantities of potentially toxic materials come from the construction materials of the waste packages themselves. The main source is the Alloy-22 material used in the corrosion-resistant layer. The possible maximum concentrations of these materials (chromium, nickel, molybdenum, manganese, and vanadium) were developed by examining the corrosion process. Corrosion was modeled in the EQ6 code

(Wolery and Daveler 1992, all), starting with the same repository water as used in the solubility calculations described above. In the corrosion step, EQ6 was run in the titration mode (that is, a confined area in which essentially stagnant water reacts with iron from existing corrosion-allowance material fragments and Alloy-22). Oxygen is fixed at atmospheric fugacity (which is analogous to partial pressure adjusted for nonidealities). After a few hundred years, the chemistry of the resultant solution stays relatively constant for a long period. Following that, ionic strength eventually exceeds limits for +EQ6. The chemistry during this "flat period" was used as the resultant solution, which contained very high quantities of dissolved chromium (as hexavalent chromium), nickel, and molybdenum, and small dissolved quantities of manganese and vanadium. The reaction of this solution with tuff was then modeled. The resultant solution showed that essentially all of the nickel and manganese were precipitated and that the original dissolved concentrations of chromium, molybdenum, and vanadium remained.

Two types of geochemical analyses were performed. The first was an analysis of the solution concentration obtained when J-13 water, adjusted for the presence of repository materials such as concrete (that is, the same water chemistry used for other process modeling work supporting the Total System Performance Assessment-Viability Assessment), reacts with a large mass of carbon steel and Alloy-22 for an extended period. The second was an analysis of the reaction of the solution from the first analysis with volcanic tuff. The resultant solution from the second analysis would represent a bounding value for the source term solution at the floor of the emplacement drift.

At each step of the reaction progress in which the titration mode of EQ6 was used, a small quantity of reactants (steel and Alloy-22) was added to the solution (starting as J-13 water). After each addition, the increment of reactant dissolves and all product phases would reequilibrate with the aqueous solution. After a long time, this process would produce a bounding concentration for the solution. This would be the case if the water had a very long contact time with the metals and a very limited amount of water was used.

The composition of J-13 water was taken from earlier studies (TRW 1997b, page A-5). The carbon dioxide and oxygen levels are maintained at atmospheric conditions during the reaction. This process promotes the formation of the chromate (CrO_{4}^{--}) ion, which represents the hexavalent (and most toxic) state of chromium. The complete oxidation of chromium and the formation of chromate creates a very low pH environment in the area immediately adjacent to the corrosion process. The result of a low pH level in the presence of sufficient oxygen would be dissolved chromium existing in the hexavalent state. Large amounts of soluble hexavalent molybdenum are also formed.

Once the corrosion solution left the waste package, it would quickly encounter rock material. The second analysis evaluated the effect of rock on the solution. The analysis used the option for a "Fluid-Centered Flow-Through Open System" in EQ6. In this type of simulation the solution is permitted to react with solid materials (in this case, the tuff) for some specified interval (either time or reaction progress). The solution is then moved away from the solid reaction products that would be created and allowed to react with the same initial solids for a further interval. In this way, the model simulates reaction of the solution as it percolates through a rock.

This analysis simulated the tuff rock with the elemental composition characteristics of volcanic tuff. Earlier waste package criticality studies used this formulation for tuff reactants (TRW 1997c, page 17).

The resultant solution from the simulated reaction of J-13 water with carbon steel and Alloy-22 has a very low pH and a high concentration of dissolved chromium, molybdenum, and nickel. The resulting pH 2.0 solution would have the elemental concentrations listed in the second column of Table I-12. When the solution from corrosion contacts the rock, it would be neutralized to a pH of 8. The availability of silica in the rock would promote the formation of silicates, which would precipitate most of the nickel and manganese but virtually none of the chromium, molybdenum, or vanadium. Some chromium would change to $Cr_2O_7^{--}$ (still hexavalent and very soluble). The molybdenum would behave in a very similar

Table I-12. EQ6-modeled concentrations (milligrams per liter)[a] in solution from reaction of J-13 water with carbon steel and Alloy-22.

Element	After corrosion of Alloy-22	After reaction with tuff rock
Chromium	299	299
Manganese	32	4.40×10^{-11}
Molybdenum	218	218
Nickel	750	9.9×10^{-5}
Vanadium	4.8	4.8

a. To convert milligrams per liter to pounds per cubic foot, multiply by 0.00000624.

fashion and remain in solution as hexavalent species. The resultant solution would have the elemental concentrations listed in the third column of Table I-12.

The mechanism for mass loss of the Alloy-22 remains an issue at this time. There is no reliable evidence to support or refute the idea that the chromium that is carried away from Alloy-22 is dissolved hexavalent chromium. What is known fairly well is that trivalent chromium is the likely constituent (as Cr_2O_3) of the passivation film and that it has a very low solubility. It is not known whether the film grows thick until it sloughs off or if the film oxidizes in place so that it loses hexavalent chromium into solution. It is also not known if the film would oxidize and dissolve if it did slough off. EQ6 simulates a process whereby the trivalent chromium oxidizes to hexavalent chromium by reaction with O_2. It is well known that if chromium is in solution, the predominant species will be hexavalent chromium, especially in oxidizing conditions. At the Eh for atmospheric oxygen, it is known that the ratio of hexavalent chromium to For purposes of analysis, DOE assumes hexavalent chromium is mobilized as a dissolved constituent, and its source term is represented by 0.22 times the bulk loss rate of Alloy-22. A parallel assumption has been made about hexavalent molybdenum, which is also present in meaningful quantities in the results of the corrosion simulation.

I.3.2.3.2 *Well Concentration of Chemically Toxic Materials*

After the materials would begin to be released from the repository, they would be transported through the unsaturated zone to the saturated zone and on to the accessible environment. The screening study assumed that the chemicals would flow to a well from which an individual received all of their drinking water. Table I-13 lists the concentrations for the chemically toxic materials.

The well concentrations listed in Table I-13 were based on a series of simple calculations. First, the release concentrations for each material were calculated. The release rate for the material in the carbon steel is based on a degradation rate of 0.025 millimeter (0.001 inch) per year and a thickness of 100 millimeters (3.9 inches); thus, the annual fractional release rate for carbon steel is 0.00025. The degradation rate for Alloy-22 is 0.000006 millimeter (0.00000024 inch) per year and the material thickness is 20 millimeters (0.79 inch); the resulting annual fractional release rate is 0.0000003. The internal materials were assumed to be released at the same rate as the carbon steel (a conservative assumption). The release rate for the high-level radioactive waste was taken from earlier studies (TRW 1998f, Section 6.4). The annual fractional release rate for the high-level radioactive waste is 0.000054. The well concentrations in Table I-13 are very conservative concentration estimates that are not used directly for impact estimates. Instead, they are used to screen potentially toxic chemicals for more detailed analyses. These estimates were then compared to the Maximum Contaminant Levels for each material, if available (40 CFR 141.2). Some of the estimated concentrations were orders of magnitude below their respective Maximum Contaminant Levels. As a result of this screening study, barium, copper, lead, mercury, and selenium were eliminated from further detailed analysis. All the other chemically toxic materials, including boron, cadmium, chromium, manganese, molybdenum, nickel, uranium, vanadium, and zinc, were carried forward for further detailed analysis (see Chapter 5, Section 5.6.1).

Table I-13. Concentrations (milligrams per liter)[a] of waterborne chemically toxic materials for screening purposes.[b]

Element	Concentration limit	Release concentration: Non-package	Carbon steel	Alloy-22	Internal	HLW	Maximum	Well concentration	Maximum contaminant level[c]
Barium	0.00412	0	0	0	0	0.99	0.00412	1.5×10^{-5}	2.0
Boron	6,400	0	0	0	50	0	52	1.9×10^{-1}	NA[d]
Cadmium	23	0	0	0	0	2.2	2.2	7.7×10^{-3}	0.005
Chromium	300	0	0	2.7	940	0	300	1.1	0.1
Copper	0.018	0.018	0	0	0	0	0.018	6.4×10^{-5}	1.3
Lead	NA	0	0	0	0	0.09	0.09	3.2×10^{-4}	0.015
Manganese	4.4×10^{-11}	4.4×10^{-11}	707	0.077	0.44	0	4.4×10^{-11}	1.6×10^{-13}	NA
Mercury	NA	0	0	0	0	0.01	0.01	3.6×10^{-5}	0.002
Molybdenum	218	0	0	2.07	71	0	71	2.5×10^{-1}	NA
Nickel	1.0×10^{-6}	0	0	8.4	1,310	0	1.0×10^{-6}	3.5×10^{-9}	NA
Selenium	NA	0	0	0	0	0.014	0.014	4.9×10^{-5}	0.05
Uranium	0.0023	0	0	0	16,500	0	0.0023	8.2×10^{-6}	NA
Vanadium	4.8	0	0	0.054	0	0	0.054	1.9×10^{-4}	NA
Zinc	63	0	0	0	0.73	0	0.73	2.6×10^{-3}	NA

a. To convert grams per cubic meter to pounds per cubic foot, multiply by 0.00000624.
b. Note that these concentrations are not used for transport modeling (as discussed in Section I.6), but only for screening analysis purposes. Refer to Section I.6 for groundwater concentrations of chemically toxic materials that were selected for further consideration based on the screening analysis.
c. Maximum contaminant levels are specified in 40 CFR 141.2.
d. NA = not available (no Maximum Contaminant Level established by the U.S. Environmental Protection Agency for this element).

For the chemicals in the nonpackaged materials, the degradation was assumed to be limited by the solubility of the chemical in water. The release concentration (in grams per cubic meter) was assumed to be equal to the elemental solubility for those chemicals with a nonzero inventory in the nonpackaged materials. For the remaining material categories, all part of the waste packages, the release concentration was calculated based on the per-package inventory and the release rate from a waste package.

The per-package inventory (in grams for each material category) was calculated by dividing the total inventory (in grams) of the material type by the total number of waste packages in the repository (assumed to be 11,969). The release of material per cubic meter would be the fractional release rate divided by the rate of water flow past a waste package, based on an average 20-millimeter (0.79-inch) annual water flow rate through the repository. The release concentration is the per-package inventory in grams multiplied by the release per cubic meter.

To estimate the concentration in a well, two steps were performed. First, the maximum release concentration from the four material groups was selected. Then, two dilution factors were applied to the maximum release concentration. An unsaturated zone dilution factor was calculated as the ratio of the total cross-sectional area of all waste packages to the total surface area of the repository. Each of the 11,969 waste packages would have a cross-sectional area of 8.9 square meters (96 square feet), and the assumed repository surface area would be about 3 square kilometers (740 acres). This calculation resulted in an unsaturated zone dilution factor of 0.035. A dilution factor of 10 was applied to the saturated zone so the dilution factor, when combined for the unsaturated and saturated zones, would be 0.0035.

I.3.2.3.3 *Health Effects Screening for Chemically Toxic Materials*

The potential for human health impacts was estimated using a hazard index. The hazard index was determined by dividing the intake of a chemical by the *oral reference dose* for that chemical. A hazard index of 1.0 or above indicated the potential for human health impacts. Table I-14 lists the human health hazard indices.

ORAL REFERENCE DOSE

The *oral reference dose* is based on the assumption that thresholds exist for certain toxic effects such as cellular necrosis. This dose is expressed in units of milligrams per kilogram per day. In general, the oral reference dose is an estimate (with uncertainty spanning perhaps an order of magnitude) of a daily exposure to the human population (including sensitive subgroups) that is likely to be without an appreciable risk of deleterious effects during a lifetime (EPA 1999, all).

Table I-14. Human health hazard indices for chemically toxic materials.

Element	Intake (milligram per kilogram per day)	Oral reference dose[a] (milligram per kilogram per day)	Hazard index
Boron	0.0053	0.09	0.059
Cadmium	0.00022	0.0005	0.44
Chromium	0.030	0.005	6.1
Manganese	4.5×10^{-15}	0.14	3.2×10^{-14}
Molybdenum	0.0072	0.005	1.4
Nickel	1.0×10^{-10}	0.02	5.1×10^{-9}
Uranium	0.00000023	0.003	0.000078
Vanadium	0.0000054	0.007	0.00078
Zinc	0.000074	0.3	0.00025

a. Source: EPA (1999, all).

Intake was based on a 2-liter (0.53-gallon) daily consumption rate of drinking water, at the concentrations in the well, by a 70-kilogram (154-pound) adult. The oral reference doses were from the Integrated Risk Information System (EPA 1999, all), with the exception of doses for uranium (EPA 1994, all) and vanadium (International Consultants 1997, all).

Of the proposed chemically toxic materials in the repository, only chromium and molybdenum have a hazard index above 1.0. Because the inventories of a given material category in the repository should no more than double under any of the inventory modules, all chemically toxic materials (except chromium and molybdenum) can be eliminated from detailed analyses. However, the analysis also considered uranium in recognition of the special attention this element attracts and as a check for the screening analyses.

I.3.2.4 Chromium Inventory for Use in the Performance Assessment Model

The Alloy-22 that would comprise the inner corrosion-resistant material layer of the waste packages for the Yucca Mountain Repository design would contain 21.25 percent chromium and 55 percent nickel. In addition, stainless-steel containers and fuel cladding would contribute a meaningful but much smaller quantity of chromium. Table I-15 lists the chromium that would be present in the waste packages under the Proposed Action. Tables I-16 and I-17 list the chromium that would be present in the waste packages under Inventory Modules 1 and 2, respectively.

The performance assessment model simulates a number of abstracted waste packages for each waste category with a generalized inventory. Tables I-18 and I-19 summarize the assignment of the chromium inventory under the Proposed Action derived from the actual inventory listed in Table I-15 to the number of abstracted waste packages simulated with the model. The inventory is separated between interior stainless steel (Table I-18) and waste package Alloy-22 (Table I-19) because these two portions of the chromium inventory are modeled separately in a two-step process (see Section I.6 for details). Similarly, Tables I-20 and I-21 summarize the assignment of the chromium inventory derived from the actual inventory under Inventory Module 1, listed in Table I-16, to the number of abstracted waste packages

Table I-15. Chromium content (kilograms) of waste packages for the Proposed Action.[a]

Waste category	Waste package type[c]	Quantity actual waste packages[d]	Alloy-22 per waste package		SS/B[b] alloy per waste package		Chromium mass per waste package type
			Alloy mass	Chromium mass[e]	Alloy mass	Chromium mass[f]	
Commercial spent nuclear fuel	21 PWR UCF (no absorber)	1,369	4,458	947	0	0	1,296,888
	21 PWR UCF (absorber plates)	2,641	4,458	947	1,883	546	3,944,056
	21 PWR UCF (control rods)	169	4,458	947	0	0	160,098
	12 PWR UCF (high heat)	394	3,282	697	0	0	274,785
	12 PWR UCF (South Texas)	179	3,717	790	1,071	311	196,981
	44 BWR UCF (no absorber)	773	4,261	905	0	0	699,923
	44 BWR UCF (absorber plates)	2,024	4,261	905	3,999	1,160	4,179,909
	24 BWR UCF (thick absorber)	93	3,342	710	2,141	621	123,789
High-level radioactive waste	5 HLW co-disposal	1,270	4,066	864	0	0	1,097,312
	5 HLW long co-disposal	1,007	5,687	1,208	0	0	1,216,947
DOE spent nuclear fuel	Navy SNF long	300[g]	6,306	1,340	0	0	381,907
Totals		**10,204**					**13,572,595**

a. To convert kilograms to pounds, multiply by 2.2046.
b. SS/B = stainless-steel boron.
c. Abbreviations: PWR = pressurized-water reactor; UCF = uncanistered fuel; BWR = boiling-water reactor; HLW = defense high-level radioactive waste; SNF = spent nuclear fuel.
d. Source: TRW (1999b, pages 6-5 to 6-12); quantities of waste packages modeled for results reported in Section I.6 differ slightly (because of the use of earlier estimates), resulting in a total chromium inventory about 1 percent less than indicated in this table. Final chromium impacts were not expected to differ because the inventory would not be exhausted during the period simulated.
e. Chromium constitutes 21.25 percent of Alloy-22.
f. Chromium constitutes 29 percent of SS/B alloy.
g. The analysis used 285 Navy SNF long waste packages in models for results discussed in Section I.6. The difference resulted in a chromium inventory that was about an additional 0.02 percent less than indicated in this table.

Table I-16. Chromium content (kilograms) of waste packages for Inventory Module 1.[a]

Waste category	Waste package type[c]	Quantity actual waste packages[d]	Alloy-22 per waste package		SS/B[b] alloy per waste package		Chromium mass per waste package type
			Alloy mass	Chromium mass[e]	Alloy mass	Chromium mass[f]	
Commercial spent nuclear fuel	21 PWR UCF (no absorber)	2,339	4,458	947	0	0	2,215,793
	21 PWR UCF (absorber plates)	4,228	4,458	947	1,883	546	6,314,074
	21 PWR UCF (control rods)	314	4,458	947	0	0	297,460
	12 PWR UCF (high heat)	646	3,282	697	0	0	450,537
	12 PWR UCF (South Texas)	428	3,717	790	1,071	311	470,994
	44 BWR UCF (no absorber)	1,242	4,261	905	0	0	1,124,584
	44 BWR UCF (absorber plates)	3,195	4,261	905	3,999	1,160	6,598,226
	24 BWR UCF (thick absorber)	186	3,342	710	2,141	621	247,578
High-level radioactive waste	5 HLW co-disposal	1,557	4,066	864	0	0	1,345,287
	5 HLW long co-disposal	3,000	5,687	1,208	0	0	3,625,463
DOE spent nuclear fuel	Navy SNF Long	300	6,306	1,340	0	0	402,008
Totals		**17,435**					**23,092,003**

a. To convert kilograms to pounds, multiply by 2.2046.
b. SS/B = stainless-steel boron.
c. Abbreviations: PWR = pressurized-water reactor; UCF = uncanistered fuel; BWR = boiling-water reactor; HLW = defense high-level radioactive waste; SNF = spent nuclear fuel.
d. Source: TRW (1999b, pages 6-5 to 6-12); quantities of waste packages modeled for results reported in Section I.6 differ slightly (because of the use of earlier estimates), resulting in a total chromium inventory about 1 percent less than indicated in this table. Final chromium impacts were not expected to differ because the inventory would not be exhausted during the period simulated.
e. Chromium constitutes 21.25 percent of Alloy-22.
f. Chromium constitutes 29 percent of SS/B alloy.

Table I-17. Chromium content (kilograms) of waste packages for Inventory Module 2.[a]

Waste category	Waste package type[c]	Quantity actual waste packages[d]	Alloy-22 per waste package		SS/B[b] alloy per waste package		Chromium mass per waste package type
			Alloy mass	Chromium mass[e]	Alloy mass	Chromium mass[f]	
Commercial spent nuclear fuel	21 PWR UCF (no absorber)	2,339	4,458	947	0	0	2,215,793
	21 PWR UCF (absorber plates)	4,228	4,458	947	1,883	546	6,314,074
	21 PWR UCF (control rods)	314	4,458	947	0	0	297,460
	12 PWR UCF (high heat)	646	3,282	697	0	0	450,537
	12 PWR UCF (South Texas)	428	3,717	790	1,071	311	470,994
	44 BWR UCF (no absorber)	1,242	4,261	905	0	0	1,124,584
	44 BWR UCF (absorber plates)	3,195	4,261	905	3,999	1,160	6,598,226
	24 BWR UCF (thick absorber)	186	3,342	710	2,141	621	247,578
High-level radioactive waste	5 HLW co-disposal	1,557	4,066	864	0	0	1,345,287
	5 HLW long co-disposal	3,000	5,687	1,208	0	0	3,625,463
DOE spent nuclear fuel	Navy SNF long	300	6,306	1,340	0	0	402,008
GTCC and SPAR[g]	5 HLW long co-disposal	608	5,687	1,208	0	0	734,760
Totals		**18,043**					**23,826,763**

a. To convert kilograms to pounds, multiply by 2.2046.
b. SS/B = stainless-steel boron.
c. Abbreviations: PWR = pressurized-water reactor; UCF = uncanistered fuel; BWR = boiling-water reactor; HLW = defense high-level radioactive waste; SNF = spent nuclear fuel.
d. Source: TRW (1999b, pages 6-5 to 6-12); quantities of waste packages modeled for results reported in Section I.6 differ slightly (because of the use of earlier estimates), resulting in a total chromium inventory about 1 percent less than indicated in this table. Final chromium impacts were not expected to differ because the inventory would not be exhausted during the period simulated.
e. Chromium constitutes 21.25 percent of Alloy-22.
f. Chromium constitutes 29 percent of SS/B alloy.
g. GTCC = Greater-Than-Class-C waste; SPAR = Special-Performance-Assessment-Required waste.

Table I-18. Modeled waste package interior chromium inventory for Proposed Action (kilograms).[a]

Waste category	Waste package type[b]	Mass per waste package type[c]	Mass per waste category	Number of abstracted waste packages	Mass per abstracted waste package
Commercial spent nuclear fuel	21 PWR UCF (no absorber)	0	3,902,762	7,760	503
	21 PWR UCF (absorber plates)	1,442,171			
	21 PWR UCF (control rods)	0			
	12 PWR UCF (high heat)	0			
	12 PWR UCF (South Texas)	55,596			
	44 BWR UCF (no absorber)	0			
	44 BWR UCF (absorber plates)	2,347,253			
	24 BWR UCF (thick absorber)	57,743			
High-level radioactive waste	5 HLW co-disposal	0	0	1,663	0
	5 HLW long co-disposal	0			
DOE spent nuclear fuel	Navy SNF long	0	0	2,546	0
Totals		**3,902,762**	**3,902,762**	**11,969**	

a. To convert kilograms to pounds, multiply by 2.2046.
b. Abbreviations: PWR = pressurized-water reactor; UCF = uncanistered fuel; BWR = boiling-water reactor; HLW = defense high-level radioactive waste; SNF = spent nuclear fuel.
c. Source: Table I-15.

Table I-19. Modeled corrosion-resistant material (Alloy-22) chromium inventory (kilograms) for Proposed Action.[a]

Waste category	Waste package type[b]	Mass per waste package type[c]	Mass per waste category	Number of abstracted waste packages	Mass per abstracted waste package
Commercial spent nuclear fuel	21 PWR UCF (no absorber)	1,296,888	6,973,667	7,760	899
	21 PWR UCF (absorber plates)	2,501,885			
	21 PWR UCF (control rods)	160,098			
	12 PWR UCF (high heat)	274,785			
	12 PWR UCF (South Texas)	141,385			
	44 BWR UCF (no absorber)	699,923			
	44 BWR UCF (absorber plates)	1,832,656			
	24 BWR UCF (thick absorber)	66,046			
High-level radioactive waste	5 HLW co-disposal	1,097,312	2,314,259	1,663	1,392
	5 HLW long co-disposal	1,216,947			
DOE spent nuclear fuel	Navy SNF long	381,907	381,907	2,546	150
Totals		**9,669,833**	**9,669,833**	**11,969**	

a. To convert kilograms to pounds, multiply by 2.2046.
b. Abbreviations: PWR = pressurized-water reactor; UCF = uncanistered fuel; BWR = boiling-water reactor; HLW = defense high-level radioactive waste; SNF = spent nuclear fuel.
c. Source: Table I-15.

Table I-20. Modeled waste package interior chromium inventory (kilograms) for Inventory Module 1.[a]

Waste category	Waste package type[b]	Mass per waste package type[c]	Mass per waste category	Number of abstracted waste packages	Mass per abstracted waste package
Commercial spent nuclear fuel	21 PWR UCF (no absorber)	0	6,262,475	12,932	484
	21 PWR UCF (absorber plates)	2,308,784			
	21 PWR UCF (control rods)	0			
	12 PWR UCF (high heat)	0			
	12 PWR UCF (South Texas)	132,933			
	44 BWR UCF (no absorber)	0			
	44 BWR UCF (absorber plates)	3,705,273			
	24 BWR UCF (thick absorber)	115,486			
High-level radioactive waste	5 HLW co-disposal	0	0	4,456	0
	5 HLW long co-disposal	0			
DOE spent nuclear fuel	Navy SNF long	0	0	4,340	0
Totals		**6,262,475**	**6,262,475**	**21,728**	

a. To convert kilograms to pounds, multiply by 2.2046.
b. Abbreviations: PWR = pressurized-water reactor; UCF = uncanistered fuel; BWR = boiling-water reactor; HLW = defense high-level radioactive waste; SNF = spent nuclear fuel.
c. Source: Table I-16.

simulated with the performance assessment model for interior stainless steel and corrosion-resistant material, respectively.

Inventory Module 2 is simulated as an incremental impact over Inventory Module 1, where the difference is in the Greater-Than-Class-C and Special-Performance-Assessment-Required wastes added under Inventory Module 2. Table I-22 summarizes the assignment of the additional chromium inventory derived from the actual inventory for Inventory Module 2 to the number of abstracted waste packages simulated with the performance assessment model. No interior stainless steel would be included in the additional waste packages under Inventory Module 2.

Table I-21. Modeled corrosion-resistant material (Alloy-22) chromium inventory (kilograms) for Inventory Module 1.[a]

Waste category	Waste package type[b]	Mass per waste package type[c]	Mass per waste category	Number of abstracted waste packages	Mass per abstracted waste package
Commercial spent nuclear fuel	21 PWR UCF (no absorber)	2,215,793	11,456,771	12,932	886
	21 PWR UCF (absorber plates)	4,005,290			
	21 PWR UCF (control rods)	297,460			
	12 PWR UCF (high heat)	450,537			
	12 PWR UCF (South Texas)	338,061			
	44 BWR UCF (no absorber)	1,124,584			
	44 BWR UCF (absorber plates)	2,892,953			
	24 BWR UCF (thick absorber)	132,093			
High-level radioactive waste	5 HLW co-disposal	1,345,287	4,970,749	4,456	1,116
	5 HLW long co-disposal	3,625,463			
DOE spent nuclear fuel	Navy SNF long	402,008	402,008	4,340	93
Totals		**16,829,528**	**16,829,528**	**21,728**	

a. To convert kilograms to pounds, multiply by 2.2046.
b. Abbreviations: PWR = pressurized-water reactor; UCF = uncanistered fuel; BWR = boiling-water reactor; HLW = high-level radioactive waste; SNF = spent nuclear fuel.
c. Source: Table I-17.

Table I-22. Additional corrosion-resistant material (Alloy-22) chromium inventory for Inventory Module 2 in excess of inventory for Module 1 (kilograms).[a]

Waste category	Waste package type[b]	Mass per waste package type[c]	Mass per waste category	Number of abstracted waste packages	Mass per abstracted waste package
GTCC+SPAR[d]	5 HLW long co-disposal	734,760	734,760	1,642	447

a. To convert kilograms to pounds, multiply by 2.2046.
b. Abbreviations: HLW = high-level radioactive waste.
c. Source: Table I-17.
d. GTCC = Greater-Than-Class-C waste; SPAR = Special-Performance-Assessment-Required waste.

I.3.2.5 Elemental Uranium Inventory for Use in the Performance Assessment Model

Table I-23 lists the total inventory of elemental uranium (that is, all isotopes of uranium) for consideration as a chemically toxic material for the Proposed Action and Inventory Modules 1 and 2. The total uranium inventory for both Inventory Modules 1 and 2 would be about 70 percent greater than that for the Proposed Action. The uranium content in high-level radioactive waste was set to the equivalent of metric tons of heavy metal (MTHM) for this analysis, though much of the uranium would have been removed during reprocessing operations. The elemental uranium inventory for Modules 1 and 2 would be essentially equivalent because Greater-Than-Class-C and Special-Performance-Assessment-Required wastes (the only additional waste in Module 2 over Module 1) do not contain substantial quantities of uranium.

I.3.2.6 Molybdenum Inventory

The Alloy-22 used for the corrosion-resistant material contains 13.5 percent molybdenum. During the corrosion of the Alloy-22, molybdenum behaves almost the same as chromium. Due to the corrosion conditions, molybdenum also dissolves in a highly soluble hexavalent form. Therefore, the source term for molybdenum will be exactly 13.5/21.25 times the source term for chromium (or 64 percent) from Alloy-22 only.

Table I-23. Total elemental uranium inventory (kilograms)[a] for Proposed Action and Inventory Modules 1 and 2.[b,c,d]

Inventory	Commercial SNF[e]	HLW[f]	DOE SNF	Totals
Proposed Action	63,000,000	4,700,000	2,300,000	70,000,000
Modules 1 and 2[g]	105,000,000	13,000,000	2,500,000	120,000,000

a. To convert kilograms to pounds, multiply by 2.2046.
b. The uranium content in high-level radioactive waste was set to the MTHM equivalent for this analysis, even though much of the uranium would have been removed during reprocessing operations.
c. Rounded to two significant figures.
d. Source: Appendix A, Tables A-12, A-13, A-19, A-29 to A-34.
e. SNF = spent nuclear fuel.
f. HLW = high-level radioactive waste.
g. Inventory Module 1 and 2 will have the same total uranium inventory because Greater-Than-Class-C and Special-Performance-Assessment-Required waste (the only additional waste in Module 2 over Module 1) does not contain a substantial quantity of uranium.

I.3.3 ATMOSPHERIC RADIOACTIVE MATERIALS

The only radionuclide that would have a relatively large inventory and a potential for gas transport would be carbon-14. Iodine-129 can exist in a gas phase, but it is highly soluble and therefore likely to dissolve in groundwater rather than migrate as a gas. After carbon-14 escaped from the waste package, it could flow through the rock in the form of carbon dioxide. About 2 percent of the carbon-14 in commercial spent nuclear fuel occurs in a gas phase in the space (or *gap*) between the fuel and the cladding around the fuel (Oversby 1987, page 92). The gas-phase inventory consists of 0.23 curie of carbon-14 per commercial spent nuclear fuel waste package. Table I-24 lists the total carbon-14 inventory for the repository under the Proposed Action and Inventory Modules 1 and 2.

Table I-24. Total carbon-14 inventory (curies).[a]

Inventory	Solid[b]	Gaseous[c]	Totals[d]
Proposed Action	92,000	1,800	93,000
Module 1	150,000	3,200	160,000
Module 2	240,000	3,200	240,000

a. Source: Appendix A, Table A-10.
b. Impacts of carbon-14 in solid form are addressed as waterborne radioactive material impacts.
c. Based on 0.234 curie of carbon-14 per commercial spent nuclear fuel waste package.
d. Totals are rounded to two significant figures.

I.4 Extension of Total System Performance Assessment Methods and Models for EIS Analyses

DOE conducted analyses for the Total System Performance Assessment – Viability Assessment to evaluate potential long-term impacts to human health from the release of radioactive materials from the Yucca Mountain Repository. The analyses for this EIS were conducted in conjunction with, but distinct from, the calculations for the Viability Assessment (DOE 1998a, Volume 3, all). The methodologies and assumptions for the Viability Assessment are detailed in TRW (1998a,b,c,d,e,f,g,h,i,j,k, all). Extensions of the Viability Assessment analyses to meet distinct EIS requirements (for example, consideration of different thermal load scenarios or inventories) were made using the same overall methodology, and details of these extensions are provided in this section. Additional information on EIS performance-assessment analyses can be found in TRW (1999a, all).

I.4.1 REPOSITORY DESIGN FOR ALTERNATIVE THERMAL LOADS

The spatial density at which the waste packages are emplaced in the repository is generally quantified using *thermal load*, which is the MTHM emplaced per acre of repository area. The higher the thermal load, the smaller the spacing between waste packages, resulting in a higher thermal output per unit area.

The area required for emplacement is based on the target thermal loads attained by varying the spacing between the waste packages and the distance between the emplacement drifts. The commercial spent nuclear fuel heat output dominates the overall heat load and thus the total emplacement area required. Thus, for purposes of thermal modeling, the Proposed Action inventory implies the nominal value of 63,000 MTHM commercial spent nuclear fuel, whereas Inventory Modules 1 and 2 have the same expanded inventory of 105,000 MTHM commercial spent nuclear fuel.

Table I-25 gives the estimates of repository area required for the emplacement of wastes, ranging from a low of 740 acres for the high thermal load scenario with the Proposed Action inventory case to a high of 4,200 acres for the low thermal load scenario with the Inventory Module 1 or 2 case. Most of the options require waste emplacement in areas beyond the primary, or *upper*, emplacement block, which is juxtaposed between the Solitario Canyon Fault and the Ghost Dance Fault. The upper emplacement block is the reference repository region in the Viability Assessment base case facility design (63,000 MTHM high thermal load scenario). Selection of potential expansion blocks near the upper block was carried out using several criteria:

- Availability of 200 meters (660 feet) of overburden
- Consistency of elevation and dip with the upper block
- Distance from the saturated zone
- Favorable excavation characteristics

These considerations are described in detail in TRW (1999b, all).

Table I-25. Estimates of repository emplacement area.[a]

Thermal load (MTHM per acre)	Drift spacing (meters)[c]	Area (acres)[b]	
		Proposed Action	Inventory Modules 1 and 2
85	28	740	1,240
60	40	1,050	1,750
25	38[d]	2,520	4,200

a. Source: TRW (1999a, Table 2.3-1, page 2-12) based on 63,000 MTHM of commercial spent nuclear fuel.
b. To convert acres to square miles, divide by 640.
c. To convert meters to feet, multiply by 0.3048.
d. Under the low thermal load, the waste packages would be placed in an approximately square pattern so that the thermal load was distributed evenly. To accomplish this, the emplacement drift spacing and the spacing of the waste packages in the emplacement drift would be approximately equal (TRW 1999c, page F-2).

The selected inventory layouts for the Proposed Action and Inventory Modules 1 and 2 for the high, intermediate, and low thermal load scenarios are shown in Figures I-2 through I-7. These layouts, simplified from the original engineering layouts presented in TRW (1999c, Figures 3.3-1 through 3.3-6), indicate that the wastes for these thermal loads can be accommodated within the upper blocks, the lower block, and one additional region (Block 1a) to the west of the Solitario Canyon Fault.

As described in TRW (1999c, all), additional subsurface blocks for emplacement of waste according to intermediate and low thermal load scenarios were identified by:

- Expanding the upper block to the north and south
- Expanding the lower block to the north and east
- Lowering the elevation of Block 1a, combining it with Block 1b, and designating the combined area as Block 5
- Raising the elevation of Block 2 by 15 meters (50 feet) and designating it as Block 6
- Raising the elevation of Block 3 by 12 meters (39 feet) and designating it as Block 7
- Raising the elevation of Block 4 by 2 meters (6.6 feet), extending the area to the south, and designating it as Block 8

The corresponding layouts for the low thermal load scenario for the Proposed Action and for Inventory Modules 1 and 2 are shown in Figures I-6 and I-7, respectively. Figure I-8 shows the relationship between the early Proposed Action designs and the design areas considered in these EIS analyses.

I.4.2 THERMAL HYDROLOGY MODEL

Evaluation of the intermediate (60 MTHM per acre) and low (25 MTHM per acre) thermal load scenarios for this EIS diverged from the high thermal load base case evaluated in the Viability Assessment. Extensions of the thermal-hydrologic modeling supporting the total systems performance assessment model were required to evaluate these additional thermal load scenarios. These extensions are detailed in this section.

I.4.2.1 Thermal-Hydrologic Scenarios

The analysis of waste package degradation and engineered barrier system release for the EIS requires information regarding waste package temperature and relative humidity, and liquid saturation and temperature within the repository invert. These data were derived from the development and application of a suite of three-dimensional, drift-scale models for predicting the thermal-hydrologic environment near the waste packages. Six sets of calculations were carried out to handle the two inventory options (63,000 and 105,000 MTHM) and the three thermal load scenarios (85, 60, and 25 MTHM per acre). The simulations were performed using NUFT, an integrated finite-difference code capable of modeling multidimensional fluid flow, solute migration, and heat transfer in porous and/or fractured media (Nitao 1998, all).

These calculations closely parallel the thermal-hydrologic modeling study performed in support of Total System Performance Assessment – Viability Assessment (TRW 1998c, all). The main difference between the two studies is in the treatment of thermal-hydrologic conditions at the edge of the repository. In Total System Performance Assessment – Viability Assessment, a hybrid methodology with complementary thermal-hydrologic and thermal conduction models is used to delineate different thermal-hydrologic zones within the repository horizon (TRW 1998c, all). In this study, a less detailed scaling methodology is used to divide the repository into center and edge regions because of the computational complexities associated with larger inventories and expanded emplacement regions. This less detailed scaling methodology is not expected to adversely impact the results.

I.4.2.2 Waste Package and Drift Geometry

Following the approach taken in Total System Performance Assessment – Viability Assessment, the basic three-dimensional drift-scale model was developed around a discrete waste package symmetry element. This model extends:

- In the x-direction, from the drift centerline to the midpoint between adjacent drifts
- In the y-direction, over a representative number of packages to capture the package-to-package variability in heat output
- In the z-direction, from the ground surface to the water table

The vertical discretization between the ground surface and the water table was chosen to be consistent with the Lawrence Berkeley National Laboratory three-dimensional, site-scale unsaturated flow model (Bodvarsson, Bandurraga, and Wu 1997, all). The basis for the model discretization in the other two dimensions is described in the following paragraphs.

The Proposed Action inventory consists of 63,000 MTHM of commercial spent nuclear fuel, 4,667 MTHM of high-level radioactive waste, and 2,333 MTHM of DOE spent nuclear fuel. As described in DOE (1998a, Volume 3, Figure 3-18, page 3-31), the corresponding symmetry element contains seven packages:

- Three 21-pressurized-water-reactor waste packages
- Two 44-boiling-water-reactor waste packages
- One-half of a 12-pressurized-water-reactor waste package
- One-half of a direct-disposal waste package (containing four DOE spent nuclear fuel N-reactor canisters)
- One co-disposal waste package (containing five high-level radioactive waste glass-filled canisters with or without a DOE spent nuclear fuel canister)

Inventory Module 1 consists of 105,000 MTHM of commercial spent nuclear fuel, 12,600 MTHM of high-level radioactive waste (based on MTHM equivalency discussion in Section A.2.3.1 of Appendix A of this EIS), and 2,500 MTHM of DOE spent nuclear fuel. Accordingly, the expanded inventory symmetry element was created using a total of nine packages:

- Three and one-half 21-pressurized-water-reactor waste packages
- Two and one-half 44-boiling-water-reactor waste packages
- One 12-pressurized-water-reactor waste package
- Two co-disposal waste packages containing five high-level radioactive waste glass-filled canisters (with or without a DOE spent nuclear fuel canister)

Note that this symmetry element model maintains the relative percentage (and heat output) of different package types while minimizing the total number of discrete packages for computational convenience. This package discretization model was deemed adequate from the standpoint of thermal-hydrologic modeling, although it is only an approximation of the true inventory.

For the high (85 MTHM per acre) and intermediate (60 MTHM per acre) thermal load scenarios, the waste package arrangement within the drifts was kept constant, and the drift spacing was adjusted to attain the correct thermal load levels. Thus, the high thermal load scenario yields drift spacing of 28 meters (about 92 feet) and the intermediate thermal load scenario yields drift spacing of 40 meters (about 130 feet). For the low (25 MTHM per acre) thermal load scenario, maintaining the same waste package arrangement as for the high and intermediate thermal load scenarios would have required the drifts to be spaced too far apart in the x-direction, resulting in localized heating effects. Therefore, the package-to-package spacing in the y-direction was increased for the low thermal load scenario to create an approximately square symmetry element, including drift spacing of 38 meters (about 120 feet). Waste package spacing for the Proposed Action and for Inventory Modules 1 and 2 is summarized in Table I-26 and Table I-27, respectively.

Table I-26. Waste package spacing for the Proposed Action inventory.[a]

		Spacing of gap after given package (meters)[b]	
Waste package type	Waste package width (meters)	High and intermediate thermal load	Low thermal load
12-PWR	½ (5.87)	6.021	26.424
21-PWR	5.3	9.276	31.215
21-PWR	5.3	2.949	15.415
Co-disposal	5.37	2.2535	13.676
21-PWR	5.3	8.929	30.345
44-PWR	5.3	7.98	27.969
44-BWR	5.3	1.305	11.2996
Direct-disposal	½ (5.37)		

a. Source: TRW (1999a, Table 3.2-1, page 3-3).
b. To convert meters to feet, multiply by 0.3048.

Table I-27. Waste package spacing for Inventory Modules 1 and 2.[a]

		Spacing of gap after given package (meters)[b]	
Waste package type	Waste package width (meters)	High and intermediate thermal load	Low thermal load
21-PWR	½ (5.3)	2.949	11.3055
Co-disposal	5.37	2.2535	17.79
21-PWR	5.3	9.95	32.902
21-PWR	5.3	10.02	33.081
21-PWR	5.3	7.39	26.9175
12-PWR	5.87	6.368	24.3615
44-PWR	5.3	7.98	27.969
44-BWR	5.3	1.305	12.599
Direct-disposal	5.37	1.305	10.0
44-BWR	½ (5.3)		

a. Source: TRW (1999a, Table 3.2-2, page 3-4).
b. To convert meters to feet, multiply by 0.3048.

I.4.2.3 Selection of Submodels

Engineering layouts developed for waste emplacement were shown in Figures I-2 through I-7. These layouts suggest that multiple, discontinuous heated regions will develop in the postclosure period for some of the options. A full three-dimensional representation of all heated regions (such as emplacement areas) was not considered computationally practical. Therefore, for modeling purposes each region was treated as an isolated entity by assuming that boundaries existed for no heat flow and no fluid flow between the regions. Furthermore, to capture the effects of varying stratigraphy and variable surface

infiltration on the thermal-hydrology response at the repository, each emplacement block was modeled by a representative stratigraphic column or submodel. These submodel solution assumptions are unlikely to affect adversely the results reported in this EIS.

Based on the original design layouts (see Figure I-2), each thermal load scenario was to be modeled using some combination of each of the following seven stratigraphic columns:

- Upper Block (stratigraphic column 1)
- Lower Block (stratigraphic column 2)
- Block 1a (stratigraphic column 3)
- Block 1b (stratigraphic column 7)
- Block 2 (stratigraphic column 5)
- Block 3 (stratigraphic column 6)
- Block 4 (stratigraphic column 4)

These submodels were used for the high and intermediate thermal load scenarios. However, because of the large areal extent required for the low thermal load scenario, the engineering layout changed for those two design options. In the new design layout, Block 1b has been combined with part of Block 1a to form Block 5, while part of Block 1a has been combined with Block 4 to form Block 8. These two new areas can be represented by two existing submodels: stratigraphic column 7 for Block 5 and stratigraphic column 4 for Block 8. This information is summarized in Table I-28 and shown on Figure I-8.

Table I-28. Areas of submodels (stratigraphic columns) used in thermal-hydrologic calculations.[a]

Thermal-hydrologic scenario	Loading (MTHM per acre)	Waste package inventory module	Emplacement block	Stratigraphic column number	Actual area (acres)	Percent of area
1	85	Proposed Action	Upper Block	1	740	100.0
2	60	Proposed Action	Upper Block	1	1,050	100.0
3	25	Proposed Action	Upper Block	1	1,110	44.0
			Lower Block	2	596	23.7
			Block 5	7	814	32.3
4	85	Inventory	Upper Block	1	1,180	95.5
		Modules 1 and 2	Lower Block	2	55	4.5
5	60	Inventory	Upper Block	1	1,180	67.4
		Modules 1 and 2	Lower Block	2	380	21.7
			Block 1a	3	190	10.9
6	25	Inventory	Upper Block	1	1,110	26.4
		Modules 1 and 2	Lower Block	2	596	14.2
			Block 5	7	814	19.4
			Block 6	5	420	10.0
			Block 7	6	440	10.5
			Block 8	4	820	19.5

a. Source: TRW (1999a, Table 3.2-3, page 3-5).

For all submodels, the vertical stratigraphic data for the model stratigraphic columns were extracted from the Lawrence Berkeley National Laboratory site-scale model (Bodvarsson, Bandurraga, and Wu 1997, all), with the exception of Block 2 and Block 3, which lie outside the boundaries of the site-scale model. The geologic framework model (TRW 1997d, all) was used to develop the stratigraphy for the columns corresponding to Block 2 and Block 3 even though very little information is available regarding the stratigraphy, hydrology, and infiltration conditions in this sector of the Yucca Mountain site. Thermal-hydrologic simulations were carried out with these two submodels for the low thermal load with expanded inventory scenario, but the simulations were not used for the subsequent total-system calculations. It was assumed that the thermal-hydrologic results for these regions could be approximated by the neighboring regions within the Berkeley model domain. Thus, the submodel for Block 8

(stratigraphic column 4) was assumed also to represent Block 3, and the submodel for Block 5 (stratigraphic column 7) was assumed also to represent Block 2.

I.4.2.4 Hydrology and Climate Regime

Hydrologic properties for the thermal-hydrologic models were taken to be the same as the Total System Performance Assessment – Viability Assessment base case (TRW 1998c, Section 3.5). These properties include matrix and fracture characteristics describing capillary retention and relative permeability for a dual-permeability model, including fracture-matrix-interaction area-reduction factor terms that were adjusted to match observed borehole saturations. As described in RamaRao, Ogintz, and Mishra (1998, pages 116 to 118), the dual-permeability model parameters have been adjusted for the present study using the "satiated saturation" concept in the generalized equivalent continuum model. Using a porosity-weighted average, the dual-permeability model fracture and matrix parameters (porosity and permeability) are combined to create corresponding parameters for the generalized equivalent continuum model, while the satiated saturation concept is used to set the threshold for the initiation of flow in fractures (before the attainment of full matrix saturation). Subsequently, the composite medium capillary characteristics are generated by a porosity-weighted average of the individual media curves. These hydrologic properties, as well as other thermal properties used in the thermal-hydrologic calculations, are discussed in TRW (1998c, Section 3.2.1, pages 3-21 to 3-26).

This EIS performance assessment considered three climate scenarios: *present-day, long-term average* (wetter than the present-day climate), and *superpluvial*, which are added at short-duration, fixed intervals on a periodic basis during the 100,000-year period after waste emplacement. In the performance assessment model, the initial conditions (that is, the present-day climate) are multiplied by 5.45 to obtain the long-term average climate and by 14.30 to obtain the super-pluvial climate (DOE 1998a, Volume 3, Figure 4.2, page 4-4). The climate changes are measured in step-changes for the duration of the climate periods, and the sequence lengths are 10,000 years for the present-day dry climate and the super-pluvial climate, and 90,000 years for the long-term average climate. The sequence of climate changes used for expected-value simulations (which use the mean value of probabilistically defined input variables) is:

- 0 to 5,000 years - present-day (dry) climate
- 5,001 to 95,000 years - long-term average climate
- 95,001 to 105,000 years - present-day (dry) climate
- 105,001 to 195,000 years - long-term average climate
- 195,001 to 205,000 years - present-day (dry) climate
- 205,001 to 285,000 years - long-term average climate
- 285,001 to 295,000 years - super-pluvial climate
- 295,001 to 305,000 years - present-day (dry) climate

This sequence is repeated for the duration of the simulation period.

Expected-value simulations were carried out for the first 1 million years after closure, to include the complete decay of waste heat caused by radioactive decay and a return to ambient conditions. To establish appropriate initial conditions for the thermal-hydrologic simulations, the nominal present-day (dry) climate scenario, as used in the Viability Assessment base case (TRW 1998c, Section 3.5), was used for the ambient hydrologic calculations. A separate set of thermal-hydrologic simulations was then performed for each climate condition, as required. This approach is consistent with that used in the Viability Assessment, in which climate effects on thermal hydrology for the entire period were included by making three sets of calculations (for present-day, long-term average, and superpluvial climates). The influence of climate change on thermal-hydrologic system response was then approximated in the performance assessment model total-system simulator by switching from one set of results to the other at the time of climate change.

For both the present-day and long-term average climate, the infiltration flux at the top of each representative column was extracted from the flux associated with the nearest element in the Lawrence Berkeley National Laboratory site-scale model (Bodvarsson, Bandurraga, and Wu 1997, all). However, there was no infiltration information available for stratigraphic columns 5 and 6, which are located outside the Berkeley model boundary. Therefore, the infiltration fluxes for these columns were assumed to be equal to the fluxes at the nearest element within the Berkeley model boundary. Note that these infiltration rates were assumed to be constant throughout the 1-million-year postemplacement period with climate changes implemented by multiplying the infiltration rate as described above.

I.4.2.5 Treatment of Edge Effects

The drift-scale modeling results, developed using a representative symmetry element with periodic lateral boundary conditions, best represents the conditions at the center of the repository. To account for the edge-cooling effects experienced by exterior drifts located near unheated rock mass, a scaling methodology was developed based on the hypothesis that the repository can be divided into at least two thermal-hydrologic regions for grouping waste packages, a center region and an edge region. The center region was designed so periodic boundary conditions (no-flow thermal and hydrologic boundaries) could be assigned in a lateral direction. The edge region has a more complicated response because of edge-cooling effects. However, it is believed that the thermal-hydrologic response at the edge is similar to that for the center, albeit at a lower thermal load. Thus, the objective of the scaling methodology was two-fold:

1. Devise a strategy for generating the thermal load scale factors so models representative of the center can be used to simulate the edge response.

2. Estimate the fraction of the repository area enclosed within the center or edge regions.

The following sections briefly describe the development and testing of the components of this scaling methodology.

I.4.2.5.1 *Scaling Factors for Edge Effects*

Based on the conceptual model that the edge response is similar to the center response at a lower thermal load, two-dimensional results from an east-west cross-section scale model of the mountain were compared to a set of one-dimensional runs representing the edge at a series of different thermal loads. The objective was to find a scaling factor for the thermal loads which would provide agreement between the two-dimensional and one-dimensional runs with respect to (1) time history of temperature, liquid saturation, and the mass fraction of air at the repository horizon; and (2) vertical profiles of temperature, liquid saturation, and the mass fraction of air at different points in time.

These calculations were carried out for the base case hydrologic properties and infiltration regime described earlier. The selection of the optimal scaling factor was performed by visual examination and restricted to one scaling factor for the early-time period (0 to 1,000 years) and a second scaling factor for the late-time period (1,000 years to 100,000 years).

Figure I-9 shows the comparison between the two-dimensional and one-dimensional model results using scale factors of 0.8 and 0.6. This comparison suggests that a scale factor of 0.8 is more appropriate for the early-time period, and a scale factor of 0.6 is more suitable for the late-time period. Although not shown here, examining vertical profiles of the primary variables at two different points in time (100 years and 10,000 years) yielded similar observations. Note that a single scaling factor can only provide a gross average match of all stated variables; thus, the match between two-dimensional and scaled one-dimensional results is never perfect. Furthermore, categorization of only two scale factors (early-time and late-time periods) is primarily for computational convenience. These simplifications notwithstanding, the

scaling methodology appears to be a reasonable and practical strategy for generating the edge response without resorting to more complex three-dimensional models containing both heated drifts and unheated rock mass.

I.4.2.5.2 *Definition of Thermal-Hydrologic Zones*

The spatial division of the repository into center and edge regions is based on the approximation of the diffusive temperature profile at the repository by a step function. The temperature profile at selected time steps was extracted and fitted with equivalent step functions. The fraction of area enclosed within the temperature discontinuity was then taken as the fraction of repository belonging to the center region. This process is schematically demonstrated for the high thermal load scenario in Figure I-10.

The fractional areas were found to be time-dependent. For the high thermal load scenario, the thermal-hydrologic response is nearly the same for the entire repository as long as the boiling period is active. Thereafter, for all practical purposes, the fraction belonging to the center stabilizes at about 0.66 (this is the recommended fraction to be used at all times for waste package degradation calculations). For the intermediate thermal load scenario, the fractional area belonging to the center region is found to be close to unity at early- and late-time periods, dropping to approximately 0.6 at intermediate times. Therefore, a time-averaged value of 0.8 is recommended as the fractional area belonging to the center for this thermal load. Edge effects are not considered important for the low thermal load scenario, because the use of multiple emplacement blocks will tend to elevate the temperature between adjacent blocks, thus minimizing edge-cooling effects.

I.4.2.6 Results

As mentioned earlier, thermal-hydrologic modeling results in the form of waste package temperature and relative humidity are required for waste package degradation calculations in WAPDEG. In addition, temperature and liquid saturation within the invert supporting the waste packages is required for Engineered Barrier System release calculations in the repository integration program model. Such information is extracted from NUFT output files and archived in tabular form for input to WAPDEG and the repository integration program model. In this section, a brief discussion of the sensitivity of the thermal-hydrologic simulation results to various design options and natural-system uncertainties will be presented.

I.4.2.6.1 *Variability Among the Waste Packages*

Figures I-11 and I-12 show the temperature and relative humidity histories for the various waste package types for the Proposed Action inventory at high and low thermal loads, respectively. For the high thermal load scenario, the highest peak temperature would result from the use of the 21-pressurized-water-reactor design package, whereas the lowest peak temperature would result from the use of the direct disposal package. These peaks differ by approximately 80°C (176°F). The temperature history for the 21-pressurized-water-reactor average waste package falls near the middle of this range. Note, however, the convergence in temperature and relative humidity for all packages as the temperature drops below the nominal boiling point [100°C (212°F)]. The small differences in temperature and relative humidity histories for the waste packages from this time onward would not affect the WAPDEG-predicted package degradation rates in a meaningful manner. Therefore, results from only the 21-pressurized-water-reactor average waste package are provided as representative inputs to WAPDEG.

I.4.2.6.2 *Sensitivity to Thermal Loads*

Figure I-13 shows the temperature and relative humidity histories for the three thermal loads and both Proposed Action and Inventory Modules 1 and 2 scenarios. As expected, the relative peak temperatures correspond to the magnitude of the thermal loads. For each thermal load, the expanded inventory gives a

slightly higher peak temperature result, but the two inventories converge quickly at later times. Calculations for the high and intermediate thermal load scenarios result in similar curves, both in terms of temperature and relative humidity. For the low thermal load scenario, the shape of the curve is much flatter and the temperature drops below 100°C (212°F) much earlier than the other scenarios.

I.4.2.6.3 *Comparison Between Center and Edge Locations*

Figure I-14 shows a comparison between temperature and relative humidity histories calculated for the high thermal load scenario using both center and edge models. The edge model is essentially the center model with a lower heat load. As described in Section I.4.2.5, the heat flux for the center model is scaled by 0.8 prior to 1,000 years and by 0.6 after 1,000 years, to provide the thermal input for the edge model. As expected, the temperature history for the edge model falls below, and the relative-humidity history lies above, the response for the center model.

I.4.3 WASTE PACKAGE DEGRADATION MODEL

Evaluation of Inventory Modules 1 and 2 for this EIS diverged from the Proposed Action, or base case, inventory evaluated in the Viability Assessment. Extensions of the waste package degradation modeling supporting the total systems performance assessment model were required to evaluate the additional inventories. These extensions are detailed in this section.

One component of the EIS and Total System Performance Assessment – Viability Assessment performance assessments pertains to quantifying the degradation of the metallic waste packages. A waste package would be a double-walled disposal container consisting of an outer 10-centimeter (4-inch)-thick layer of carbon steel (the corrosion-allowance material), and an inner 2-centimeter (0.8-inch)-thick layer of chromium-molybdenum Alloy-22 (the corrosion-resistant material) (DOE 1998a, Volume 3, page 3-74). A statistically based waste package degradation numerical code, WAPDEG (TRW 1998l, all), was developed to quantify the ranges in expected degradation of the waste packages. The corrosion rates for the corrosion-allowance materials and corrosion-resistant materials included in the code were abstracted from several sources (TRW 1998e, pages 5-11 to 5-16). The development of WAPDEG indicated that the major environmental factors in waste package degradation were temperature and moisture availability. These data were input into WAPDEG after conducting thermal-hydrologic modeling to establish the temperature and relative humidity histories, as described in Section I.4.2.

I.4.3.1 WAPDEG Development and Application to Total System Performance Assessment – Viability Assessment

The EIS WAPDEG calculations were based on the Total System Performance Assessment – Viability Assessment model configuration of this code (TRW 1998e, page 5-3). The performance assessment analysis conducted for the Total System Performance Assessment – Viability Assessment considered a repository thermal load of 85 MTHM per acre, with the base case waste inventory of 63,000 MTHM commercial spent nuclear fuel and 7,000 MTHM DOE spent nuclear fuel and high-level radioactive waste. Numerical thermal-hydrologic modeling was conducted to generate transient temperature and relative humidity histories within the emplacement drift. These histories were then used as input into the WAPDEG code to determine the time of initiation, type, and rate of waste package corrosion during a 100,000-year simulation. The WAPDEG simulations generated a suite of waste package failure distributions that were incorporated into the Total System Performance Assessment – Viability Assessment model.

Two corrosion modes were implemented by the WAPDEG code for each waste package, general corrosion and localized corrosion. These modes were applicable to both the corrosion-allowance-material outer wall/barrier and the corrosion-resistant-material inner wall/barrier. The conditions under which the

corrosion modes applied in WAPDEG depended primarily on temperature, relative humidity, the geochemistry of the water, and the presence or absence of dripping or pooled water.

The corrosion-allowance material undergoes general corrosion according to one of two models, a humid-air corrosion model and an aqueous corrosion model, depending on the relative humidity at the waste package surface. Both models are based on statistical analysis of corrosion data observed for carbon-steel corrosion (DOE 1998a, Volume 3, pages 3-81 to 3-82). However, neither corrosion model will be applicable if the temperature at the waste package surface is too high. The thermal calculations for the potential repository typically show an initial postclosure increase in repository temperature due to radioactive decay, followed by a cooling period that eventually reaches ambient temperature. Laboratory and modeling studies indicate that general corrosion of the corrosion-allowance material can only start when the temperature cools to a value near the boiling point of water (DOE 1998a, Volume 3, page 3-82). The temperature-dependent corrosion data are input into the model and applied to waste packages based on a user-defined temperature threshold either in the form of a fixed value or a probability distribution that is sampled for each package.

Relative humidity generally increases as the temperature cools and vaporized moisture condenses. If the relative humidity is sufficiently high and the temperature threshold is met, the corrosion-allowance material can undergo humid-air corrosion. An input to the model is the relative humidity threshold sufficient for initiation of humid-air general corrosion either as a fixed value or a probability distribution that is sampled for each package.

The relative humidity may rise sufficiently to cause a thin film of water to form on the waste package surface. At that point, the aqueous corrosion model more appropriately describes general corrosion. The relative humidity threshold is input either as a fixed value or a probability distribution that is sampled for each package. When the relative humidity exceeds the threshold, WAPDEG transitions from the humid-air corrosion model to the aqueous corrosion model.

Neither general corrosion model for corrosion-allowance materials is expected to behave in a uniform manner over the entire waste package surface. WAPDEG includes a provision for nonuniform corrosion in two ways; it discretizes the waste package surface into segments called *patches* with roughness factors applied to each patch. The number of patches per waste package and the roughness factors are input, with the latter either as a fixed value or a probability distribution. WAPDEG obtains a statistical sample of the distribution (if provided) to be used for each patch on the package. The product of the general corrosion depth at a given time and the roughness factor gives the total corroded depth at a particular location on the patch at that time. When the corroded depth at any point on a patch equals or exceeds the thickness of the corrosion-allowance material, WAPDEG assumes that the patch has failed.

When a patch is breached on the corrosion-allowance material, WAPDEG assumes that part of the surface area of the corrosion-resistant material is then subject to corrosion. In fact, there is a one-to-one correspondence of patches for corrosion-allowance material and corrosion-resistant material. Even though only a fraction of the corrosion-allowance material patch may be breached, the crevice between the two materials will likely grow over time to allow water and air to access the entire corrosion-resistant material patch. WAPDEG conservatively assumes that the entire area of this patch is immediately subject to corrosion upon breach of its overlying corrosion-allowance material patch.

The general corrosion of the two materials differs due to the composition of the two waste package wall materials. The general corrosion rate applied by WAPDEG to the corrosion-resistant material was derived from data gained from the Waste Package Degradation Expert Elicitation. A compilation of the elicited results was then used to create a cumulative distribution function for general corrosion rates of corrosion-resistant materials at temperatures of 25°C, 50°C, and 100°C (77°F, 122°F, and 212°F, respectively) (DOE 1998a, Volume 3, pages 3-85 to 3-88). WAPDEG samples a corrosion rate from each cumulative distribution function for a package in such a manner that, if the points were joined on a plot

comparing corrosion rates and temperatures, the curve for a waste package is parallel to the curves for all the other waste packages. When WAPDEG encounters a temperature between the specified temperatures, it linearly interpolates the logarithm of the corrosion rate versus the reciprocal of the temperature to estimate the corrosion rate at the given temperature.

According to a follow-up question for the Waste Package Degradation Expert Elicitation, the spread of the general corrosion rates at a given temperature was due to a combination of uncertainty and natural variability. Waste Package Degradation Expert Elicitation panelists estimated the Alloy-22 general corrosion rate and the allocation of the total variance to its variability and uncertainty. The effect of the corrosion rate variability among waste packages, patches, and the corrosion rate uncertainty on waste package failure and, ultimately, radiological dose was evaluated by splitting the total variance into three different variability and uncertainty combinations: 75-percent variability and 25-percent uncertainty; 50-percent variability and 50-percent uncertainty; and 25-percent variability and 75-percent uncertainty. Uncertainty was interpreted as the uncertainty of the mean of the distribution. To capture this uncertainty, a given percentage was used to establish three possible values for the mean which were based on the 5th, 50th, and 95th percentiles of the uncertainty about the global mean. Three uncertainty splits, combined with these three estimates of the mean, produced nine new cumulative distribution functions for general corrosion rate, which implied nine WAPDEG runs. These runs are summarized in Table I-29.

Table I-29. Uncertainty/variability splitting sets for corrosion rate of corrosion-resistant material[a]

	Uncertainty/variability splitting ratios		
Percentile	25% and 75%	50% and 50%	75% and 25%
5th	Set 1	Set 2	Set 3
50th	Set 4	Set 5	Set 6
95th	Set 7	Set 8	Set 9

a. Source: TRW (1999a, Table 3.3-1, page 3-12).

In the presence of water or water vapor, localized corrosion could occur on the corrosion-resistant material in the form of pitting or crevice corrosion. Information from the Waste Package Degradation Expert Elicitation indicates that localized corrosion would begin only if the temperature was sufficiently high. The user supplies the temperature threshold for initiating pitting either in the form of a fixed value or a probability distribution that is sampled for each waste package. If pitting is allowed to begin as the result of sufficient water and heat levels, WAPDEG implements an Arhennius model for pit growth. Thus, the corrosion-resistant material could be breached either by the general corrosion of patches on the waste package surface or by pit penetration. WAPDEG output files indicate the number of patch failures and pit penetrations over time for each waste package.

The local environment in the waste-emplacement areas could differ from package to package, a factor treated as variability in WAPDEG. To implement this concept, WAPDEG assumes that the variances of the probability distributions that describe general corrosion are due to spatial variability and the variances should be allocated. Using the treatment described above for splitting the cumulative distribution functions for general corrosion of the corrosion-resistant material, the variance of each of the resulting nine distributions is due to natural variability. Some variance accounts for package-to-package variability, and the rest accounts for variable conditions along a waste package (patch-to-patch variability). The user supplies the fraction of variance to be shared by the waste packages, and the remaining fraction is applied to patches. In the Viability Assessment analysis, variance between packages and between patches is 35 percent/65 percent for patches dripped on and 50 percent/50 percent otherwise.

In practice, WAPDEG samples a corrosion parameter using the global distribution but with only a fraction of its variance. The sampled value is then treated as the mean value for the patches on that waste package. For each patch, WAPDEG samples the distribution using the waste package mean and the remaining variance. The results are used to model general corrosion for the patch. WAPDEG also

applies this variance-sharing technique to the general corrosion of the corrosion-allowance material and to the temperature threshold for pitting initiation on the corrosion-resistant material.

One difference between waste package environments would be the presence or absence of dripping or pooled water. WAPDEG allows the user to specify the fraction of patches that contact such water, either as a fixed value or using a probability distribution. The user can also specify when drips start, stop, or experience a change in water chemistry. For dripping conditions, model inputs can be used to specify roughness factors on the corrosion-allowance material, the cumulative distribution functions of general corrosion rates for corrosion-resistant material, and all the temperature and relative humidity thresholds as different from those for nondripping conditions. WAPDEG determines if an individual patch is dripped on or not and uses the appropriate model parameters.

For the Total System Performance Assessment – Viability Assessment configuration, waste package failure distributions were generated based on always-dripping or no-dripping conditions. For each infiltration (I) case where I varied from I multiplied by 3 to I divided by 3 (I, I × 3, and I) 3), nine simulations were conducted based on the always-dripping corrosion rates. Because of the small number of failures for the no-dripping case, only one case was simulated (Set 6).

I.4.3.2 Application of WAPDEG for the EIS

This EIS analyzes the effects of three different thermal loads (high, intermediate, and low) and three waste inventories (Proposed Action, Inventory Module 1, and Inventory Module 2) to determine their impact, if any, on total system performance. The comparison of thermal output versus time for the Inventory Module 1 and Inventory Module 2 waste inventories were considered identical for the thermal-hydrologic modeling (see Section I.4.2). Therefore, only the Proposed Action inventory and Inventory Module 1 (the expanded inventory) were considered.

Section I.4.2 describes the number of repository regions that were simulated depending on the thermal load requirements for each scenario. To incorporate the potential cooling effects around the edges of a repository region, some regions were simulated using a conceptualized center and edge, resulting in multiple NUFT simulations for certain regions. Table I-30 lists the number of individual simulations conducted for each thermal load/inventory combination, for each climate scenario.

As with the Total System Performance Assessment-Viability Assessment analyses, only the long-term average climate scenario was used in the EIS WAPDEG simulations. Therefore, the six thermal-hydrologic scenarios listed in Table I-30 were used in the generation of an equal suite of WAPDEG simulations that assumed long-term average infiltration conditions. Table I-30 lists 18 total individual thermal-hydrologic simulations for the six scenarios. WAPDEG simulations were performed using the temperature and relative humidity histories generated from each of the 18 simulations. Each set of WAPDEG simulations consisted of nine always-dripping and one no-dripping case, based on uncertainty/variability splitting.

The EIS analyses used one always-dripping case and the no-dripping base case input files from the Total System Performance Assessment – Viability Assessment as starting points. The EIS models used the same corrosion model configuration and the same corrosion rate probability distribution functions as those used in the Total System Performance Assessment – Viability Assessment base case configuration. However, the EIS analysis used a lower, fixed relative humidity threshold for corrosion initiation of the corrosion-resistant material than that used in the Total System Performance Assessment – Viability Assessment analysis. The threshold used in the EIS analysis is based on a better understanding of the factors that initiate corrosion. This difference resulted in an earlier estimate of failure of the corrosion-resistant material for the EIS analysis. This earlier failure is evident in the results of the 10,000-year analysis but does not affect the 1-million-year analysis.

Table I-30. Thermal-hydrologic and waste package degradation simulation matrix.[a]

Thermal-hydrology scenario	Inventory module	Thermal load (MTHM per acre)	Repository block(s)	Stratigraphic column	Block simulation location	WAPDEG simulation number
1	Proposed Action	85	Upper Block	1	Center	1-10
					Edge	11-20
2	Proposed Action	60	Upper Block	1	Center	21-30
					Edge	31-40
3	Proposed Action	25	Upper Block	1	Center	41-50
			Lower Block	2	Center	51-60
			Block 5	7	Center	61-70
4	Inventory Modules 1 and 2	85	Upper Block	1	Center	71-80
					Edge	81-90
			Lower Block	2	Center	91-100
					Edge	101-110
5	Inventory Modules 1 and 2	60	Upper Block	1	Center	111-120
			Lower Block	2	Center	121-130
			Block 1a	3	Center	131-140
6	Inventory Modules 1 and 2	25	Upper Block	1	Center	141-150
			Lower Block	2	Center	151-160
			Block 8	4	Center	161-170
			Block 5	7	Center	171-180

a. Source: TRW (1999a, Table 3.3-2, page 3-13).

Each WAPDEG run generated a failure curve that contained a probability distribution function of the first corrosion-resistance-material breach, average pit failures, and average patch failures (as a function of time). These files were transferred to the repository integration program model.

I.4.3.3 Results

Figure I-15 shows the temperature and drift relative humidity history curves, respectively, for all three thermal loads (high, intermediate, and low) with the Proposed Action inventory. Figure I-16 shows the temperature and relative humidity history curves, respectively, for all three thermal load scenarios with the expanded inventory (Inventory Modules 1 and 2). These figures show that when the temperature threshold [100°C (212°F)] for corrosion initiation is met, the relative humidity within the drifts for most of the runs is within the range of aqueous corrosion (80 to 100 percent). The time to reach the temperature threshold is less for the low thermal load scenario (less than 100 years) than for the high and intermediate thermal load scenarios (200 to 700 years). Corrosion of the corrosion-allowance material for the low thermal load scenario is initiated sooner but only by a few hundred years. This difference will become relatively small when discussing the differences in package failure rates at times greater than 10,000 years.

The thermal histories generated from the thermal-hydrologic modeling indicate that the hottest and coolest thermal histories correspond to the high thermal load, expanded-inventory scenario and the low thermal load, Proposed Action inventory scenarios, respectively. Thus, the results from these two configurations bound the range of potential WAPDEG failure responses. In addition, the waste package failure results were dominated by the packages that were dripped on; therefore, the failure results for the packages that were not dripped on are not presented.

WAPDEG simulations for the low thermal load with Proposed Action inventory case were generated for three repository regions corresponding to the upper (primary) block, lower block, and Block 5. The thermal output for this layout did not include edge effects (see Section I.4.2); therefore, only one thermal simulation per repository block was generated. Temperature and relative humidity histories generated from each repository block were used to define the conditions within the drifts. Figure I-17 shows the time to first breach or failure of the corrosion-allowance material for the always-dripping packages in each of the three emplacement blocks. The failures of the corrosion-allowance material are very similar for all three stratigraphic columns, with failures starting at approximately 800 years and extending approximately 4,000 years. Figure I-18 shows the time to first breach of the corrosion-resistant material for the always-dripping packages in each of the three emplacement blocks, for each of the nine uncertainty/variability splitting sets (defined in Table I-29). The failure of the corrosion-resistant material barriers in the three regions were very similar, given the same uncertainty/variability splitting set (set 5). For example, the responses observed for stratigraphic columns 2 and 7 overlie each other. The variability in the failure of the corrosion-resistant material in a particular region (for example, stratigraphic column 1), due to the introduction of the uncertainty/variability splitting, ranges from a few thousand years (set 7) to no failures within 1 million years (set 3).

Given the relatively cool thermal history for the low thermal load scenario and the 70,000 MTHM inventory, no pits (localized corrosion) would penetrate through the corrosion-resistant material for the always-dripping packages for all three emplacement blocks. All failures (see Figure I-18) would be due to general corrosion because the temperature threshold for localized corrosion was not reached. Figure I-19 shows the average number of patches penetrated through the corrosion-resistant material as a function of time for the always-dripping packages, all three emplacement blocks, and the uncertainty/variability splitting sets. Figures I-20 through I-22 show that the variability in the results of the failure for the three emplacement blocks is dominated by the corrosion rate uncertainty/variability splitting of corrosion-resistant material, with little variability attributed to the different thermal-hydrologic inputs.

WAPDEG simulations for the high thermal load scenario with the expanded inventory were generated for the upper (primary) and lower repository blocks. The repository blocks were simulated with both a center and an edge region (see Section I.2). Figure I-20 shows the time to first breach or failure of the corrosion-allowance material for the always-dripping packages, for all four simulations, and the uncertainty/variability splitting sets. Figure I-21 shows the time to first breach of the corrosion-resistant material. Figure I-22 shows the average number of patches penetrated through the corrosion-resistant material as a function of time. Previous analyses have shown that the releases from the waste packages are dominated by advection through the patch. Therefore, the patch failure history is a representative indicator of the overall performance. The results shown in Figure I-22 also show that the variability in the failures for the four center and edge simulations is dominated by the uncertainty/variability splitting, with little variability attributed to the different thermal-hydrologic inputs.

These results show that the variability in the corrosion-resistant material failures as a function of time has a greater dependency on the variability/uncertainty splitting associated with the corrosion-resistant material corrosion rate than on the variation in the temperature and relative humidity histories. The results for the high and intermediate thermal load scenarios for the Proposed Action inventory and the intermediate and low thermal load scenarios for the expanded inventory simulations showed similar behavior to the results discussed above.

I.4.3.4 Discussion

Corrosion of the corrosion-allowance material is not initiated until the waste package temperature decreases below the thermal threshold selected for the model [100°C (212°F)]. For the majority of the thermal-hydrologic simulations conducted for the EIS, once the thermal threshold is satisfied, the humid-air corrosion is initiated. Figure I-23 shows the time to the first breach of the corrosion-allowance

material for all expected-value always-dripping WAPDEG simulations (Set 5). The time to first breach of the corrosion-allowance material is earliest for the low thermal load scenarios as expected from the temperature profiles shown in Figures I-15 and I-16. Because the thermal threshold is satisfied sooner, corrosion of the corrosion-allowance material is initiated sooner.

Figure I-23 also shows that by 5,000 years, almost each waste package has had at least a single corrosion-allowance material failure, thereby allowing corrosion of corrosion-resistant material. Figure I-24 shows the time to the first breach of the corrosion-resistant material for all expected-value always-dripping WAPDEG simulations (Set 5). The first corrosion-resistant-material breach for most scenarios occurs between 20,000 to 30,000 years, with the high thermal load, expanded-inventory scenario having a very low fraction of packages failing within 10,000 years. Figure I-24 also shows that the higher thermal loads generate the earliest corrosion-resistant material failures, even with later corrosion-allowance material failures. This behavior is due to the temperature-dependent, corrosion-resistant-material corrosion models, which have higher corrosion rates at higher temperatures. The thermal profiles in Figures I-23 and I-24 show that temperature is lower for the lower thermal load scenarios, resulting in slower corrosion rates and delayed failure relative to the higher loads.

Figure I-25 shows the average number of patches that failed per package as a function of time for all thermal loads and inventories, all regions, always-dripping, and uncertainty/variability splitting (set 9). Figure I-26 shows the average number of patches that failed per package as a function of time for all thermal loads and inventories, all regions, always-dripping, and uncertainty/variability splitting (set 5). These plots show a factor-of-five difference between the failure results for the two different uncertainty/variability-splitting sets.

The degradation results show that for each thermal-hydrologic scenario, the variability in the failures due to the uncertainty/variability splitting in the corrosion rate of the corrosion-resistant material would be considerably greater than the variability due to the different thermal histories. Therefore, for each thermal and inventory scenario, a set of -failure distributions from a single region was selected and included in the RIP model simulations.

I.4.4 WASTE FORM DISSOLUTION MODELS

Evaluation of Inventory Modules 1 and 2 for this EIS diverged from the Proposed Action, or base case, inventory evaluated in the Viability Assessment. Specifically, additional waste forms were included in Inventory Modules 1 and 2 that were not considered in the Viability Assessment base case, and waste form dissolution models were required to model these additional waste forms. Extensions of the waste form dissolution modeling that supported the Total Systems Performance Assessment model were required to evaluate the additional inventories. These extensions are detailed in this section.

I.4.4.1 Spent-Fuel Dissolution Model

A semi-empirical model for intrinsic dissolution (alteration) rate of the spent fuel matrix was developed from experimental data (TRW 1995, page 6-2). If the postclosure environment inside the potential repository can be assumed to maintain the atmospheric oxygen partial pressure of 0.2 atmosphere (TRW 1995, page 6-1), the dissolution model becomes a function of temperature, total carbonate concentration, and pH of contacting water. The dissolution rate strongly depends on temperature and total carbonate concentration but is less influenced by pH. The spent fuel dissolution rate increases with temperature and is enhanced by the total carbonate concentration of the contacting water, although to a smaller extent than by temperature. The mixed oxide spent nuclear fuel from plutonium disposition was modeled as commercial spent nuclear fuel.

I.4.4.2 High-Level Radioactive Waste Glass

As in the spent fuel alteration/dissolution modeling discussed above, the entire surface area of defense high-level radioactive waste in the glass waste form is assumed to be exposed to the near-field environment as soon as the first pit penetrates the waste package. The waste forms are assumed to be covered by a "thin" water film when the water contacts the glass and the alteration/dissolution processes are initiated. The "can-in-canister" ceramic from plutonium disposition was modeled as high-level radioactive waste.

High-Level Radioactive Waste Glass Dissolution Model

Details concerning the intrinsic glass dissolution rate model, as a function of temperature and pH, are presented along with rate data (TRW 1995, pages 6-4, 6-5, and 6-37). The relationship indicates that the rate model represented by the equation predicts a monotonically increasing dissolution rate with temperature.

This dissolution conceptualization contains several assumptions and limitations. The radionuclides are assumed to be released as fast as the glass structure breaks down, which is a conservative assumption because it does not account for solubility-limited radionuclides. No credit is taken for the fact that "experiments have shown that the actinides more commonly are included in alteration phases at the surface of the glass either as minor components of other phases or as phases made up predominantly of actinides" (TRW 1995, page 6-5). The model includes neither solution chemistry (other than pH and dissolved-silica concentration) nor vapor-phase alteration of the glass. Glass has been observed to undergo hydration in a humid environment and, on subsequent contact with water, radionuclide releases from a hydrated glass layer were several orders of magnitude higher than those from an unhydrated (fresh) glass waste form (TRW 1995, page 6-5).

I.4.4.3 Greater-Than-Class-C and Special-Performance-Assessment-Required Waste

The alteration/dissolution processes for Greater-Than-Class-C and Special-Performance-Assessment-Required waste forms were assumed to be similar to those for high-level radioactive waste glass.

I.4.5 RIP MODEL MODIFICATIONS

The EIS RIP model simulations are based on the Total System Performance Assessment – Viability Assessment (Revision 1) base case RIP model (TRW 1998n, all). To perform the EIS performance assessment analyses, the base case model was modified primarily to allow input of the different repository areas corresponding to the thermal load scenarios and the expanded waste inventories of Modules 1 and 2, and the repository-block configurations used in the thermal-hydrologic modeling. The EIS analysis also considered the impact to individuals at distances other than the 20 kilometers (12 miles) used for the Viability Assessment. Therefore, the analysis expanded the saturated-zone convolution model used in the Viability Assessment to include development of convolution stream tubes from the repository to distances of 30 kilometers (19 miles) and 80 kilometers (50 miles) and postprocessing of the 20-kilometer output to extract the radiological dose to individuals at the 5-kilometer (3-mile) distance described in Section I.4.5.4. This section describes the modifications. Knowledge and understanding of the RIP model (Golder 1998, all) and the Viability Assessment model (TRW 1998a,b,c,d,e,f,g,h,i,j,k, all) are necessary to fully understand the differences discussed in this section.

I.4.5.1 Modifications to the RIP Model in the Repository Environment

The RIP model conceptualization for the Yucca Mountain Repository performance assessment considers waste forms in discrete regions of the repository as source terms for flow and transport. The RIP model conceptualization for the Viability Assessment considered the primary repository block, corresponding to the high thermal load scenario, to be comprised of six regions. For any particular case analyzed for the

EIS, the EIS thermohydrologic simulations were used to determine the number of repository regions used. In adapting the Viability Assessment base case as the model for the EIS analyses, the repository regions had to conform to the center/edge model conceptualization. For each of the unused Viability Assessment regions, the source terms (commercial spent nuclear fuel, high-level radioactive waste, and DOE spent nuclear fuel) and all associated RIP model cells were removed from the model, and the remaining source terms and associated connecting cells were adapted to the center/edge model. In all cases, a total of 60 concentration parameters and all of the "connection" groups, except the 10 groups that provided total radiological dose at various points, were removed from the model. Then, the new region-specific connection groups were added as appropriate to account for the calculation of advective and diffusive releases from the center and edge regions of the EIS simulations. The calculated flux data, developed from the Lawrence Berkeley National Laboratory hydrologic model of the repository area (Bodvarsson, Bandurraga, and Wu 1997, all), was used to modify the flux into and fluid saturations applicable to the various source terms in the EIS RIP model.

Another modification resulted from the fact that although the Total System Performance Assessment – Viability Assessment considered sensitivity variations in the infiltration to the repository, the EIS simulations used only the infiltration (I) option. This was done to reduce the number of calculations, because the three thermal loads and two extra inventories greatly multiplied the number of cases to be simulated. The (I × 3) and (I × 3) options of the Total System Performance Assessment – Viability Assessment were not considered. Therefore, only the WAPDEG results for the "always-dripping" and "no-drip" scenarios were selected for model input. This change resulted in appropriate changes to the fraction-of-packages-failed parameters to allow the appropriate (I) WAPDEG to be incorporated into the model. To accommodate these differences to the RIP model, the fraction-of-packages-failed parameters for the (I × 3) and (I × 3) options were redirected to call the applicable WAPDEG tables for the long-term average climate case. The effect of neglecting this variation is minor. Sensitivity studies with the Viability Assessment model for the high thermal load scenario (DOE 1998a, Volume 3, pages 5-3 to 5-5) showed that the 10,000-year peak dose is actually decreased by 30 percent for the I × 3 case, while the peak is moved back from 10,000 years to about 5,000 years and the 1-million-year peak dose is increased about 30 percent.

The EIS simulations used only one thermal table rather than the six used in the Viability Assessment base case. Therefore, the thermal parameters were updated to refer to only one unique thermal table for each of the thermal load scenarios and inventory combinations:

- High thermal load, Proposed Action inventory
- Intermediate thermal load, Proposed Action inventory
- Low thermal load, Proposed Action inventory
- High thermal load, Inventory Modules 1 and 2
- Intermediate thermal load, Inventory Modules 1 and 2
- Low thermal load, Inventory Modules 1 and 2

The thermal hydrology modeling indicated that a single invert saturation was sufficient for all regions and all layers of the invert. Based on this information, all invert saturation parameters were fixed to a value of 0.993.

I.4.5.2 Modifications to Input and Output FEHM Model

The particle-tracking files used in the Viability Assessment (TRW 1998g, all) were modified for each EIS case to allow a different number of FEHM input regions to be used, depending on the number of input regions used in the engineered barrier system model. The "Zone 6" interface file was modified for each EIS case by changing the FEHM nodes to be used for input of mass from the engineered barrier system. The FEHM nodes were chosen to correspond to the coordinates of the EIS repository emplacement

blocks. For the low thermal load scenario for Inventory Modules 1 and 2 shown in Figure I-7, proposed Blocks 6 and 7 fell outside the model boundaries. To allow the unsaturated zone particle tracker in the FEHM model to account for all mass in the repository, the mass from areas 6 and 7 were allocated to Blocks 5 and 8, respectively. Figures I-27 through I-32 show the repository emplacement blocks used for each case.

The "Zone 6" interface file was also modified for each EIS case by defining the saturated zone area that would capture the mass coming out of the FEHM model. It was necessary to modify the capture regions in order to ensure inclusion of all of the mass and to distribute the mass amongst the six stream tubes based on its repository emplacement block of origin. For the high and intermediate thermal load scenarios with Proposed Action inventories, the same regions were used for this EIS as were used for the Viability Assessment base case (Figure I-33). Figure I-34 shows the capture regions used for the low thermal load scenario with the Proposed Action inventory; the low thermal load scenario with Inventory Modules 1 and 2, and the intermediate thermal load scenario with Inventory Modules 1 and 2. Figure I-35 shows the capture regions used for the high thermal load scenario with Inventory Modules 1 and 2.

I.4.5.3 Modifications to Saturated Zone Stream Tubes for Different Repository Areas

The saturated zone stream tubes consist of a unit-breakthrough curve and a scaling factor. The unit-breakthrough curves are all the same for a given radionuclide at a given distance. The scaling factor is the product of the flux coming from the repository and a dilution factor. The dilution factor is a lumped parameter that is used to account for mixing and lateral dispersion. For the multiple-realization cases, the dilution factor is assumed to have lognormal distribution with a mean value of ten.

In order to use the stream tubes for different repository regions, flux multiplier values were calculated for each stream tube. The flux multiplier value is the ratio of the new flux into a stream tube to the flux into that stream tube in the base case (Proposed Action inventory, high thermal load scenario). The saturated zone module of RIP requires the concentration of water entering the saturated zone from the unsaturated zone, so the water flux at this interface is needed to compute the mass concentration of contaminants in the water. The resulting flux multiplier is used to scale the water flux predicted by the FEHM transport module in RIP to properly account for the larger capture zone areas for other cases. Each stream tube is associated with one of the unsaturated zone capture regions described above. The flux into a given stream tube is the sum of the fluxes from the repository regions that are in that capture region. The high thermal load scenario with Proposed Action-inventory used the same fluxes as the Viability Assessment base case. Tables I-31 and I-32 list the contribution to each of the stream tubes from each of the repository areas for the intermediate and low thermal load scenarios with Proposed Action inventory, respectively. The same information is provided for the high, intermediate, and low thermal load scenarios with Inventory Modules 1 and 2 inventory, respectively, in Tables I-33 through I-35. The fluxes used in these tables were obtained from the results of the base case Lawrence Berkeley National Laboratory site-scale unsaturated zone flow model (Bodvarsson, Bandurraga, and Wu 1997, all).

Table I-31. Summary of fluxes (cubic meters per year) from repository area to convolution stream tubes for intermediate thermal load scenario with Proposed Action inventory.[a]

	Flux from each repository area into each stream tube						
Stream tube	Upper block	Lower block	Blocks 5 & 6	Blocks 7 & 8	Total flux	85-MTHM-per acre, base case inventory flux	Flux multiplier
1	6,410	0	0	0	6,410	3,162	2.03
2	3,480	0	0	0	3,480	3,482	1.00
3	3,990	0	0	0	3,990	3,993	1.00
4	4,060	0	0	0	4,060	4,060	1.00
5	8,090	0	0	0	8,090	10,103	0.801
6	5,320	0	0	0	5,320	2,077	2.56

a. Source: TRW (1999a, Table 3.5-1, page 3-19).

Table I-32. Summary of fluxes (cubic meters per year) from repository area to convolution stream tubes for low thermal load scenario with Proposed Action inventory.[a]

	Flux from each repository area into each stream tube						
Stream tube	Upper block	Lower block	Blocks 5 & 6	Blocks 7 & 8	Total flux	85-MTHM-per acre, base case inventory flux	Flux multiplier
1	16,570	0	0	0	16,570	3,162	5.24
2	16,570	0	0	0	16,570	3,482	4.76
3	0	5,250[b]	0	0	5,250[b]	3,993	0.131
4	0	5,250[b]	0	0	5,250[b]	4,060	0.129
5	0	0	6,750	0	6,750	10,103	0.668
6	0	0	6,750	0	6,750	2,077	3.25

a. Source: TRW (1999a, Table 3.5-2, page 3-19).
b. Typographical error in source document.

Table I-33. Summary of fluxes (cubic meters per year) from repository area to convolution stream tubes for high thermal load scenario with Inventory Modules 1 and 2.[a]

	Flux from each repository area into each stream tube						
Stream tube	Upper block	Lower block	Blocks 5 & 6	Blocks 7 & 8	Total flux	85-MTHM-per acre, base case inventory flux	Flux multiplier
1	7,050	0	0	0	7,050	3,162	2.23
2	7,050	0	0	0	7,050	3,482	2.02
3	7,050	0	0	0	7,050	3,993	1.77
4	7,050	0	0	0	7,050	4,060	1.74
5	7,050	0	0	0	7,050	10,103	0.698
6	0	969	0	0	969	2,077	0.466

a. Source: TRW (1999a, Table 3.5-3, page 3-20).

Table I-34. Summary of fluxes (cubic meters per year) from repository area to convolution stream tubes for intermediate thermal load scenario with Inventory Modules 1 and 2.[a]

	Flux from each repository area into each stream tube						
Stream tube	Upper block	Lower block	Blocks 5 & 6	Blocks 7 & 8	Total flux	85-MTHM-per acre, base case inventory flux	Flux multiplier
1	17,620	0	0	0	17,620	3,162	5.57
2	17,620	0	0	0	17,620	3,482	5.06
3	0	3,350	0	0	3,350	3,993	0.838
4	0	3,350	0	0	3,350	4,060	0.824
5	0	0	0	4,090	4,090	10,103	0.404
6	0	0	0	4,090	4,090	2,077	1.97

a. Source: TRW (1999a, Table 3.5-5, page 3-20).

Table I-35. Summary of fluxes (cubic meters per year) from repository area to convolution stream tubes for low thermal load scenario with Inventory Modules 1 and 2.[a]

	Flux from each repository area into each stream tube						
Stream tube	Upper block	Lower block	Blocks 5 & 6	Blocks 7 & 8	Total flux	85-MTHM-per acre, base case inventory flux	Flux multiplier
1	17,620	0	0	0	17,620	3,162	5.57
2	17,620	0	0	0	17,620	3,482	5.06
3	0	5,250	0	0	5,250	3,993	1.31
4	0	5,250	0	0	5,250	4,060	1.29
5	0	0	10,240	0	10,240	10,103	1.01
6	0	0	10,240	54,200	64,440	2,077	31.0

a. Source: TRW (1999a, Table 3.5-4, page 3-20).

REPOSITORY SIZE AND SATURATED ZONE DILUTION FACTORS

Increasing repository size could cause either a reduction or no change in the relative lateral dispersive effects of saturated zone transport. Consider a rectangular repository oriented normal to the direction of flow in the saturated zone. The cross-sectional area of the resultant contaminant plume at a downstream well would be larger than that at the cross-sectional area of the plume at the source (below the repository), causing dilution of the radionuclide concentration at the downstream well. However, if the area of the repository was doubled, the plume at the exposure location would increase, but by less than twice. Hence, lower dilution factors would occur for larger repositories. Analytical modeling provides quantification for lower dilution factors.

The validity of using lower dilution factors for larger repositories can be illustrated by considering two hypothetical repositories with equal waste inventory, one having twice the emplacement area of the other. The concentration at the base of the unsaturated zone below the larger repository would be - half the concentration below the smaller repository (a direct result of different spacing of the waste). Using a one-dimensional saturated zone transport model without dilution, for times far greater than the groundwater travel time, the concentrations at a downstream well would be equal to those at the base of the unsaturated zone (provided the contaminant release was continuous). If the same dilution factor was applied in both cases, the downstream well concentrations for the larger repository would be half those in the smaller repository. On the other hand, if the repository was treated as a point source in each case, the dilution factor for the larger repository would be half that of the smaller repository, resulting in equal concentrations at a downstream well. These two outcomes correspond to two alternative ways of doubling the repository area. Thus, the dilution factors for expanded area repositories can be lower or equal to those of the base-case repository.

I.4.5.4 Modifications to the Stream Tubes for Distances Other Than 20 Kilometers

One-dimensional stream-tube runs for the saturated zone were conducted for generating unit-breakthrough curves at distances of 30 and 80 kilometers (19 and 50 miles) downstream from the repository. This was accomplished using the Los Alamos National Laboratory simulator FEHM (Zyvoloski et al. 1995, all) and developing a finite-element mesh that extended beyond the 25-kilometer (16-mile) mesh previously used to develop the 20-kilometer (12 mile) stream tube used for the Viability Assessment. The sets of transport parameters used in the previous model runs were also applied in the extended mesh simulations for distances up to 25 kilometers. Beyond 25 kilometers, the model properties were made identical to those assigned to the undifferentiated valley fill. On completing the FEHM runs for each of nine radionuclides, model output was postprocessed to take into account mass loadings from the unsaturated zone to each of six different stream-tube capture areas and to adjust model results for dilution attributed to transverse dispersion. This last step involved the determination of distance-dependent dilution factors by using dilution information previously developed from exposure concentrations at the 20-kilometer distance. An analytical transport solution in the program 3DADE (Leij, Scaggs, and van Genuchten 1991, all) was used to determine dispersion coefficients that resulted in dilution factors of 10, 50, and 100 at 20 kilometers and to determine corresponding dilution factors at distances of 30 and 80 kilometers. The resulting data indicated a logarithmic relationship between the 20-kilometer dilution factors and those occurring at the longer distances, making it possible to determine appropriate dilution parameters used in postprocessing of the extended-distance FEHM runs.

The saturated zone transport in the Viability Assessment is essentially based on a one-dimensional analysis that precludes lateral dispersion in the *y* and *z* directions. To simulate the realistic results of three-dimensional transport, the results of the one-dimensional analysis are divided by a dilution factor. Thus, the dilution factor accounts for attenuation of concentrations caused by the spread of the contaminant plume as the result of lateral dispersion. The dilution factor approximates numerical dispersion for the one-dimensional saturated zone model, as can be achieved using a three-dimensional advective-dispersive numerical model. This simulates the real dilution in the system.

The Viability Assessment dilution factors were based on the results of the Expert Elicitation Panel Project (TRW 1998h, Section 8.2.3.2), which assigned a median value of 10, a maximum value of 100, and a minimum value of 1.0 (no dispersion). Consideration of Inventory Modules 1 and 2 and/or the reduced thermal load resulted in a larger-area repository than that considered in the Viability Assessment analysis. Simplified logical models were developed to study the impact of the larger-area repository configurations for this EIS. In general, a larger inventory at the same thermal load results in lower concentrations at the base of the unsaturated zone (barring some exceptionally adverse infiltration conditions) because the spacing between disposal blocks results in the additional amount of waste being spread over a larger area. The larger size of the repository also tends to cause a reduction in the lateral dispersive effects of saturated zone transport, implying lower dilution factors for larger repository configurations. If the dilution factors of the Viability Assessment were to be used in this EIS, the dose rates would be predicted (albeit erroneously) to be lower than their true values for cases with expanded repository areas.

The dilution factors appropriate for the larger-area repository configurations were computed for the EIS analyses. The analytical solution for the three-dimensional transport in a one-dimensional flow field (Leij, Scaggs, and van Genuchten 1991, all) was used to relate the lateral dispersion lengths (in the *y* and *z* directions) and the dilution factors. Considering a rectangular source oriented normally to the flow direction, the steady-state concentrations at the locations [5, 20, 30, and 80 kilometers (3, 12, 19, and 50 miles)] were computed based on the assumed dispersion lengths described below.

The ratio between the concentration from the one-dimensional and three-dimensional analyses gives the dilution factor, which enables a "translation" of the Saturated Zone Expert Elicitation Panel's dilution factors to "dispersion lengths." The Panel's dilution estimates were for a 25-kilometer (16 miles) distance and the Viability Assessment adjusted this estimate for estimates at 20 kilometers (12 miles). The dispersion lengths so derived for the Viability Assessment are assumed to remain the same for larger repository configurations. Using the same dispersion lengths, as implied in the Viability Assessment, the dilution factors for the larger repository configurations were computed using the analytical solution. The Darcy flux used in the calculations for the saturated zone flow fields was the same 0.6 meters (2 feet) per year used in the Viability Assessment (DOE 1998a, Volume 3, page 3-138). The actual repository geometry was a rectangular source with an area equivalent to that of the repository configuration for the appropriate thermal load. The larger dimension of the rectangular source was normal to the flow direction and assumed equal in the unsaturated and saturated zones. The smaller dimension of the rectangular source, parallel to the flow in the saturated zone, was modified in the saturated zone to fulfill the continuity of flow requirement (that is, to reconcile large differences in the flow velocities in the unsaturated and saturated zones).

The matrix of dilution factors (given in Table I-36), calculated using the 3DADE computer code (Leij, Scaggs, and van Genuchten 1991, all), was dependent on the major influences on the calculated dilution factors, namely:

- The orientation of each repository configuration relative to the direction of groundwater flow
- The total area of each repository configuration
- The average percolation flux of each sector (or block) of the repository based on the Lawrence Berkeley National Laboratory hydrologic model

Extension of the repository area in a direction orthogonal to that of groundwater flow had little effect on the calculated dilution factor. However, for dilution factors calculated for the repository and enlarged in the direction parallel to that of groundwater flow, there were changes on the order of factors of two or three. Thus, the intermediate thermal load scenario had the same dilution factor as the high thermal load Proposed Action scenario for the 20-kilometer (12-mile) distance, because the repository shape was relatively similar with essentially no changes parallel to the flow direction. In contrast, the low thermal

Table I-36. Dilution factors for three thermal load scenarios and four exposure locations.[a]

		Proposed Action			Inventory Modules 1 and 2		
	Thermal load (MTHM per acre)[b]	High (85)	Intermediate (60)	Low (25)	High (85)	Intermediate (60)	Low (25)
Distance	Repository area (acres)	740	1,050	2,520	1,240	1,750	4,200
5 kilometers[c]	Minimum	1.0	1.0	1.0	1.0	1.0	1.0
	Median	5.15	5.15	2.9	5.15	3.8	2.5
	Maximum	50.02	50.02	24.6	50.02	354	19.2
20 kilometers	Minimum	1.0	1.0	1.0	1.0	1.0	1.0
	Median	10.0	10.0	5.1	10.0	7.2	4.1
	Maximum	100.0	100.0	49.2	100.0	70.8	38.4
30 kilometers	Minimum	1.0	1.0	1.0	1.0	1.0	1.0
	Median	12.2	12.2	6.2	12.2	8.8	4.9
	Maximum	122.0	122.0	60.2	122	86.7	47
80 kilometers	Minimum	1.0	1.0	1.0	1.0	1.0	1.0
	Median	19.894	19.84	9.9	19.84	14.2	7.8
	Maximum	200.04	200.04	98.4	200.04	141.6	76.7

a. Source: TRW (1999a, Table 4.1-1, page 4-6).
b. To convert acres to square miles, multiply by 0.0015625.
c. To convert kilometers to miles, multiply by 0.62137.

load Proposed Action scenario has almost double the area of the intermediate thermal load Proposed Action scenario. The repository is approximately twice the distance in the direction parallel to flow, resulting in a dilution factor almost twice that of the intermediate thermal load Proposed Action scenario. Thus, because of the repository geometry, the differences in the dilution factors between the low and intermediate thermal load Proposed Action scenarios resulted in less dilution in the low thermal load Proposed Action scenario.

I.4.5.5 Modifications to the RIP Model to Account for Unsaturated Zone and Saturated Zone Particle Transport

Transport through the unsaturated zone is modeled in RIP using particles that are assigned a "start location" at the level of the repository. The Viability Assessment analysis considered particle releases only in the upper block of the repository. For the EIS analyses, the Lawrence Berkeley National Laboratory model (Bodvarsson, Bandurraga, and Wu 1997, all) element centroids were mapped to the outline of the upper block, and particles were released from these locations.

Because the EIS analysis considered expanded areas for the emplacement of waste, additional particle coverage was needed to represent transport throughout the entire region of interest. This region included the additional repository blocks for the expanded waste inventories considered in Inventory Modules 1 and 2. An orthogonal grid was mapped for each of the emplacement zones within the area covered by the Lawrence Berkeley National Laboratory model, and this grid was use to determine the coordinates of particle start points at the repository horizon. These coordinates were then converted to the centroid of the nearest Lawrence Berkeley National Laboratory model elements. In this way, a file containing Lawrence Berkeley National Laboratory element numbers was created for each waste emplacement zone for the particle-start coordinates. From this functional area of the RIP model, both the EIS and Viability Assessment performance assessment analyses used the FEHM model (Zyvoloski et al. 1995, all) to model particle transport through the unsaturated zone.

At the base of the unsaturated zone, a corresponding change of coordinates was used to collect and distribute the mass transported through the unsaturated zone to the saturated zone convolution stream tubes that carried dissolved radionuclides to the various exposure locations. The unsaturated and saturated zone capture regions for the EIS analysis were scaled-up modifications of the six regions used

by the Total System Performance Assessment – Viability Assessment analysis, as extended to the edge of the Lawrence Berkeley National Laboratory model area. The nodes at the bottom of the unsaturated zone were calculated to ensure complete capture of the mass coming out of the unsaturated zone and to appropriately distribute that mass among the six stream tubes, based on those six repository regions being modified and applied to the expanded areas addressed by the EIS analysis.

Table I-37 lists the ranges of stochastic parameters that were included in the analysis of saturated zone flow and transport.

Table I-37. Stochastic parameters for saturated zone flow and transport.[a]

Parameter	Distribution type	Distribution statistics [bounds]
Effective porosity, alluvium	Truncated normal	Mean = 0.25, SD[b] = 0.075 [0, 1.0]
Effective porosity, upper volcanic aquifer	Log triangular	[1×10^{-5}, 0.02, 0.16]
Effective porosity, middle volcanic aquifer	Log triangular	[1×10^{-5}, 0.02, 0.23]
Effective porosity, middle volcanic confining unit	Log triangular	[1×10^{-5}, 0.02, 0.30]
Effective porosity [plutonium], volcanic units	Log uniform	[1×10^{-5}, 1×10^{-3}]
Distribution coefficient K_d (milliliters per gram) for:		
Neptunium (alluvium)	Uniform	[5, 15]
Neptunium (volcanic units)	Beta (approx. exp.)	Mean = 1.5, SD= 1.3 [0, 15]
Protactinium (alluvium)	Uniform	[0, 550]
Protactinium (volcanic units)	Uniform	[0, 100]
Selenium (alluvium)	Uniform	[0, 150]
Selenium (volcanic units)	Beta (approx. exp.)	Mean = 2.0, SD = 1.7, [0, 15]
Uranium (alluvium)	Uniform	[5, 15]
Uranium (volcanic units)	Uniform	[0, 4.]
Plutonium (all units)	Log uniform	[1×10^{-5}, 10]
Longitudinal dispersivity, all units (meters)	Log-normal	Log(mean) = 2.0, log(SD) = 0.753
Fraction of flow path in alluvium	Discrete CDF[c]	[0, 0.3] (see text)

a. Source: DOE (1998a, Volume 3, Table 3-20, page 3-140).
b. SD = standard deviation.
c. CDF = cumulative distribution function.

I.4.5.6 Biosphere Dose Conversion Factors for Waterborne Radionuclides

A biosphere dose conversion factor for groundwater is a number used to convert the annual average concentration of a radionuclide in the groundwater to an annual radiological dose for humans. The calculation of a biosphere dose conversion factor requires knowledge about the pathway the radionuclide would follow from the well to humans and the lifestyle and eating habits of humans. Figure I-36 illustrates the biosphere modeling components.

The approach used in this long-term performance assessment calculated the health consequences for a reference person living in the Amargosa Valley. The reference person would be an adult who lived year-round on a farm in the Amargosa Valley, grew a garden, raised livestock, and ate locally grown food. Because future human technologies, lifestyles, and activities are inherently unpredictable, the analysis assumed that the future inhabitants of the region would be similar to present-day inhabitants. This assumption has been accepted in similar international efforts at biosphere modeling and is preferable to developing a model for a future society (National Research Council 1995, all).

A lifestyle survey of people living in the area was completed in 1997 (TRW 1998i, Section 9.4, pages 9-25 to 9-35). Among other functions, the survey was intended to give an accurate representation of dietary patterns and lifestyle characteristics of residents within 80 kilometers (50 miles) of the Yucca

Mountain site. Of special interest was the proportion of locally grown foodstuff consumed by local residents and details about regularly consumed food types.

The Amargosa Valley region is primarily rural agrarian in nature and the local vegetation is primarily desert scrub and grasses. Agriculture consists mainly of growing livestock feed (for example, alfalfa); however, gardening and animal husbandry are common. Water for household uses, agriculture, horticulture, and animal husbandry is primarily from local wells.

Another component of the dose to people would be the inadvertent ingestion of contaminated soil, usually from vegetables. The inhalation pathways would include breathing small soil particles that became airborne during outdoor activities, especially farming, mining, and construction activities that would disturb the soil or bedrock. Proximity to a radiation source external to the body would result in an external pathway. This pathway is called "groundshine" when the contaminants are on the ground, "submersion" when they are in the atmosphere, and "immersion" when they are in water.

The analysis calculated biosphere dose conversion factors for the exposure pathways described above. Although many of the input parameters were derived from site-specific data obtained from the Yucca Mountain regional survey and weather data tabulations, some were from other published sources. The input parameters used in the biosphere modeling are described in the Viability Assessment (DOE 1998a, Volume 3, Section 3.8). The estimated consumption rates for vegetables, fruits, grains, beef, poultry, milk, eggs, and water were from the results of the survey (TRW 1998i, Tables 9-14 through 9-20, pages T9-20 to T9-26). Generic food-transfer factors were from IAEA (1994, pages 5 to 58). The amount of plant uptake of radionuclides used in the calculations was taken from LaPlante and Poor (1997, pages 2-12 to 2-14).

The analysis calculated the dose from each radionuclide that would reach the reference person by multiplying the amount of radionuclide ingested, inhaled, or deposited near that person by the dose conversion factor for that radionuclide. Dose conversion factors have important uncertainties associated with them. However (as is customary for radiological compliance evaluations and EISs), this analysis used only fixed values derived by methods from the *International Commission on Radiological Protection Publication 30* (ICRP 1979, all). These methods are similar to those specified by the Environmental Protection Agency (Eckerman, Wolbarst, and Richardson 1988, all).

The long-term performance assessment calculations used the statistical distributions of biosphere dose conversion factors. When the postulated climate change occurred during the model run, the biosphere dose conversion factors changed to reflect the precipitation patterns associated with the new climate. The major impact of a wetter climate would be to reduce the amount of well water required for irrigation. The analysis did not consider other climate-related effects such as the appearance of springs, seeps, or other surface water, because they would be unlikely to cause a large change in the consequences for a maximally exposed individual. The result was the annual dose rate that the reference person would receive from that radionuclide at a given time. The reference person (referred to in this EIS as a maximally exposed individual) was developed from a series of lifestyle assumptions based on the surveys of lifestyles in the region. Details on the reference person development are in the Viability Assessment (DOE 1998a, Volume 3, pages 3-150 to 3-155).

In the analyses for this EIS, the same biosphere dose conversion factors were used for the four locations considered [5, 20, 30, and 80 kilometers (3, 12, 19, and 50 miles)]. The biosphere dose conversion factors are appropriate for the 30-kilometer location due to its similarity to the 20-kilometer location. However, using the same factors for the other locations resulted in a systematic dose overestimation at 5 and 80 kilometers. This overestimate resulted because not all of the exposure pathways considered in the calculation of biosphere dose conversion factors for the 20-kilometer location were appropriate for the 5-and 80-kilometer locations. The 5-kilometer location would be a drinking-water-only pathway (ingestion dose only) because this location is not suitable to irrigation or farming. The 80-kilometer

location is a lake playa, where evaporating contaminated water would result in deposits of contaminated dust. Resuspension of the contaminated dust present the only exposure pathway for this location (that is, drinking water and irrigation water pathways would not be relevant). However, development and use of location-specific biosphere dose conversion factors for 5 and 80 kilometers would only serve to reduce the calculated impacts reported in this EIS. Therefore, using the biosphere dose conversion factors developed for the Viability Assessment (DOE 1998a, Volume 3, pages 3-158 to 3-161) for the 20-kilometer location at all other locations evaluated in this EIS is considered conservative.

I.5 Waterborne Radioactive Material Impacts

This section presents the total radiological dose to maximally exposed individuals, as calculated by the RIP model, at the following four groundwater withdrawal or discharge locations downgradient from the Yucca Mountain site where contaminated water could reach the accessible environment:

- A potential well 5 kilometers (3 miles) from the repository
- A potential well 20 kilometers (12 miles) from the repository
- A potential well 30 kilometers (19 miles) from the repository
- Franklin Lake Playa, the closest potential groundwater discharge point downstream from the repository [80 kilometers (50 miles)]

The total radiological dose was calculated from repository closure to 10,000 years following closure and at a time when the peak radiological dose would be observable. RIP model simulations carried out to 1 million years after repository closure also will include the peak radiological dose. These results are provided in Section I.5.1.

Apparent anomalous behavior of total radiological dose results predicted by the RIP model for the low and intermediate thermal load scenario under the Proposed Action inventory is explained in Section I.5.2.

The sensitivity of the estimates of waterborne radioactive material impacts to the fuel cladding model is examined in Section I.5.3.

I.5.1 TOTAL RELEASES DURING 10,000 YEARS AND 1 MILLION YEARS

The RIP model calculated radionuclide releases and radiological doses from individual nuclides and the total radiological dose due to all nine modeled radionuclides released from the repository from failed waste packages. The model calculated total radiological dose in either of two ways: as a single run using expected values of variable parameters, or in multiple realizations (runs) using randomly selected values for distributed parameters. The model can calculate the total radiological dose as the expected value of individual nuclides or the sum of all nuclides, for which sum the model chooses the mean value of all distributed parameters. In addition, the model can use the *Monte Carlo* code to stochastically, or randomly, perform any number of realizations or runs to select values of the distributed parameters. The stochastic nature of the predictions is shown by the complementary cumulative distribution function of the total radiological dose rate (that is, the sum of doses over all radionuclides) for 10,000 or 1 million years. The total radiological dose represents the radiological dose to a maximally exposed individual at the accessible environment using potentially affected groundwater for drinking water. The complementary cumulative distribution functions discussed in this section represent the result of 100 realizations of the RIP model.

The number of realizations used for a Monte Carlo simulation is an important issue with respect to the reliability of analysis results and proper allocation of resources. The number of runs required to reliably predict peak dose rates was examined (DOE 1998a, Volume 3, page 4-71). To verify that 100 realizations would be sufficient, 10,000-year and 100,000-year simulations for the high thermal load scenario with Proposed Action inventory were carried out with 1,000 and 300 realizations, respectively. The resulting distributions of peak individual radiological dose rates were compared with the 100-realization base case results for both periods. The complementary cumulative distribution functions for each time period were found to nearly match. The 100-realization complementary cumulative distribution functions did not go below a probability of 0.01 because each predicted dose rate has a probability of occurrence of one one-hundredth, or 0.01. Similarly, the 1,000- and 300-realization distributions display minimum probabilities of 0.001 and 0.003, respectively. Peak dose rates did continue to increase as probability decreased. Increased dose rates at these low probabilities were caused by combinations of extremely uncertain parameter values sampled from the tails of the parameter probability distributions. However, 100 realizations appear to be sufficient for a good compromise between cost and precision.

Figures I-37 through I-39 show the 10,000-year and 1-million-year complementary cumulative distribution functions of total peak radiological dose for the Proposed Action inventory (see Section I.3.1.2) at 5, 20, 30, and 80 kilometers (3, 12, 19, and 50 miles). In sequence, these figures show the total radiological dose at human exposure locations for the high, intermediate, and low thermal load scenarios and show that the maximum peak radiological dose (total for all nuclides) would occur well after 10,000 years. Further, the 10,000-year complementary cumulative distribution functions show that the distance (of the four distances analyzed) at which the highest total radiological dose would occur is 5 kilometers from the repository. As groundwater moves downgradient from the Yucca Mountain site, it flows from tuffaceous rocks to an alluvial aquifer. The pattern of the complementary cumulative distribution reflects the fact that there would be greater natural retardation in the alluvium than in the tuff portions of the hydrostratigraphic units.

Figures I-40 through I-42 show the 10,000-year and 1-million-year complementary cumulative distribution functions of total peak radiological doses for the Inventory Module 1 inventory at 5, 20, 30, and 80 kilometers (3, 12, 19, and 50 miles). In sequence, these figures show the total radiological doses at human exposure locations for the high, intermediate, and low thermal load scenarios. As for the Proposed Action inventory, these figures show that the maximum peak radiological dose (total, all nuclides) would occur well after 10,000 years. Again, the 10,000-year complementary cumulative distribution functions show that the distance (of the four distances analyzed) at which the highest total radiological dose would occur is 5 kilometers from the repository.

For the Viability Assessment and this EIS, the mean peak dose is the average peak dose of the 100 realizations of radiological dose to a maximally exposed individual (that is, the peak for each realization is determined and all peaks are averaged). The 95th-percentile peak dose is the average of the 95th- and 96th-highest ranked peak doses of the 100 realizations of radiological dose to a maximally exposed individual (that is, the peak for each realization is determined, those peaks are ordered from lowest to highest, and the average of the 95th- and 96th-highest is computed).

I.5.2 APPARENT ANOMALOUS BEHAVIOR BETWEEN LOW AND INTERMEDIATE THERMAL LOAD RESULTS FOR PROPOSED ACTION INVENTORY

Comparison of the expected-value simulations for the different thermal load scenarios at the same distance from the repository reveals apparent anomalous behavior. The differences between the scenarios involving low and intermediate thermal loads under the Proposed Action inventory, which show that the low thermal load curve crosses over the intermediate thermal load curve, require further explanation.

The analysis of three thermal load scenarios revealed some differences in performance as measured by the calculation of total radiological dose to maximally exposed individuals at various distances from the

repository. In particular, there is an apparent inconsistent relationship between the total dose-rate history curves for the low and intermediate thermal load scenarios at 20 kilometers (12 miles) from the repository. The apparent differences can be explained by the following factors:

- The effect of repository-area shape on the calculation of the dilution factor using the 3DADE analytical solution (Leij, Scaggs, and van Genuchten 1991, all)
- Waste package degradation differences resulting in the solubility-limited transport, among the different repository blocks being considered for disposal, of neptunium-237 from waste-form degradation
- The correlative differences in the percolation flux

I.5.2.1 Effect of the Dilution Factor

The saturated zone dilution factors were presented and discussed in Section I.4.5.4. As noted in that section, the major influences on the calculated dilution factors were the geometry of the total repository, the orientation of the repository relative to the direction of groundwater flow, and the average estimated infiltration for each repository block. The important finding was that for each repository configuration, extension of the repository area in a direction orthogonal to that of groundwater flow had little effect on the calculated dilution factor. However, when calculated for an enlargement parallel to groundwater flow, there were changes in the range of two to three times the dilution factors.

Thus, the intermediate thermal load Proposed Action scenario for the 20-kilometer (12-mile) distance had the same dilution factor as the high thermal load Proposed Action scenario, because the repository shape was relatively similar with essentially no change orthogonally to the flow direction. In contrast, the low thermal load Proposed Action scenario for the 20-kilometer distance has almost double the area of the intermediate thermal load Proposed Action scenario. Moreover, the repository is approximately twice as long in the direction parallel to groundwater flow, resulting in a dilution factor almost two times less than that of the intermediate thermal load Proposed Action scenario. Thus, because of the repository geometry, the dilution factors between the low and intermediate thermal load Proposed Action scenarios would result in less dilution under the low thermal load scenario.

I.5.2.2 Effect of Waste Package Degradation

Figure I-43 shows the total-radiological-dose-history curve for the Proposed Action inventory for the intermediate and low thermal load scenarios. The peak radiological dose from the low thermal load scenario is slightly delayed compared to the intermediate thermal load scenario, due to the delay in package failure initiation for the low thermal load scenario. An examination of the waste package failure distribution between these two scenarios (Figure I-44) shows that after the initial juvenile package failure (one package fails early for every case) stipulated by the Viability Assessment analysis, the first failure of the intermediate thermal load scenario is about 9,000 years after repository closure, whereas the first failure of the low thermal load scenario is about 27,000 years after repository closure. Thus, the amount of neptunium-237 available for removal from the repository is less for the low thermal load scenario than for the intermediate thermal load scenario.

The disparity in amount of neptunium-237 available for removal persists until the time of the super-pluvial climate. Figure I-43 shows that until the super-pluvial climate cycle (about 300,000 years after repository closure) the low thermal load total radiological dose history curve lies below and later than the intermediate thermal load total radiological dose history curve. Essentially, the peak radiological doses occur at different times by that same amount of material removed. At this time, the number of waste package failures has increased to allow differences in removal rates from the repository due to the solubility limitations of neptunium-237. A larger proportion of the neptunium-237 is removed under the

intermediate thermal load conditions because of the relatively higher amount of percolation flux and larger number of waste packages for the upper block for this scenario. However, more of the neptunium-237 remains in the repository under the low thermal load case because it can not all be removed from the larger repository area due to the reduced amount of water. The total-radiological-dose-to-receptor curve then crosses over the intermediate thermal load curve at about 300,000 years after closure. Thereafter, the two curves slowly approach one another during the remainder of the simulation but never recross during the simulated period.

I.5.2.3 Effect of Percolation Flux Distribution

The percolation flux differs across Yucca Mountain, especially in relation to the proposed areas. Figure I-45 shows the average percolation flux for the different repository areas. Note that Block 5 has the lowest percolation flux and Block 8 has the largest percolation flux. The intermediate thermal load Proposed Action scenario includes only the upper block (Block 1) and the capture areas are similar to the high thermal load Proposed Action scenario. The average infiltration flux for the upper block is larger than that for Block 8.

A sensitivity analysis using only the long-term average climate shows that the release rate of neptunium-237 at the top of the water table has two peaks. One is influenced by percolation flux in capture regions 1, 2, and 4, and the other is influenced by percolation flux in capture regions 3, 5, and 6. The reason for the two-peak aspect of the total release-rate curve is that neptunium-237 is solubility limited, and the lower percolation flux in the lower block and Block 8 does not completely remove all of the available neptunium-237 from these blocks at the same rate as in areas with greater percolation flux. The comparable curve for the intermediate thermal load Proposed Action scenario shows that all neptunium-237 is released at approximately the same time. Figures I-46 through I-49 show a comparison of the neptunium-237 radiological dose-rate histories for the low and intermediate thermal load scenarios for only the average long-term climate at the engineered barrier system and at the exposure location [20 kilometers (12 miles)]. These figures show that the difference in percolation flux is apparent at the engineered barrier system and accentuated in the saturated zone because of the retarded release of neptunium-237 under lower percolation flux. Because neptunium-237 is the dominant radionuclide contributing to the total radiological dose at times greater than 100,000 years, the curves indicating the low and intermediate thermal load total radiological-dose rate history cross. After crossing, the curves do not maintain their separation but tend to approach one another without recrossing for the remainder of the 1-million-year simulation period. It appears that they would likely cross again between 1 million and 1.5 million years at the observed rate of closure if the simulation were extended.

I.5.2.4 Conclusion

The analysis of the three thermal loads proposed for the planned repository configuration revealed anomalous differences in performance as measured by the calculation of total radiological dose to maximally exposed individuals at various distances from the repository. The apparent differences can be explained by three factors:

- The effect of repository area shape on the calculation of the saturated zone dilution factor using the 3DADE numerical code, based on an analytical solution to flow and transport from the repository
- Differences in waste package failure under the different thermal loads
- Differences in the percolation flux and the correlative neptunium-237 solubility-limited transport among the different repository blocks being considered for disposal

I.5.3 SENSITIVITY TO FUEL CLADDING MODEL

Section 5.4.4 of this EIS describes a sensitivity analysis DOE conducted to assess the importance of fuel pin cladding protection on radiological dose. This section contains additional details for the sensitivity analysis.

The average radionuclide inventory listed in Table I-1 for each commercial spent nuclear fuel waste package was used in the sensitivity analysis. Under the Proposed Action, approximately 1.2 percent of the spent nuclear fuel would have stainless-steel cladding rather than zirconium-alloy cladding. The stainless steel would degrade much faster than zirconium alloy, so the sensitivity analysis neglected stainless-steel cladding as a protective barrier. In addition, approximately 0.1 percent of the fuel pins are proposed to fail in the reactor environment. Thus, under the Proposed Action, 1.3 percent of the radionuclides in every spent nuclear fuel waste package would be available for degradation and transport as soon as the waste package failed.

For the purposes of comparison, the analysis performed additional stochastic runs for 10,000 and 1 million years after repository closure assuming the zirconium-alloy cladding would provide no resistance to water or radionuclide movement after the waste package failed. Table I-38 compares the peak radiological dose rate from groundwater transport of radionuclides for the base case and this case, which assures zirconium-alloy cladding would not be present. The analysis used data representing the high thermal load scenario to calculate individual exposures for a 20-kilometer (12-mile) distance only for purposes of comparison.

Table I-38. Comparison of consequences for a maximally exposed individual from groundwater releases of radionuclides using different fuel rod cladding models under the high thermal load scenario.

	Mean consequence[a]		95th-percentile consequence[b]	
Maximally exposed individual	Dose rate (millirem/year)	Probability of an LCF[c]	Dose rate (millirem/year)	Probability of an LCF
Peak at 20 kilometers[d] within 10,000 years after repository closure with cladding credit	0.22	7.6×10^{-6}	0.58	2.0×10^{-5}
Peak at 20 kilometers within 10,000 years after repository closure without cladding credit	5.4	1.9×10^{-4}	15	5.3×10^{-4}
Peak at 20 kilometers within 1 million years after repository closure with cladding credit	260	9.0×10^{-3}	1,400	5.0×10^{-2}
Peak at 20 kilometers within 1 million years after repository closure without cladding credit	3,000	1.1×10^{-1}	10,800	3.8×10^{-1}

a. Based on sets of 100 simulations of total system performance, each using random samples of uncertain parameters.
b. Represents a value for which 95 out of the 100 simulations yielded a smaller value.
c. LCF = latent cancer fatality; incremental lifetime (70 years) risk of contracting a fatal cancer for individuals, assuming a risk of 0.0005 latent cancer per rem for members of the public (NCRP 1993a, page 31).
d. To convert kilometers to miles, multiply by 0.62137.

Figure I-50 shows complementary cumulative distribution functions of the peak radiological dose rates for the four suites of model runs. Approximately 25 percent of the 10,000-year runs did not show any releases to the locations at a distance of 20 kilometers (12 miles). The zero releases are the reason the 10,000-year curves in Figure I-50 start at an exceedance probability of 0.73 and decrease with increasing radiological dose rate. All of the 1-million-year runs show releases at 20 kilometers.

The analysis assumed that the zirconium-alloy cladding would provide no barrier to water movement and radionuclide mobilization after the failure of the waste package. However, DOE expects that the zirconium alloy would provide some impediment to radionuclide mobilization when the waste package is breached. Therefore, the results for no cladding listed in Table I-38 should be viewed as an upper boundary.

I.6 Waterborne Chemically Toxic Material Impacts

Further transport analysis is warranted because the screening analysis (Section I.3.2.3.3) indicated that the repository could release chromium into groundwater in substantial quantities and thus could represent a human-health impact. Surrogate calculations were performed using the RIP model and inputs based on the radiological materials transport simulations. This approach selected a long-lived unretarded isotope (iodine-129) to serve as a surrogate for chromium. Iodine is highly soluble and exhibits little or no sorption so when corrected for radioactive decay, its movement represents scalar transport. This method avoided the extensive inputs necessary to define a new species for the RIP model and revision of the associated external function modules that the analysis had carefully constructed for the nine modeled radionuclides.

I.6.1 CHROMIUM

The screening analysis for chemically toxic materials (Section I.3.2.3) identified chromium from the waste packaging as a potential impact of concern. This section describes a chromium inventory for use in the RIP model and evaluates chromium impacts.

I.6.1.1 RIP Model Adaptations for Chromium Modeling

The following assumptions were applied to the chromium surrogate calculation approach:

1. Iodine-129 will serve adequately as a surrogate for chromium because it has a long radioactive half-life, lacks decay ingrowth by predecessors in a decay chain in the RIP model calculations, and is not retarded in groundwater (chromate is also unretarded). A small error introduced by the slight radioactive decay of iodine-129 during the model simulations can be corrected by an analytical expression as a postprocessing step.

2. Alloy-22 degradation and release is modeled using general corrosion depth of the corrosion-resistant material taken from WAPDEG modeling results (Mon 1999, all) for both dripping and nondripping conditions. The WAPDEG modeled the general corrosion depth (in millimeters per year) of corrosion-resistant material for 400 waste packages were averaged to produce a general degradation rate for dripping and nondripping conditions and converted to a fraction of corrosion-resistant material per year rate for use in the RIP model. The fractional degradation rate curves are show in Figure I-51.

3. Chromium associated with stainless-steel components used in many commercial spent nuclear fuel waste packages would be released proportionately with Alloy-22 chromium. This conservative assumption effectively assumes no credit for the delay of the onset of interior stainless-steel degradation or for the degradation rate of the interior stainless steel itself.

The treatment of Alloy-22 corrosion-resistant material degradation and chromium mobilization required the redefinition of the RIP container model. This calculation used the “Primary Container” in the RIP model to represent only the corrosion-allowance material (outer layer) of the waste package. The “Secondary Container” in the RIP model (used to represent cladding in the radiological material transport simulations) was not used. The waste matrix was used to represent the corrosion-resistant inner layer made of Alloy-22. These steps, with the proper material inventory and degradation coefficients, enabled the use of the current RIP model structure for this calculation.

The following additional changes were made to the radiological RIP model input files to conduct the surrogate chromium mobilization and migration calculation:

1. Iodine-129 solubility was specified as 1,976 grams per cubic meter (0.12 pounds per cubic foot), based on the near-field geochemistry screening study results for chromium (iodine-129 serving as a surrogate for chromium). Section I.3.2.3.1 contains details on determining this solubility limit.

2. For each source term, the inventory of all radionuclides (except iodine-129) received a value of zero.

3. The inventory of iodine-129 in each source term were specified in units of grams (rather than the original units of curies) per waste package using the values in Tables I-18 through I-22 in Section I.3. All inventory was assigned to the RIP model Waste Matrix Fraction (and none to the Primary or Secondary Container Fractions) in each source term.

4. The analysis assumed that mobilized chromium from the corrosion-resistant material would advect directly from the exposed corrosion-resistant material surface onto the invert (drift floor).

5. All secondary container definitions were all changed to a "degenerate" distribution at time zero, to eliminate the effects of any cladding protection from the calculation. A degenerate distribution simply results in all secondary containers failing at the specified time. The Alloy-22 corrosion-resistant material layer would be outside the cladding and, hence, not a barrier from this perspective.

6. The primary container definitions were changed to a "Degenerate" distribution at time zero, to eliminate the effects of corrosion-allowance material protection. This step is necessary because the protective benefits of the corrosion-allowance material are implicit in the WAPDEG results used to directly incorporate corrosion-resistant material degradation into the RIP model.

7. The waste-form-degradation rate for each source term was replaced with new variables representing weight-averaged Alloy-22 degradation. The definition of these degradation rates is detailed below.

8. RIP model output was requested in grams (mass) rather than curies (radioactivity).

To arrive at a weight-averaged fractional corrosion rate to apply to all waste packages of a given category (spent nuclear fuel, high-level radioactive waste, or DOE spent nuclear fuel) in a given repository region, the following steps were taken. The Alloy-22 generalized corrosion depth for dripping and nondripping conditions was converted to a fractional degradation rate, as described above. The Alloy-22 fractional corrosion rate was computed from a weighted average (with respect to the fraction of packages subject to dripping and nondripping conditions in the current climate) of dripping and nondripping generalized corrosion rates. This weight-averaged fractional degradation rate was then used to model the release of chromium from the waste package to the near-field environment.

For the Proposed Action, 30 percent of the chromium inventory would originate from interior stainless-steel components used in some commercial spent nuclear fuel waste packages (see Table I-16). Because the waste package would have to fail before degradation and transport of interior components could begin, simply adding the two chromium inventories together would yield artificially high results.

A two-stage scoping analysis, following the steps outlined above for using the RIP model to calculate chromate migration, was performed for the Proposed Action inventory under the high thermal load scenario to predict chromate concentrations at the 5-kilometer (3-mile) distance. In the first stage, the model was run with only the chromium inventory from the Alloy-22 corrosion-resistant material [904,000 grams (about 2,000 pounds) of chromium per commercial spent nuclear fuel waste package] following the steps outlined above for chromium modeling. In the second stage, the model was run again with only the

interior stainless-steel inventory [514,000 grams (about 1,100 pounds) of chromium per commercial spent nuclear fuel waste package] but used the complete WAPDEG waste package model (as used in the Viability Assessment) to represent complete waste package containment. Only the commercial spent nuclear fuel packages would differ; no interior stainless-steel internal components would be used in high-level radioactive waste or DOE spent nuclear fuel containers. Each RIP model run was held to the same random number seed (used to "seed" the random number generator that is used to select random values of stochastic parameters) so the realizations would be replicated. The results of each simulation were summed, with respect to realization and time step, to calculate the total chromium concentration at 5 kilometers (3 miles). The results are listed in Table I-39.

Table I-39. Chromium groundwater concentrations (milligrams per liter)[a] at 5 kilometers (3 miles) under Proposed Action inventory using the high thermal load scenario and a two-stage RIP model.

	Peak chromium concentration	
Model	Mean	95th-percentile
RIP Stage 1: Corrosion-resistant material (Alloy-22) chromium inventory	0.0085	0.037
RIP Stage 2: Interior-to-waste package (SS/B[b] alloy) chromium inventory	0.000000086	0.00000048
Totals (Stage 1 + Stage 2, by realization; time step)	**0.0085**	**0.037**

a. To convert milligrams per liter to pounds per cubic foot, multiply by 0.00000624.
b. SS/B = stainless-steel boron.

The chromium concentrations obtained in this scoping analysis demonstrated that the inventory of chromium associated with interior stainless-steel components, although it would represent 30 percent of the total chromium inventory, would be small with respect to the peak chromium concentration in groundwater at the closest downgradient location considered. Including the interior stainless-steel chromium inventory increased the estimate of the mean peak chromium concentration by 0.00088 percent over modeling the corrosion-resistant material chromium alone. The 95th-percentile peak chromium concentration was increased by 0.000072 percent over modeling the corrosion-resistant material inventory of chromium alone. Therefore, an additional step to model the interior stainless-steel corrosion and transport was unnecessary to predict peak chromate concentrations.

Two factors would contribute to the inconsequential impact of the chromium inventory from the waste package interior. First, the Alloy-22 in the waste package would have to be breached before interior stainless steel was exposed to water and began to degrade. Thus, much of the chromium in the Alloy-22 would already have migrated before the interior stainless-steel chromium began to degrade and migrate. Second, the Alloy-22 degradation would depend strongly on the RIP model parameters controlling the fraction of packages exposed to dripping conditions. Packages that experienced dripping conditions would degrade much faster; only those that experienced dripping conditions would fail within 10,000 years and permit exposure of interior stainless steel. The vast majority of waste packages would not fail, so the interior chromium inventory would never be exposed for degradation and transport.

Based on this demonstration of the relative unimportance of the interior stainless-steel chromate inventory in calculating peak chromium concentrations within 10,000 years, only the corrosion-resistant material (Alloy-22) in the chromium inventory was simulated for analysis of chromium impacts as a waterborne chemically toxic material.

I.6.1.2 Results for the Proposed Action

The chromium-migration calculation was conducted for the Proposed Action inventory under the high, intermediate, and low thermal load scenarios using the same stochastic approach as that used for the waterborne radioactive material assessment. The 100 independent realizations, using randomly selected input parameter values chosen from assigned probability distributions of values, were simulated with the RIP model. Simulations were performed to estimate chromium concentrations at 5, 20, 30, and 80 kilometers (3, 12, 19, and 50 miles) for 10,000 years following closure. The resulting concentrations

were decay-corrected to remove the slight radioactive decay calculated by the RIP model for the surrogate constituent, iodine-129.

The mean peak concentrations and 95th-percentile peak concentrations computed with the RIP model, using the surrogate chromium-migration calculation described above, are listed in Table I-40 for all thermal load scenarios under the Proposed Action. Figures I-52 through I-54 show the complementary cumulative distribution function for the 100 realizations of chromium concentration under the Proposed Action at each of the four locations for the low, intermediate, and high thermal load scenarios, respectively.

Table I-40. Peak chromium groundwater concentration (milligrams per liter)[a] under the Proposed Action inventory.[b]

Thermal load	Maximally exposed individual	Mean	95th-percentile
High	At 5 kilometers[c]	0.0085	0.037
	At 20 kilometers	0.0028	0.012
	At 30 kilometers	0.0018	0.0063
	At 80 kilometers	0.00022	0.00061
Intermediate	At 5 kilometers	0.0029	0.0096
	At 20 kilometers	0.0023	0.010
	At 30 kilometers	0.00080	0.0038
	At 80 kilometers	0.000031	0.00015
Low	At 5 kilometers	0.0046	0.016
	At 20 kilometers	0.0018	0.0083
	At 30 kilometers	0.00067	0.0033
	At 80 kilometers	0.000053	0.00034

a. To convert milligrams per liter to pounds per cubic foot, multiply by 0.0000624.
b. Based on 100 repeated simulations of total system performance, each using randomly sampled values of uncertain parameters.
c. To convert kilometers to miles, multiply by 0.62137.

A simple sensitivity run, reducing the solubility limit of the iodine-129 surrogate by one order of magnitude (from 1,976 to 197.6 milligrams per liter), demonstrated that the imposed value of the solubility limit did not affect the resulting concentration at the accessible environment. This demonstration suggests that the chromium degradation rate is a major controlling factor over the release of chromium.

There are two measures for comparing human health effects for chromium. When the Environmental Protection Agency established its Maximum Contaminant Level Goals, it considered safe levels of contaminants in drinking water and the ability to achieve these levels with the best available technology. The Maximum Contaminant Level Goal for chromium is 0.1 milligram per liter (0.0000062 pound per cubic foot) (40 CFR 141.51). The other measure for comparison is the reference dose factor for chromium, which is 0.005 milligram per kilogram (0.0004 ounce per pound) of body mass per day (EPA 1999, all). The reference dose factor represents a level of intake that has no adverse effect on humans. It can be converted to a threshold concentration level for drinking water. The conversion yields essentially the same concentration for the reference dose factor as the Maximum Contaminant Level Goal.

No attempt can be made at present to estimate the groundwater concentrations of hexavalent chromate in Table I-40, in terms of human health effects (for example, latent cancer fatalities). The carcinogenicity of hexavalent chromium by the oral route of exposure cannot be determined because of a lack of sufficient epidemiological or toxicological data (EPA 1999, all; EPA 1998, page 48).

I.6.1.3 Results for Inventory Modules 1 and 2

Chromium impacts were calculated for Inventory Modules 1 and 2 using the same approach as for the Proposed Action. Peak mean and 95th-percentile chromium concentrations for Inventory Modules 1 and 2 are listed in Tables I-41 and Table I-42, respectively. Figures I-55 through I-57 show the complementary cumulative distribution function for the 100 realizations of chromium concentration for Inventory Module 1 at each of the four locations for the low, intermediate, and high thermal load scenarios, respectively.

Table I-41. Peak chromium groundwater concentration (milligrams per liter)[a] for 10,000 years after closure under Inventory Module 1.[b]

Thermal load	Maximally exposed individual	Mean	95th-percentile
High	At 5 kilometers[c]	0.032	0.14
	At 20 kilometers	0.018	0.10
	At 30 kilometers	0.0057	0.027
	At 80 kilometers	0.00029	0.00070
Intermediate	At 5 kilometers	0.023	0.083
	At 20 kilometers	0.0089	0.042
	At 30 kilometers	0.0032	0.017
	At 80 kilometers	0.00019	0.00057
Low	At 5 kilometers	0.0093	0.0353
	At 20 kilometers	0.0050	0.022
	At 30 kilometers	0.0020	0.0084
	At 80 kilometers	0.000074	0.00026

a. To convert milligrams per liter to pounds per cubic foot, multiply by 0.0000624.
b. Based on 100 repeated simulations of total system performance, each using randomly sampled values of uncertain parameters.
c. To convert kilometers to miles, multiply by 0.62137.

Table I-42. Peak chromium groundwater concentration (milligrams per liter)[a] due only to Greater-Than-Class-C and Special-Performance-Assessment-Required wastes for 10,000 years after closure under Inventory Module 2.[b]

Thermal load	Maximally exposed individual	Expected Value
High	At 5 kilometers[c]	0.0014
	At 20 kilometers	0.00058
	At 30 kilometers	0.00021
	At 80 kilometers	0.000000012
Intermediate	At 5 kilometers	0.00080
	At 20 kilometers	0.00033
	At 30 kilometers	0.00012
	At 80 kilometers	0.0000000094
Low	At 5 kilometers	0.00060
	At 20 kilometers	0.00025
	At 30 kilometers	0.000086
	At 80 kilometers	0.000000010

a. To convert milligrams per liter to pounds per cubic foot, multiply by 0.0000624.
b. Based on an expected value simulation using the mean of all stochastic parameters for the additional inventory of Inventory Module 2 over Inventory Module 1.
c. To convert kilometers to miles, multiply by 0.62137.

There are two measures for comparing human health effects for chromium. When the Environmental Protection Agency established its Maximum Contaminant Level Goals, it considered safe levels of contaminants in drinking water and the ability to achieve these levels with the best available technology. The Maximum Contaminant Level Goal for chromium is 0.1 milligram per liter (0.0000062 pound per

cubic foot) (40 CFR 141.51). The other measure for comparison is the reference dose factor for chromium, which is 0.005 milligram per kilogram (0.0004 ounce per pound) of body mass per day (EPA 1999, all). The reference dose factor represents a level of intake that has no adverse effect on humans. It can be converted to a threshold concentration level for drinking water. The conversion yields essentially the same concentration for the reference dose factor as the Maximum Contaminant Level Goal.

No attempt can be made at present to express the estimated groundwater concentrations of hexavalent chromate in Table I-42 in terms of human health effects (for example, latent cancer fatalities). The carcinogenicity of hexavalent chromium by the oral route of exposure cannot be determined because of a lack of sufficient epidemiological or toxicological data (EPA 1999, all; EPA 1998, page 48).

I.6.2 MOLYBDENUM

Alloy-22 used as a waste package inner barrier also contains 13.5 percent molybdenum (ASTM 1994, page 2). During the corrosion of Alloy-22, molybdenum behaves almost the same as the chromium. Due to the corrosion conditions, molybdenum also dissolves in a highly soluble hexavalent form. Therefore, the source term for molybdenum will be exactly 13.5/22 times (61.4 percent) the source term for chromium. All the mechanisms and parameters are the same as those used for chromium so modeling is unnecessary. It is reasonable to assume that molybdenum would be present in the water at concentrations 61.4 percent of those reported above for chromium.

There is currently no established toxicity standard for molybdenum (in particular, the Environmental Protection Agency has not established a Maximum Contaminant Level Goal for molybdenum), although this does not mean that molybdenum is not toxic. The concentrations of molybdenum would be very small, so no effect would be likely to result from the molybdenum released to the groundwater.

I.6.3 URANIUM

While the screening analysis indicated that elemental uranium would not pose a health risk as a waterborne chemically toxic material (see Section I.3.2.3.3), it was retained for consideration for other reasons. The total uranium inventory (all uranium isotopes) is listed for the inventory modules in Table I-23.

The reference dose for elemental uranium is 0.003 milligram per kilogram of body mass per day (EPA 1999, all). Assuming that a child would experience the maximum individual exposure from the drinking-water pathway, the analysis used a 1-liter (0.26-gallon) daily intake rate and a 16-kilogram (35-pound) body weight to convert the reference dose to a threshold concentration of 4.8×10^{-2} milligram per liter (2.9×10^{-6} pound per cubic foot).

I.6.3.1 RIP Model Adaptations for Elemental Uranium Modeling

To evaluate the consequences of total uranium migration, the mobilization and transport of the total uranium inventory for the Proposed Action listed in Table I-23 were simulated using the RIP model. The following steps were taken in the RIP model adaptation for the total uranium simulations:

1. The inventory of all radionuclides except uranium was set to zero (as a precaution and to prevent confusion with radiological runs).

2. The inventory of uranium (all isotopes) was changed to 8,119 kilograms (17,900 pounds) for commercial spent nuclear fuel packages, 786 kilograms (1,730 pounds) for DOE spent nuclear fuel packages, and 2,826 kilograms (6,220 pounds) for high-level radioactive waste packages.

3. Output from the RIP model was requested in grams rather than curies.

4. The radiological decay rate of uranium-234 was left to represent all uranium isotopes in the waste packages, although the resulting concentrations obtained from RIP model simulations were decay-corrected to provide undecayed concentrations. Various uranium isotopes have different half-lives, so the analysis ignored decay benefits in reducing impacts.

5. Because the chemical properties (such as sorption rate) are functions of the element and not the isotope, the other transport properties of uranium were left the same as those used for the radiological consequences simulations.

6. Use of the parameter FCSOLU, which is used in the RIP model to partition the solubility coefficient to account for the fact that radionuclide simulations model only one isotope of uranium, was omitted for full uranium elemental simulations.

DOE ran 100 simulations to model the release and transport of uranium. The Proposed Action inventory is approximately 70,000 MTHM (77,000 tons). Although a small percentage of the heavy metal in the spent fuel is not uranium, it was reasonable to assume all of it was because doing so had a very small effect on the result and would make the analysis more conservative. This assumption introduced an approximate 7-percent increase into the result. The runs are based on the high thermal load scenario, and the consequences are computed for 5 kilometers (3 miles) from the repository. In addition, the analysis neglected radioactive decay. Most of the uranium present has a very long half-life compared to the analysis period, so decay would have a very small conservative effect on the result.

I.6.3.2 Results for the Proposed Action

The Proposed Action inventory of elemental uranium would be approximately 65 million kilograms (72,000 tons) (see Table I-23). Total elemental uranium migration calculations were made using the RIP model code for the Proposed Action inventory under the high thermal load scenario for 10,000 years following closure for the 5-kilometer (3-mile) distance. The resulting concentrations of elemental uranium in groundwater at the 5-kilometer (3-mile) discharge location were obtained from the simulation results.

The reference dose for elemental uranium is 3.0×10^{-3} milligram per kilogram (4.8×10^{-8} ounce per pound) of food intake per day (EPA 1999, all). Assuming that a child would experience the maximum individual exposure for the drinking water scenario, the analysis used a 1-liter (0.26-gallon) daily intake rate and a 16-kilogram (35-pound) body weight to convert the reference dose to a threshold concentration. The threshold concentration would be 0.048 milligram per liter (3.0×10^{-6} pound per cubic foot).

The maximum uranium concentration over 10,000 years was extracted for each of the 100 sets of simulation results. The mean peak concentration of uranium would be 6.7×10^{-8} milligram per liter (5.2×10^{-9} pound per cubic foot), and the 95th-percentile peak concentration would be 2.2×10^{-8} milligram per liter (1.7×10^{-9} pound per cubic foot). These concentrations would be six orders of magnitude lower than the threshold concentration for the oral reference dose, so DOE expects no human health effects from the chemical effects of waterborne uranium under the high thermal load scenario.

Figure I-58 shows the complementary cumulative distribution function for elemental uranium concentrations at the 5-kilometer (3-mile) discharge location for 10,000 years following closure under the high thermal load scenario. The groundwater concentration information in this figure shows that uranium, as a chemically toxic material, would be far below the reference dose at any probability level.

Based on trends in waterborne radioactive material results, the concentrations of elemental uranium at locations that were more distant [20, 30, and 80 kilometers (12, 19, and 50 miles)] and for the intermediate and low thermal load scenarios at all distance would be even lower. Because of the extremely low concentrations from these simulations, further simulations were unnecessary to evaluate

other thermal loads under the Proposed Action. Elemental uranium would not present a health risk as a chemically toxic material under the Proposed Action for any thermal load scenario.

I.6.4 RESULTS FOR INVENTORY MODULES 1 AND 2

Under Inventory Modules 1 and 2, the total uranium inventory would increase from the Proposed Action total of 70,000 MTHM to 120,000 MTHM (Table I-18). The 70-percent increase in elemental uranium inventory would be likely to increase the groundwater concentration at the discharge location (1) at most, if the percentage of the inventory was increased, or (2) by less, if solubility limits were exceeded along the transport paths in groundwater in any case. Even doubling the groundwater concentrations calculated for the Proposed Action inventory would result in concentration levels that would be several orders of magnitude below the reference dose concentration level. Therefore, elemental uranium would not present a substantial health risk as a chemically toxic material under Inventory Module 1 or 2 for any thermal load scenario.

I.7 Atmospheric Radioactive Material Impacts

After DOE closed the Yucca Mountain Repository, there would be limited potential for releases to the atmosphere because the waste would be isolated far below the ground surface. Still, the rock is porous and does allow gas to flow, so the analysis must consider possible airborne releases. The only radionuclide that would have a relatively large inventory and a potential for gas transport is carbon-14. Iodine-129 can exist in a gas phase, but it is highly soluble and therefore would be more likely to dissolve in groundwater rather than migrate as a gas. Other gas-phase isotopes were eliminated in the screening analysis (Section I.3), usually because of short half-lives and because they are not decay products of long-lived isotopes. After carbon-14 escaped from the waste package, it could flow through the rock in the form of carbon dioxide. Atmospheric pathway models were used to estimate human health impacts to the local population in the 84-kilometer (52-mile) region surrounding the repository.

About 2 percent of the carbon-14 in commercial spent nuclear fuel exists as a gas in the space (or *gap*) between the fuel and the cladding around the fuel (Oversby 1987, page 92). The average carbon-14 inventory in a commercial spent nuclear fuel waste package is approximately 12 curies (see Table I-1), so the analysis used a gas-phase inventory of 0.23 curie of carbon-14 per commercial spent nuclear fuel waste package to calculate impacts from the atmospheric release pathway. The analysis described in Section 5.4 included the entire inventory of the carbon-14 in the repository in the groundwater release models. Thus, the groundwater-based impacts would be overestimated slightly (by 2 percent) by this modeling approach.

Carbon is the second-most abundant element (by mass) in the human body, constituting 23 percent of Reference Man (ICRP 1975, page 377). Ninety-nine percent of the carbon comes from food ingestion (Killough and Rohwer 1978, page 141). Daily carbon intakes are approximately 300 grams (0.7 pound) and losses include 270 grams (0.6 pound) exhaled, 7 grams (0.02 pound) in feces, and 5 grams (0.01 pound) in urine (ICRP 1975, page 377).

Carbon-14 dosimetry can be performed assuming specific-activity equivalence. The primary human-intake pathway of carbon is food ingestion. The carbon-14 in food results from photosynthetic processing of atmospheric carbon dioxide, whether the food is the plant itself or an animal that feeds on the plant. Biotic systems, in general, do not differentiate between carbon isotopes. Therefore, the carbon-14 activity concentration in the atmosphere will be equivalent to the carbon-14 activity concentration in the plant, which in turn will result in an equivalent carbon-14 specific activity in human tissues.

I.7.1 CARBON-14 RELEASES TO THE ATMOSPHERE

The calculation of regional radiological doses requires estimation of the annual release rate of carbon-14. The analysis based the carbon-14 release rate on the predicted timeline of container failures for the high thermal load scenario, using average values for the stochastic parameters that were entered. The expected number of spent nuclear fuel waste package failures in 100-year intervals was used to estimate the carbon-14 release rate after repository closure. The estimated amount of material released from each package as a function of time was reduced to account for radiological decay.

As for the waterborne releases described in Section 5.4, some credit was taken for the intact zirconium-alloy cladding (on approximately 99 percent by volume of the spent nuclear fuel) delaying the release of gas-phase carbon-14. The remaining 1 percent by volume of the spent nuclear fuel either would have stainless-steel cladding (which degrades much more quickly than zirconium alloy) or would already have failed in the reactor. The RIP model uses a waste package failure model that conceptually divides the surface area of the waste packages into many *patches.* A corrosion future for each patch is then calculated. The zirconium-alloy cladding failure model is implemented in the same fashion, with the cladding corrosion rate set to a fraction of the corrosion rate of the Alloy-22 in the inner shell of the waste package. This analysis set the cladding corrosion rate for the zirconium alloy to the same value used in the Viability Assessment (DOE 1998a, Volume 3, page 3-101). A plot of the patch-area fraction of the zirconium-alloy cladding that has failed as a function of time after repository closure is shown in Figure I-59. Although difficult to see on the plot scale, no zirconium-alloy cladding would fail during the first 5,000 years after repository closure.

The amount (in curies) of carbon-14 that would be available for transport from a failed waste package, A_T, is calculated as:

$$A_T = (F_{IF} + F_{FC}) \times 0.23 \text{ curies per package}$$

where:

F_{IF} = fraction immediately failed (fuel with stainless-steel cladding or previously failed fuel pins)

F_{FC} = fraction of failed cladding (if the value shown in Figure I-59 is less than 0.01, then that value is used; if the value shown in Figure I-59 exceeds 0.01, then a value of 0.9875 is used)

The model uses the patch failure rate on the zirconium alloy as the fraction of the failed pins until the patch failure rate reaches 1 percent. After the patch failure rate reaches 1 percent, the release rate is reset to not take further credit for zirconium-alloy cladding reducing the transport rate of gas-phase carbon-14. Rather than conducting a detailed gas-flow model of the mountain, the analysis assumed that the carbon-14 from the failed waste package would be released to the ground surface uniformly over a 100-year interval. Thus, the release rate to the ground surface for a waste package would be A_T divided by 100 (curies per year).

Figure I-60 shows the estimated release rate of carbon-14 from the repository for 50,000 years after repository closure, assuming that the spent nuclear fuel with stainless-steel cladding had failed and released its gas-phase carbon-14 prior to being placed in a waste package. This assumption is represented by F_{IF}=0 in the calculation for A_T. The results in Figure I-60 are based on the Proposed Action inventory. Each symbol in the figure represents the carbon-14 release rate to the ground surface for a period of 100 years. The general downward slope of the symbols is due to radioactive decay (carbon-14 has a half-life of 5,730 years). The symbols marking zero releases (curies per year) indicate that no waste packages failed during some 100-year periods. The jagged nature of the plot indicates a different number of waste packages failing in different 100-year intervals. Only 97 of 7,760 spent nuclear fuel waste packages would have failed during the first 10,000 years after repository closure. By 40,000 years after repository

closure, 676 of the 7,760 spent nuclear fuel waste packages would have failed. Using this expected-value representation of waste package lifetime, no more than three waste packages would have failed in any single 100-year interval before 30,000 years after repository closure. Between 30,000 and 50,000 years after repository closure, as many as five waste packages would fail in a single 100-year interval. The maximum release rate would occur about 19,000 years after repository closure. The estimated maximum release rate would be about 0.098 microcurie per year.

I.7.2 ATMOSPHERE CONSEQUENCES TO THE LOCAL POPULATION

DOE used the GENII-S code (Leigh et al. 1993, all) to model the atmospheric transport and human uptake of released carbon-14 for the 84-kilometer (52-mile) population radiological dose calculation. This calculation used 84 kilometers rather than the typical 80 kilometers (50 miles) used in an EIS to include the population of Pahrump, Nevada, in the impact estimate. Radiological doses to the regional population near Yucca Mountain from carbon-14 releases were estimated using the population distribution compiled from DOE (1998a, Volume 3, Figure 3-76), which indicates approximately 28,000 people would live in the region surrounding Yucca Mountain in the year 2000. The population by distance and sector used in the calculations are listed in Table I-43. The computation also used current (1993 to 1996) annual average meteorology. The joint frequency data are listed in Table I-44.

Table I-43. Population by sector and distance from Yucca Mountain used to calculate regional airborne consequences.[a]

	Distance from the repository (kilometers)[b]										
Direction	6[c]	16	24	32	40	48	56	64	72	84	*Totals*[d]
S	0	0	16	238	430	123	0	10	0	0	*817*
SSW	0	0	0	315	38	0	0	7	0	0	*360*
SW	0	0	0	0	0	0	868	0	0	0	*868*
WSW	0	0	0	0	0	0	0	0	87	0	*87*
W	0	0	0	638	17	0	0	0	0	0	*655*
WNW	0	0	0	936	0	0	0	0	0	20	*956*
NW	0	0	0	28	2	0	0	0	33	0	*63*
NNW	0	0	0	0	0	0	0	0	0	0	*0*
N	0	0	0	0	0	0	0	0	0	0	*0*
NNE	0	0	0	0	0	0	0	0	0	0	*0*
NE	0	0	0	0	0	0	0	0	0	0	*0*
ENE	0	0	0	0	0	0	0	0	0	0	*0*
E	0	0	0	0	0	0	0	0	0	0	*0*
ESE	0	0	0	0	0	0	0	0	1,055	0	*1,055*
SE	0	0	0	0	3	0	13	0	0	206	*222*
SSE	0	0	0	0	23	172	6	17	6,117	16,399	*22,734*
Totals	**0**	**0**	**16**	**2,155**	**513**	**295**	**887**	**34**	**7,292**	**16,625**	***27,817***

a. Source: Compiled from DOE (1998a, Volume 3, Figure 3-76).
b. To convert kilometers to miles, multiply by 0.62137.
c. The 80-kilometer (50-mile) distance typically used in an EIS analysis was increased to 84 kilometers (52 miles) in order to include the population of Pahrump in the SSE sector in the calculations.
d. Population figures are estimates for 2000.

A population radiological dose factor of 2.2×10^{-9} person-rem per microcurie per year of release was calculated by the GENII code. For a 0.098-microcurie-per-year release, this corresponds to a 7.8×10^{-15}-rem-per-year average radiological dose to individuals in the population. Thus, a maximum 84-kilometer (52-mile) population radiological dose rate would be 2.2×10^{-10} person-rem per year. This radiological dose rate represents 1.1×10^{-13} latent cancer fatalities in the regional population of 28,000

Table I-44. Meteorologic joint frequency data used for Yucca Mountain atmospheric releases (percent of time).[a]

Average wind speed (m/s)[b]	Atmospheric stability class	Direction (wind toward)															
		S	SSW	SW	WSW	W	WNW	NW	NNW	N	NNE	NE	ENE	E	ESE	SE	SSE
0.9	A	0.807	0.633	0.613	0.520	0.462	0.604	0.688	0.659	0.467	0.340	0.183	0.200	0.197	0.212	0.412	0.778
	B	0.279	0.479	0.392	0.325	0.372	0.540	1.243	2.279	1.484	0.499	0.290	0.192	0.105	0.070	0.087	0.305
	C	0.113	0.105	0.064	0.017	0.015	0.020	0.041	0.157	0.122	0.067	0.055	0.020	0.012	0.020	0.009	0.032
	D	0.003	0.003	0	0	0	0	0	0	0	0	0	0	0	0	0	0
	E	0	0	0	0	0	0	0	0	0	0	0	0	0	0	0	0
	F	0	0	0	0	0	0	0	0	0	0	0	0	0	0	0	0
2.55	A	0.099	0.073	0.026	0.020	0.026	0.017	0.023	0.061	0.041	0.029	0.023	0.017	0.029	0.029	0.052	0.096
	B	0.058	0.044	0.038	0.026	0.032	0.061	0.125	0.377	0.360	0.070	0.049	0.015	0.009	0	0.009	0.017
	C	0.229	0.267	0.256	0.116	0.110	0.105	0.328	1.193	2.404	0.909	0.671	0.302	0.157	0.142	0.125	0.174
	D	0.105	0.049	0.038	0.003	0.003	0.003	0.006	0.035	0.444	0.290	0.206	0.055	0.035	0.049	0.087	0.099
	E	0.003	0.006	0	0.003	0	0	0.003	0.003	0.003	0.006	0.003	0.003	0.003	0.003	0	0.003
	F	0	0.003	0	0	0	0	0	0	0.003	0.003	0	0	0	0	0	0.003
4.35	A	0.096	0.096	0.041	0.015	0.012	0.009	0.015	0.023	0.058	0.044	0.026	0.023	0.029	0.020	0.020	0.070
	B	0.052	0.087	0.041	0.023	0.006	0.026	0.078	0.261	0.305	0.131	0.076	0.017	0.006	0.003	0.009	0.032
	C	0.142	0.241	0.168	0.070	0.029	0.076	0.131	0.740	1.638	0.308	0.290	0.119	0.049	0.041	0.038	0.102
	D	0.253	0.264	0.163	0.049	0.020	0.020	0.020	0.392	2.375	0.447	0.285	0.081	0.046	0.058	0.139	0.346
	E	0.006	0.017	0	0	0	0	0	0.003	0.006	0.020	0.015	0.006	0.003	0.003	0.012	0.020
	F	0	0	0	0	0	0	0	0	0	0	0	0	0	0	0	0
6.95	A	1.568	0.642	0.215	0.038	0.035	0.009	0.023	0.026	0.081	0.142	0.261	0.163	0.209	0.314	0.343	0.819
	B	0.682	0.552	0.067	0.003	0.006	0.006	0.023	0.058	0.348	0.325	0.267	0.131	0.078	0.093	0.078	0.256
	C	0.993	0.560	0.105	0.012	0.009	0.078	0.090	0.244	0.984	0.526	0.337	0.192	0.067	0.076	0.073	0.189
	D	1.594	0.912	0.183	0.020	0.020	0.006	0.035	0.566	3.368	0.430	0.160	0.128	0.035	0.044	0.142	0.598
	E	0.735	0.366	0.067	0.012	0.006	0	0	0.386	2.515	0.192	0.038	0.015	0	0.015	0.064	0.804
	F	0.238	0.096	0.003	0	0.003	0	0	0.142	1.641	0.055	0.032	0	0.003	0.003	0.029	0.796
9.75	A	2.134	0.935	0.218	0.078	0.029	0.041	0.026	0.070	0.163	0.232	0.203	0.232	0.267	0.372	0.587	1.388
	B	0.865	0.627	0.081	0.009	0.003	0.017	0.020	0.046	0.319	0.267	0.154	0.131	0.070	0.052	0.113	0.302
	C	0.720	0.261	0.038	0.012	0.020	0.020	0.009	0.076	0.502	0.299	0.148	0.229	0.078	0.032	0.041	0.157
	D	0.415	0.212	0.020	0.003	0.003	0.003	0.003	0.046	0.627	0.154	0.044	0.032	0.029	0.009	0.026	0.145
	E	0.029	0.006	0	0	0.003	0	0	0	0.006	0.003	0.003	0	0	0.003	0	0.003
	F	0	0.003	0	0	0	0	0	0	0	0	0	0	0	0.003	0	0.003
12.98	A	1.661	0.706	0.418	0.322	0.247	0.244	0.366	0.343	0.407	0.380	0.302	0.299	0.357	0.537	1.083	2.038
	B	0.836	0.668	0.253	0.107	0.157	0.116	0.264	0.499	0.674	0.404	0.270	0.171	0.122	0.096	0.232	0.950
	C	0.322	0.267	0.087	0.017	0.006	0.012	0.026	0.136	0.311	0.107	0.032	0.029	0.020	0.009	0.015	0.038
	D	0.006	0.006	0	0	0	0	0	0.003	0.012	0.003	0	0	0	0	0	0.003
	E	0	0	0	0	0	0	0	0	0	0	0	0	0	0	0	0
	F	0	0	0	0	0	0	0	0	0	0	0	0	0	0	0	0

a. Source: Adapted from data in TRW (1999d, Appendix B, all)
b. To convert meters per second to feet per second, multiply by 3.2808.

persons each year at the maximum release rate. This annual population radiological dose rate corresponds to a lifetime radiological dose of 1.5×10^{-8} rem over a 70-year lifetime, which corresponds to 7.6×10^{-12} latent cancer fatalities during the 70-year period of the maximum release.

I.7.3 SENSITIVITY TO THE FRACTION OF EARLY-FAILED CLADDING

DOE performed a sensitivity analysis in which all of the cladding on commercial spent nuclear fuel that had stainless-steel cladding (about 1.3 percent of the fuel by volume) was assumed to fail immediately as the waste package failed. The commercial spent nuclear fuel with zirconium-alloy cladding was assumed to fail as shown in Figure I-57. The number of latent cancer fatalities per year in the local population at the time of maximum release would increase from 1.1×10^{-13} to 4.0×10^{-11} under the sensitivity analysis assumptions. The time of maximum release would be 2,000 years after repository closure rather than 19,000 years after repository closure.

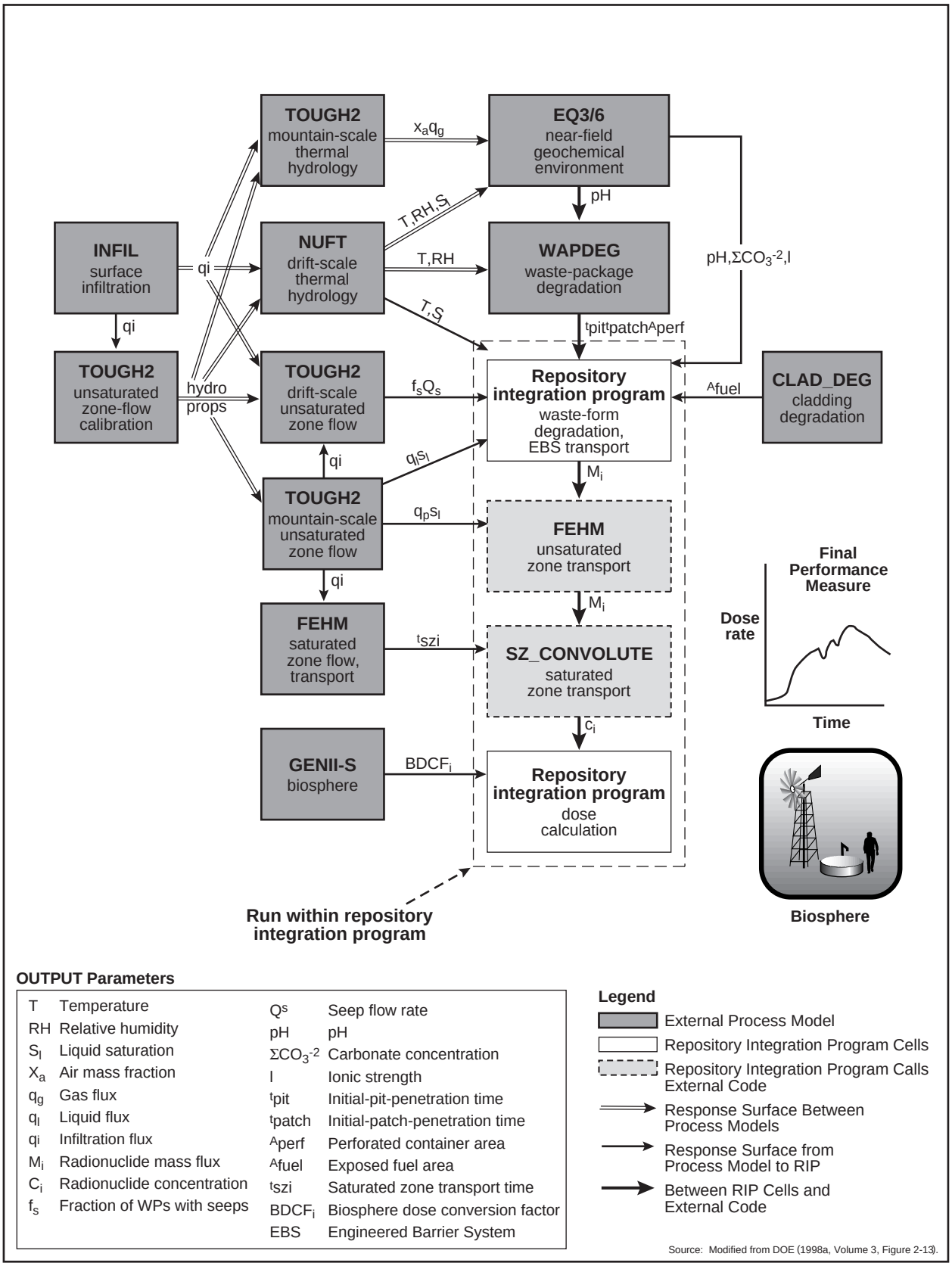

OUTPUT Parameters

T	Temperature	Q^s	Seep flow rate
RH	Relative humidity	pH	pH
S_l	Liquid saturation	ΣCO_3^{-2}	Carbonate concentration
X_a	Air mass fraction	I	Ionic strength
q_g	Gas flux	^{t}pit	Initial-pit-penetration time
q_l	Liquid flux	^{t}patch	Initial-patch-penetration time
q_i	Infiltration flux	^{A}perf	Perforated container area
M_i	Radionuclide mass flux	^{A}fuel	Exposed fuel area
C_i	Radionuclide concentration	^{t}szi	Saturated zone transport time
f_s	Fraction of WPs with seeps	$BDCF_i$	Biosphere dose conversion factor
		EBS	Engineered Barrier System

Legend

- External Process Model
- Repository Integration Program Cells
- Repository Integration Program Calls External Code
- Response Surface Between Process Models
- Response Surface from Process Model to RIP
- Between RIP Cells and External Code

Source: Modified from DOE (1998a, Volume 3, Figure 2-13).

Figure I-1. Total system performance assessment model.

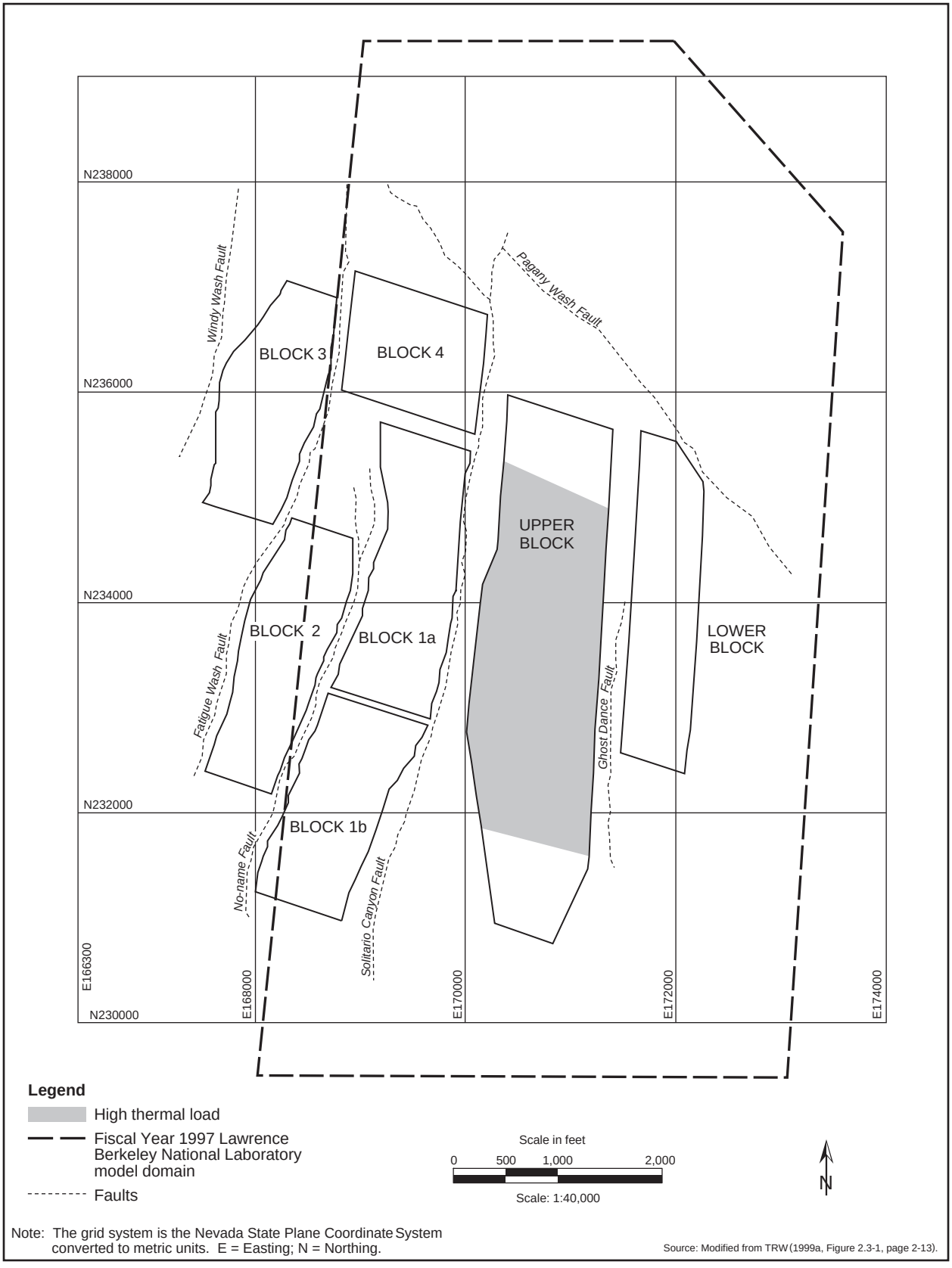

Figure I-2. Layout for Proposed Action inventory for high thermal load (85 MTHM per acre) scenario.

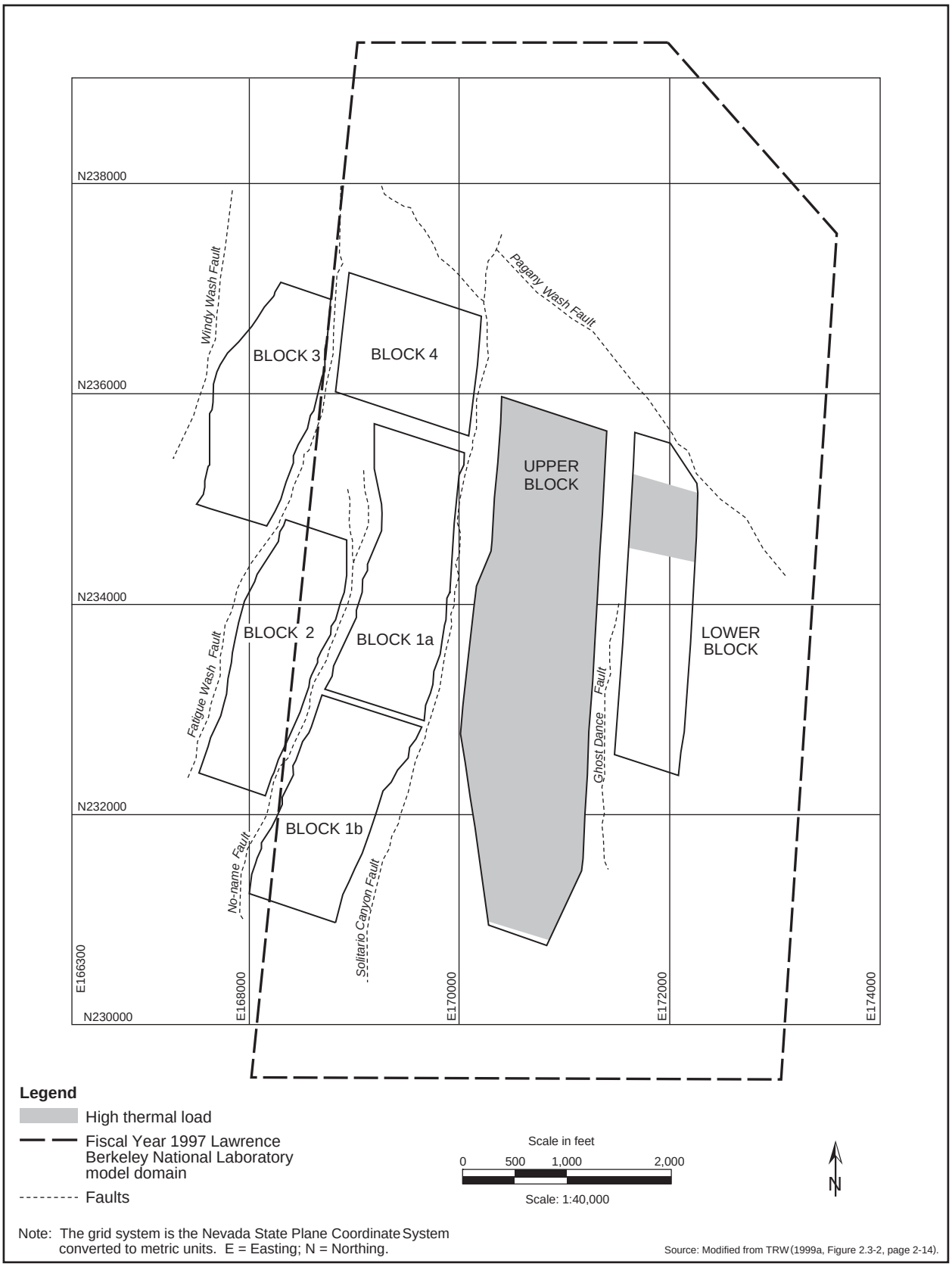

Figure I-3. Layout for Inventory Modules 1 and 2 for high thermal load (85 MTHM per acre) scenario.

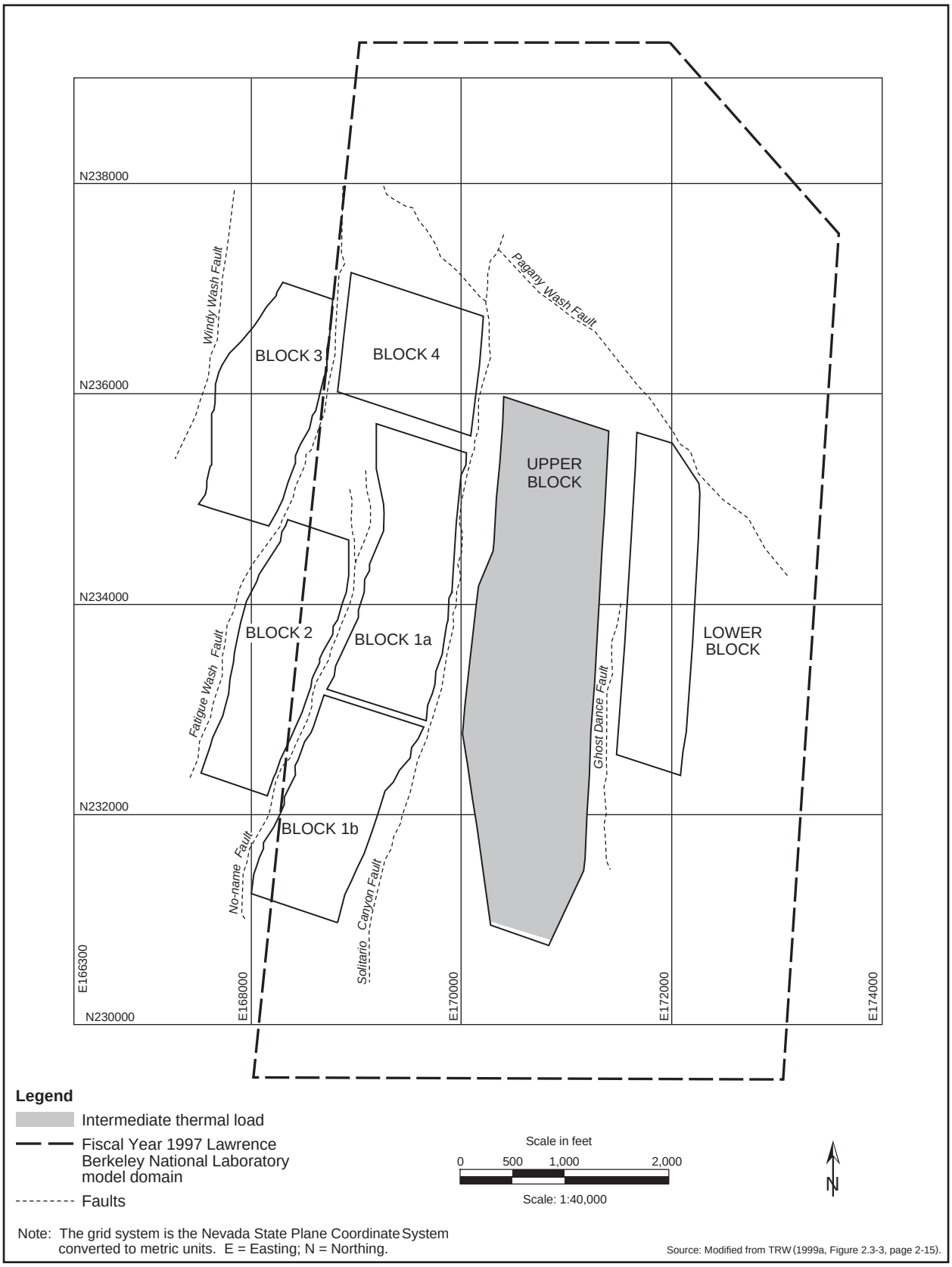

Figure I-4. Layout for Proposed Action inventory for intermediate thermal load (60 MTHM per acre) scenario.

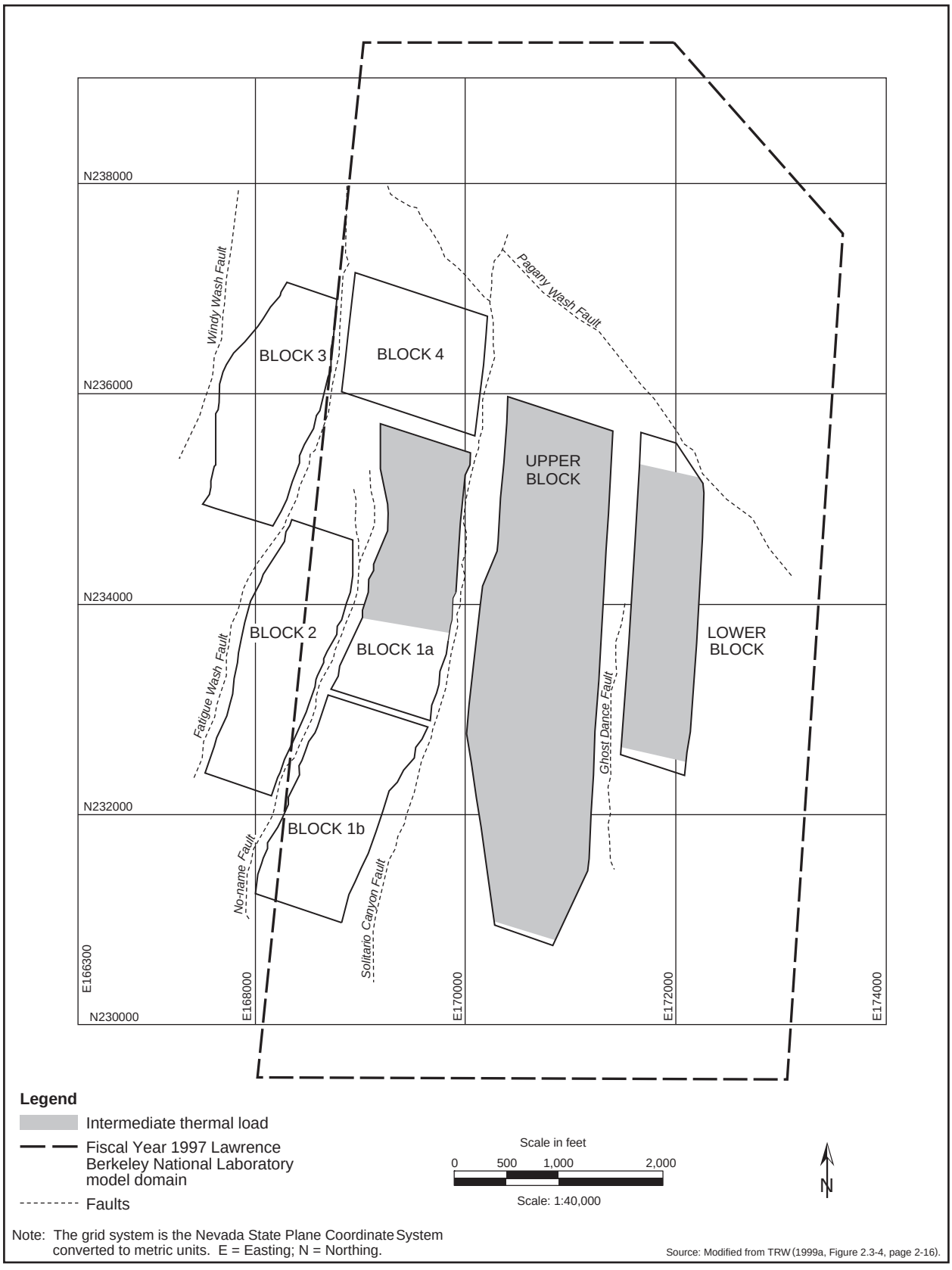

Figure I-5. Layout for Inventory Modules 1 and 2 for intermediate thermal load (60 MTHM per are) scenario.

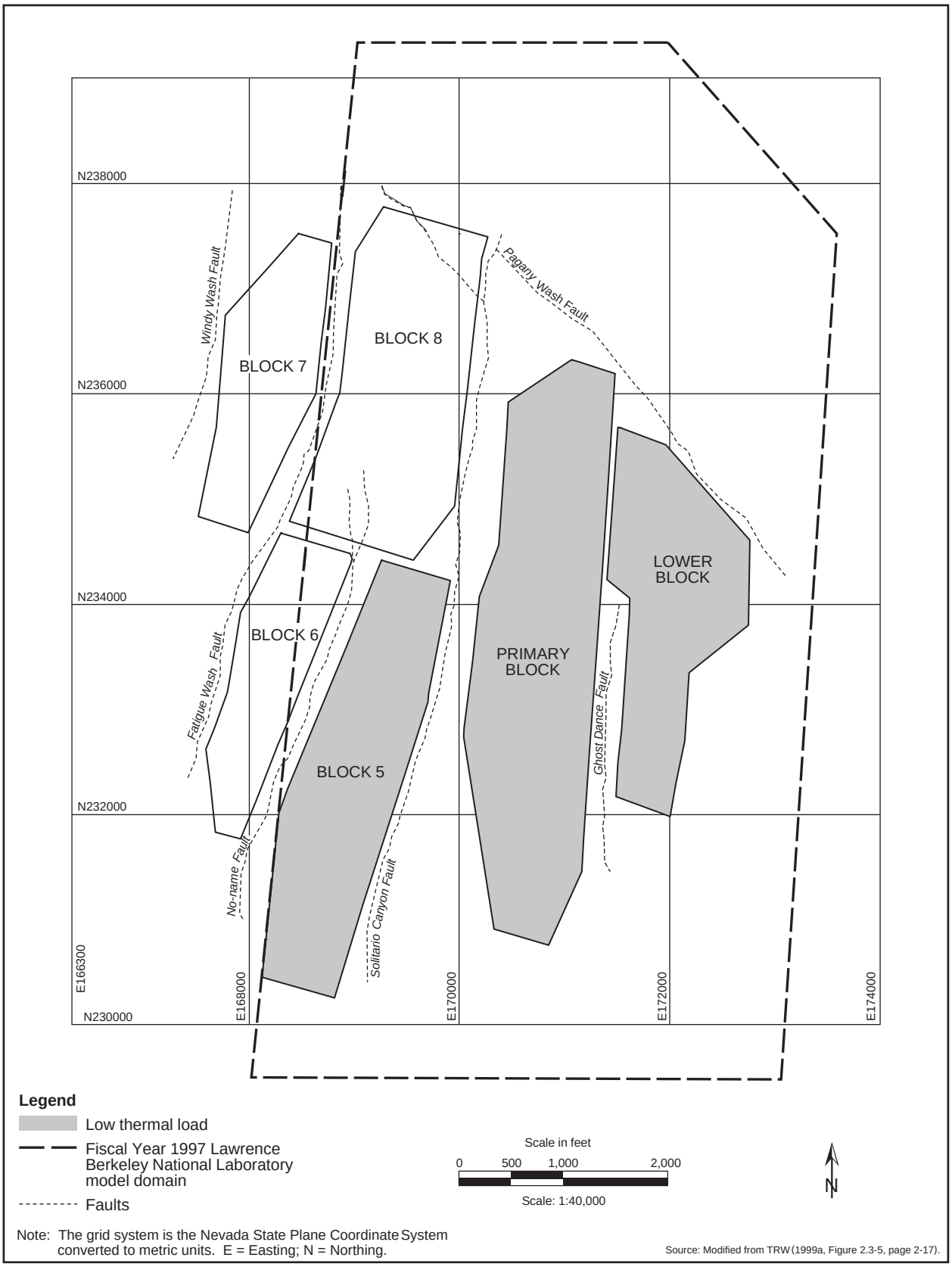

Figure I-6. Layout for Proposed Action inventory for low thermal load (25 MTHM per acre) scenario.

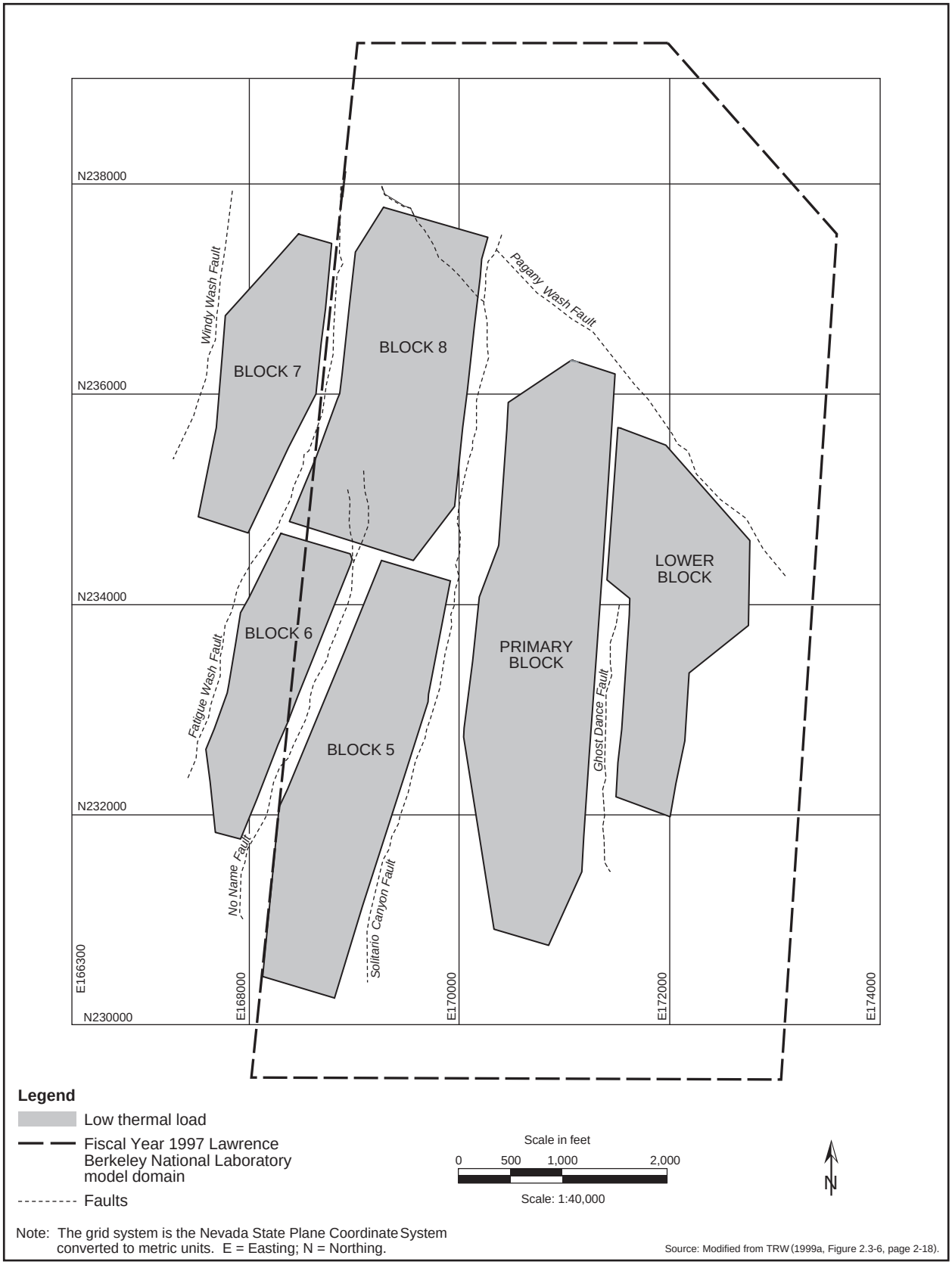

Figure I-7. Layout for Inventory Modules 1 and 2 for low thermal load (25 MTHM per acre) scenario.

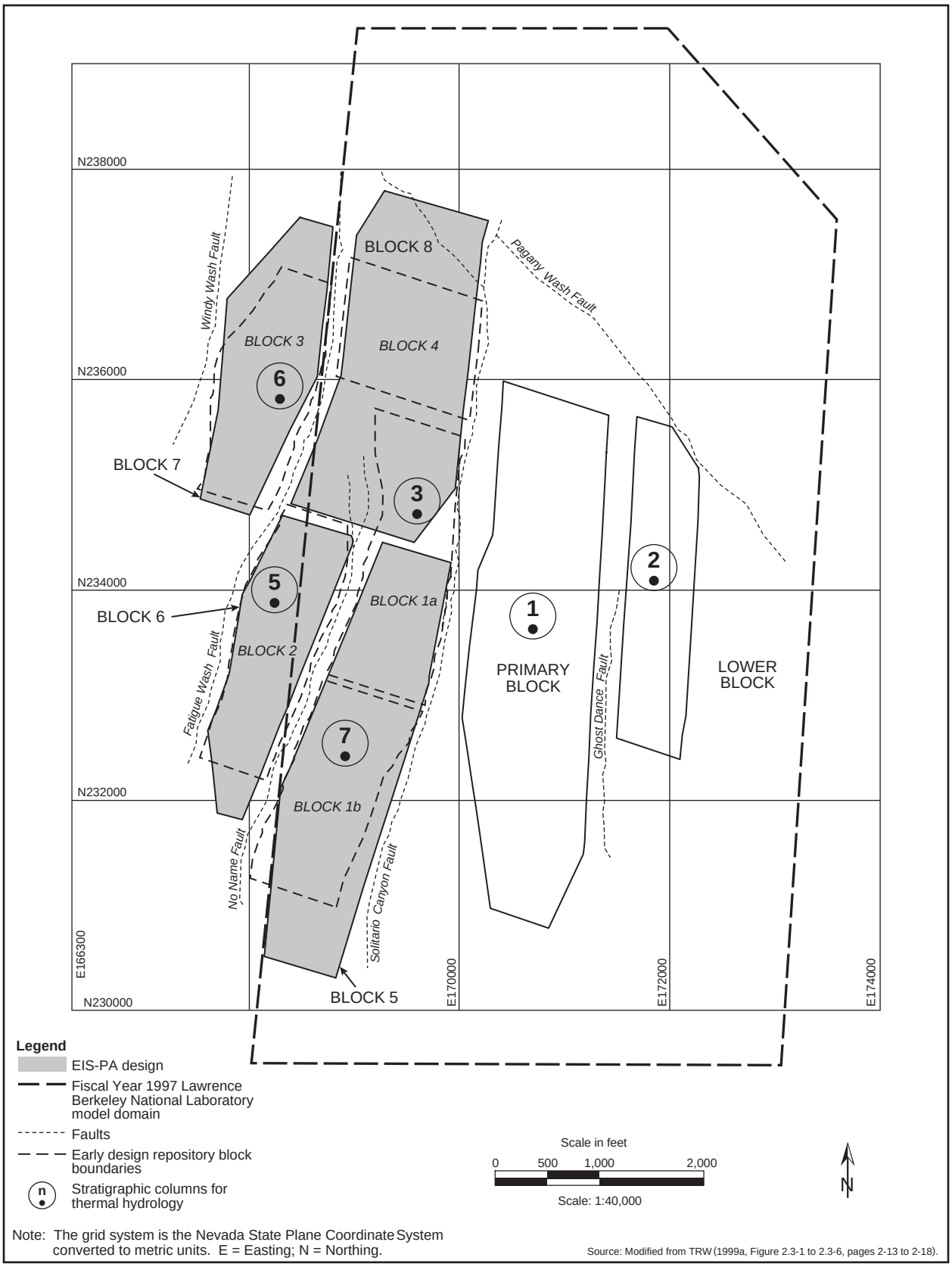

Note: The grid system is the Nevada State Plane Coordinate System converted to metric units. E = Easting; N = Northing.

Source: Modified from TRW (1999a, Figure 2.3-1 to 2.3-6, pages 2-13 to 2-18).

Figure I-8. Relationship between the early performance assessment design and emplacement block layout considered in this EIS performance assessment analysis.

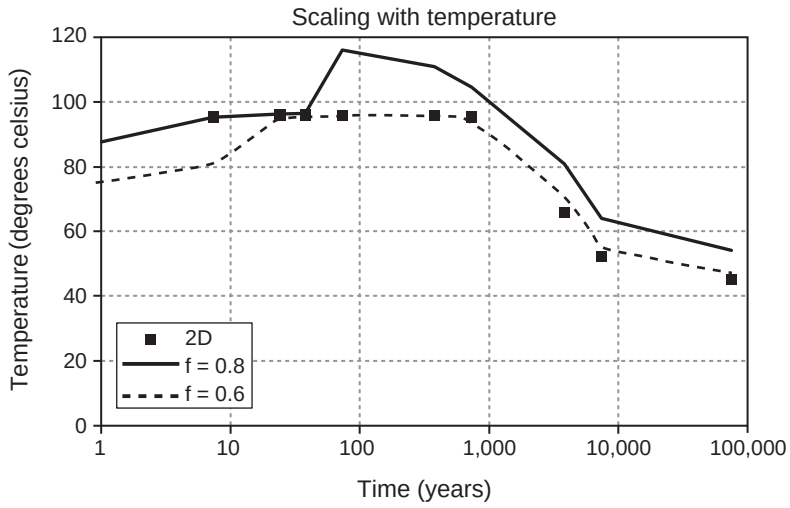

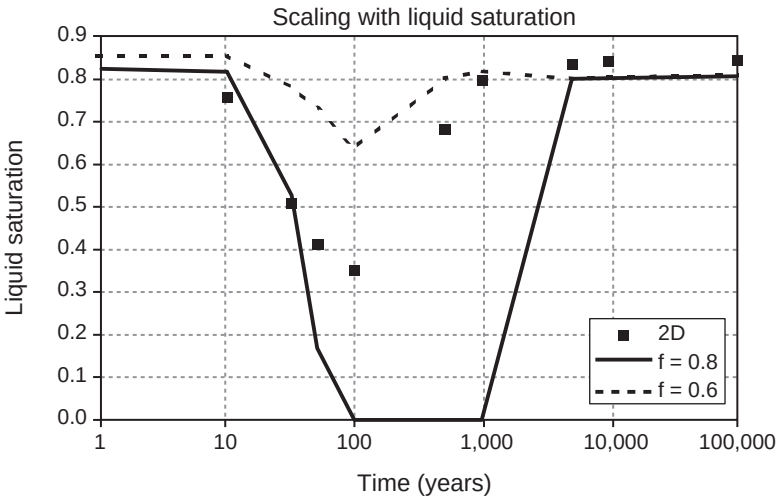

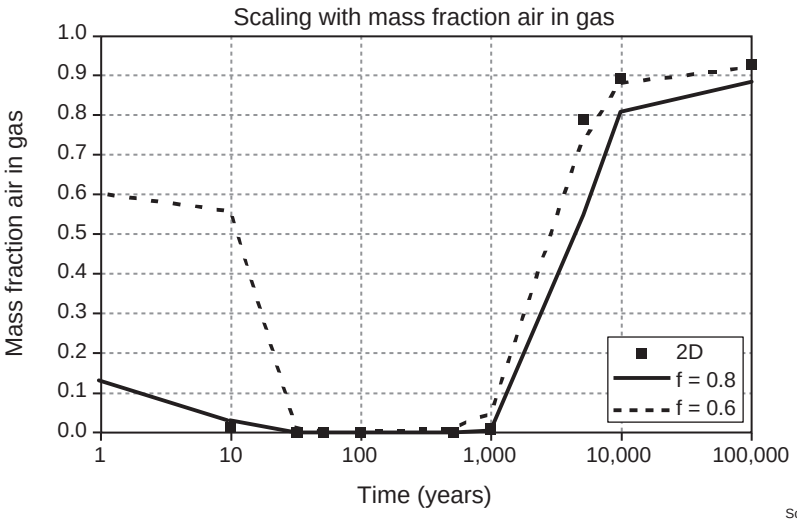

Source: Modified from TRW (1999a, Figure 3.2-1, page 3-23).

Figure I-9. Development of thermal load scale factors on the basis of two-dimensional and one-dimensional model comparisons using time history of temperature, liquid saturation, and air mass fraction.

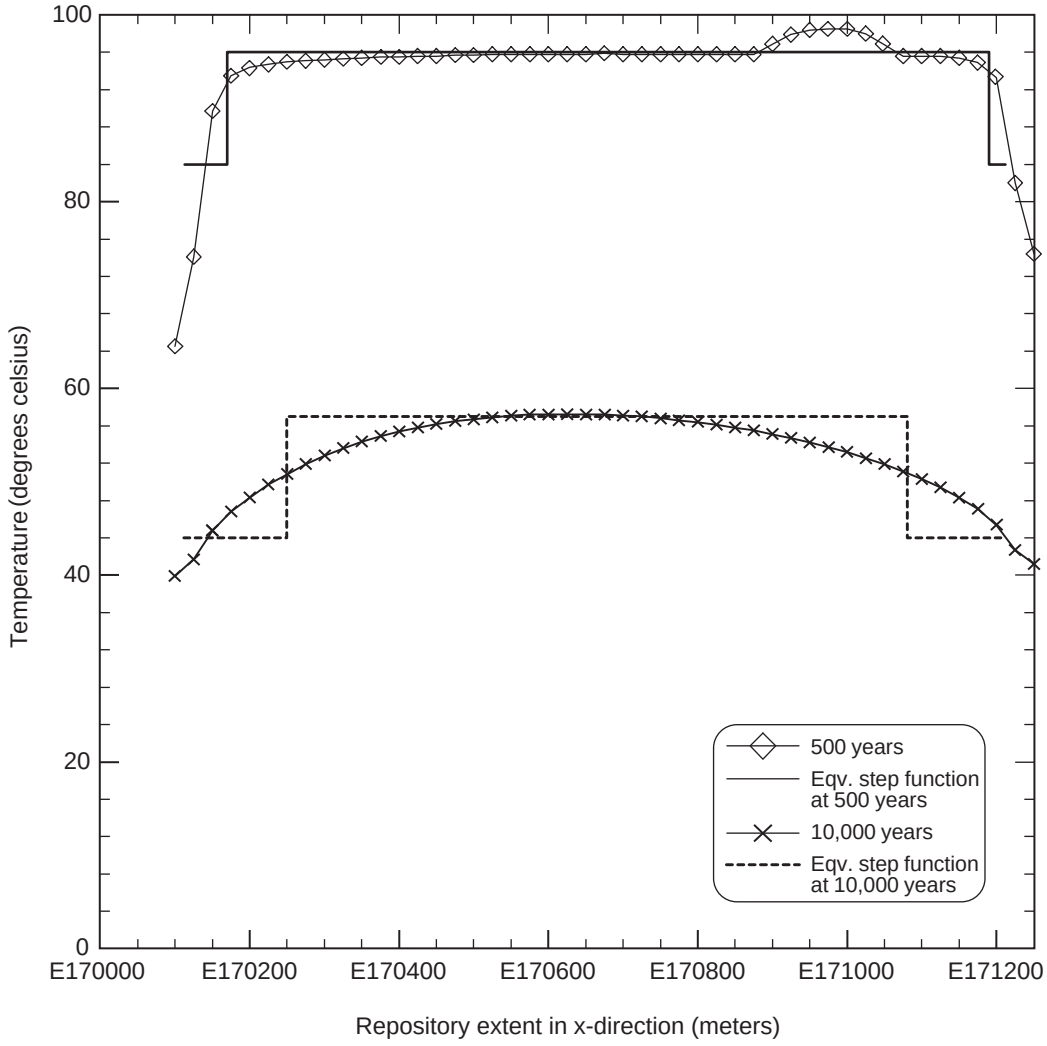

Note: The grid system is the Nevada State Plane Coordinate System converted to metric units. E = Easting; N = Northing.

Source: Modified from TRW (1999a, Figure 3.2-2, page 3-24).

Figure I-10. Partition of repository area between center and edge regions.

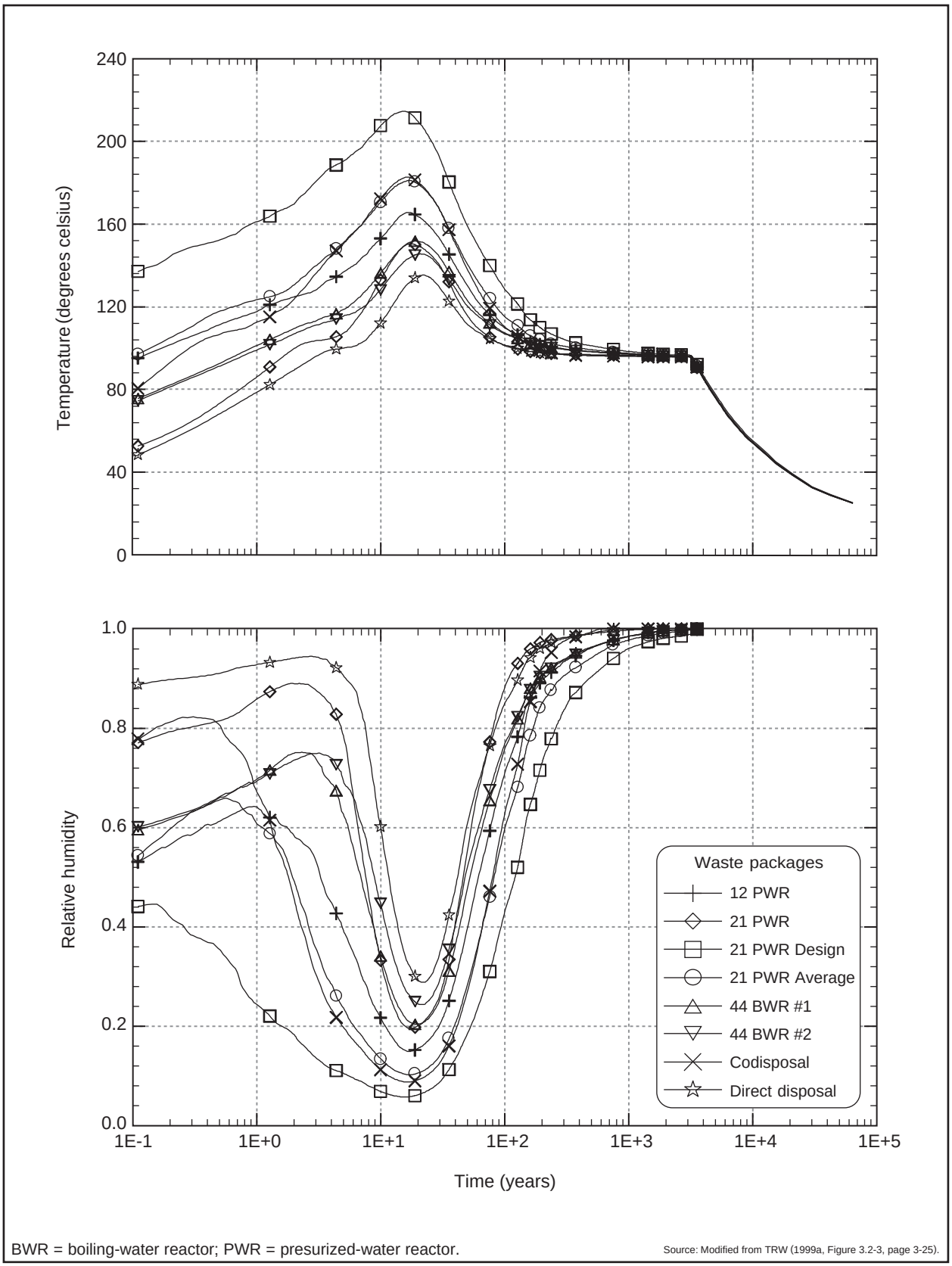

BWR = boiling-water reactor; PWR = presurized-water reactor.

Source: Modified from TRW (1999a, Figure 3.2-3, page 3-25).

Figure I-11. Temperature and relative humidity histories for all waste packages for high thermal load scenario, Proposed Action inventory, and long-term average dimate.

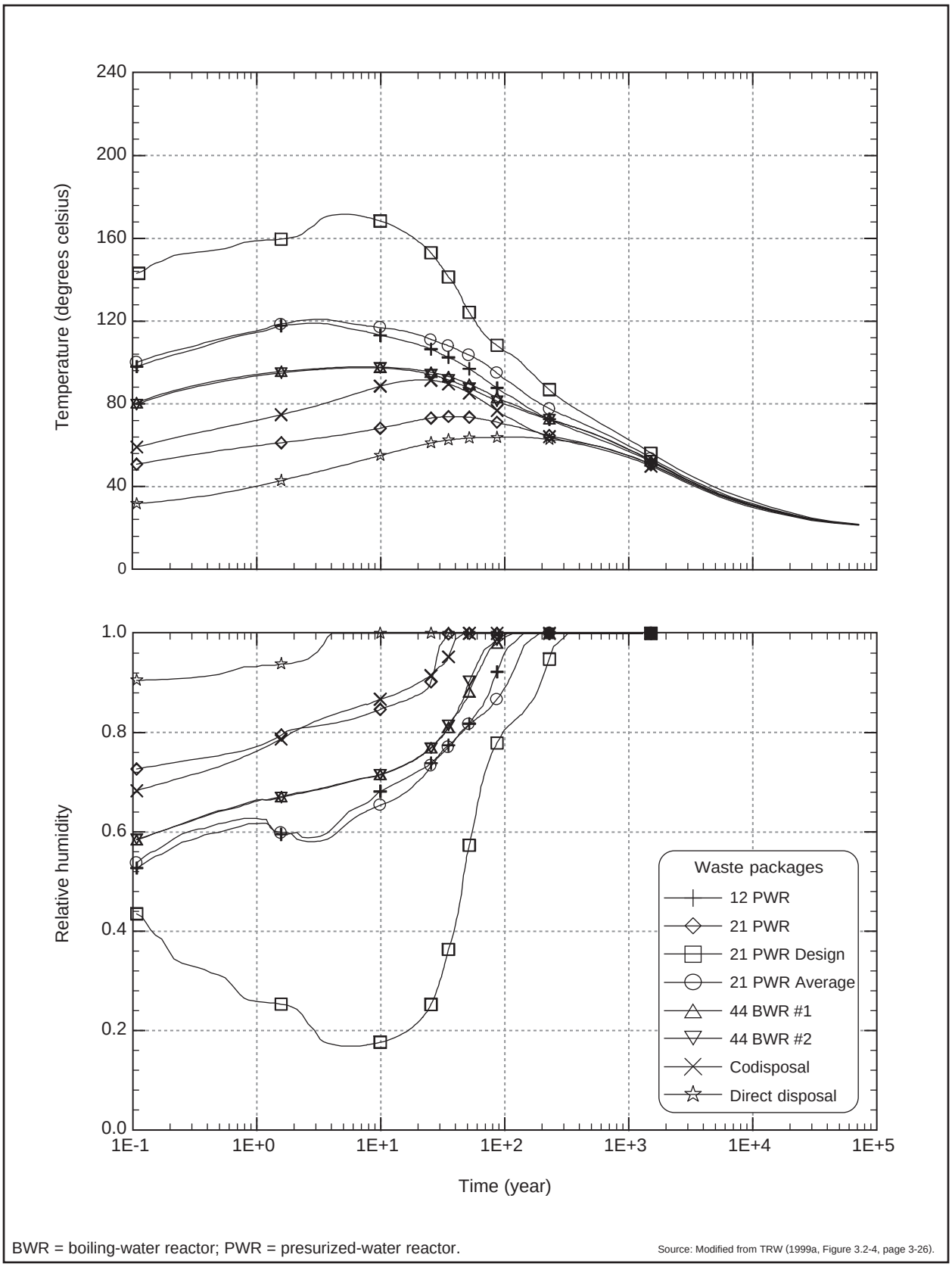

BWR = boiling-water reactor; PWR = presurized-water reactor.

Source: Modified from TRW (1999a, Figure 3.2-4, page 3-26).

Figure I-12. Temperature and relative humidity histories for all waste packages, low thermal load scenario, Proposed Action inventory, and long-term average climate.

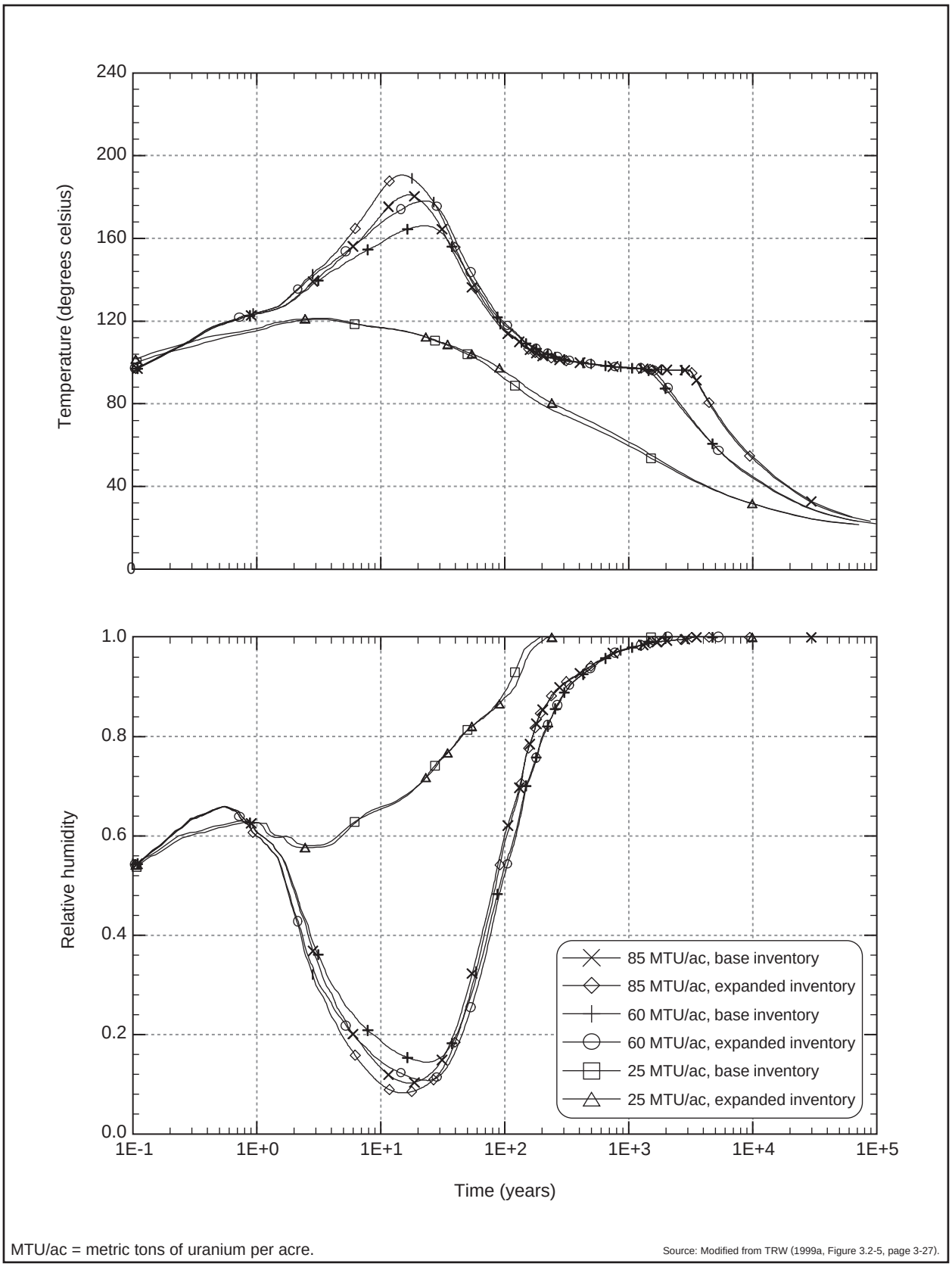

MTU/ac = metric tons of uranium per acre.

Source: Modified from TRW (1999a, Figure 3.2-5, page 3-27).

Figure I-13. Temperature and relative humidity histories for the 21 pressurized-water-reactor average waste packages, long-term average climate scenario, showing sensitivity to waste inventory.

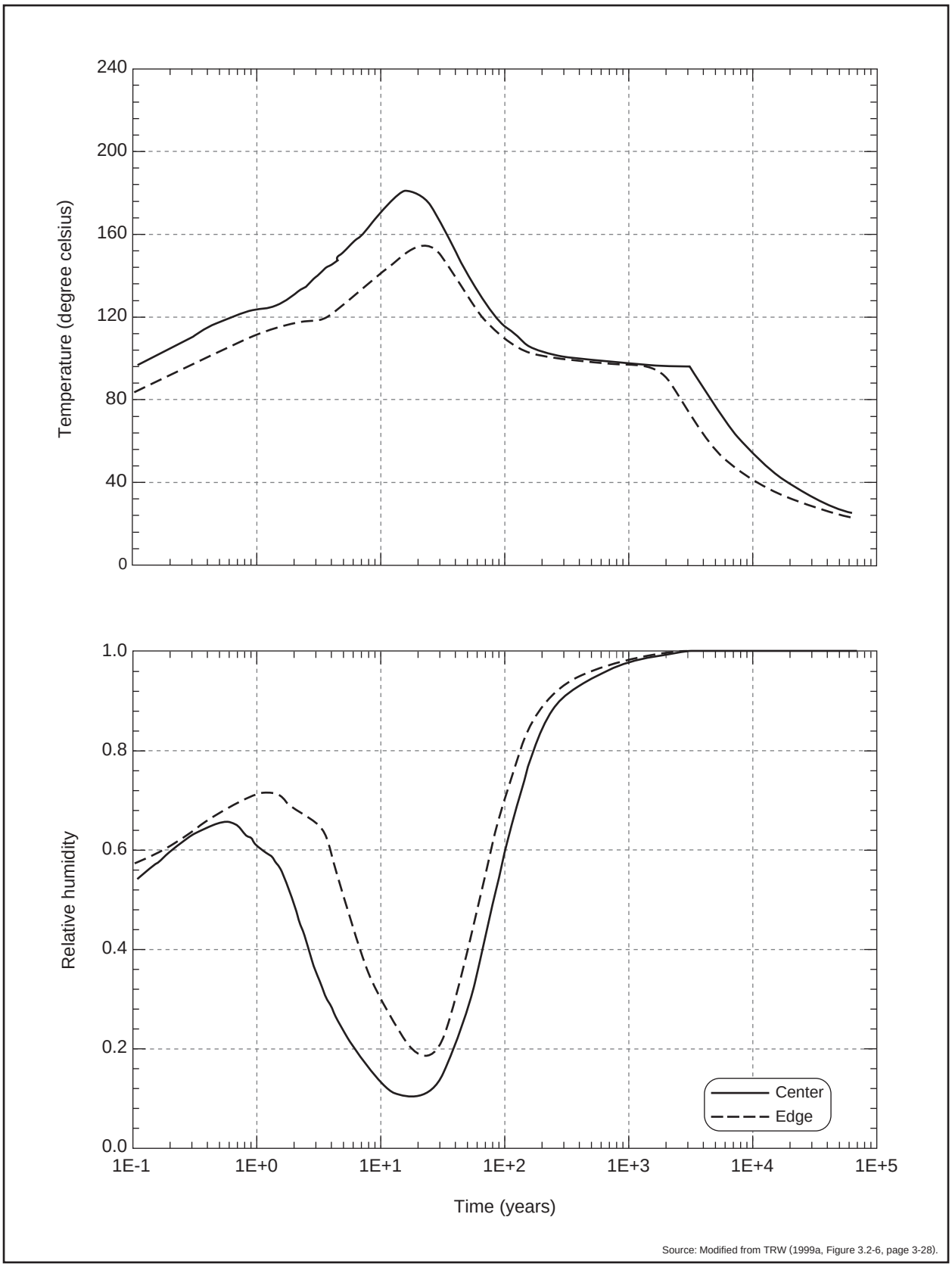

Figure I-14. Temperature and relative humidity histories for the 21 pressurized-water-reactor average waste packages, high thermal load scenario, Proposed Action inventory, long-term average climate scenario, comparing the center and edge scenarios.

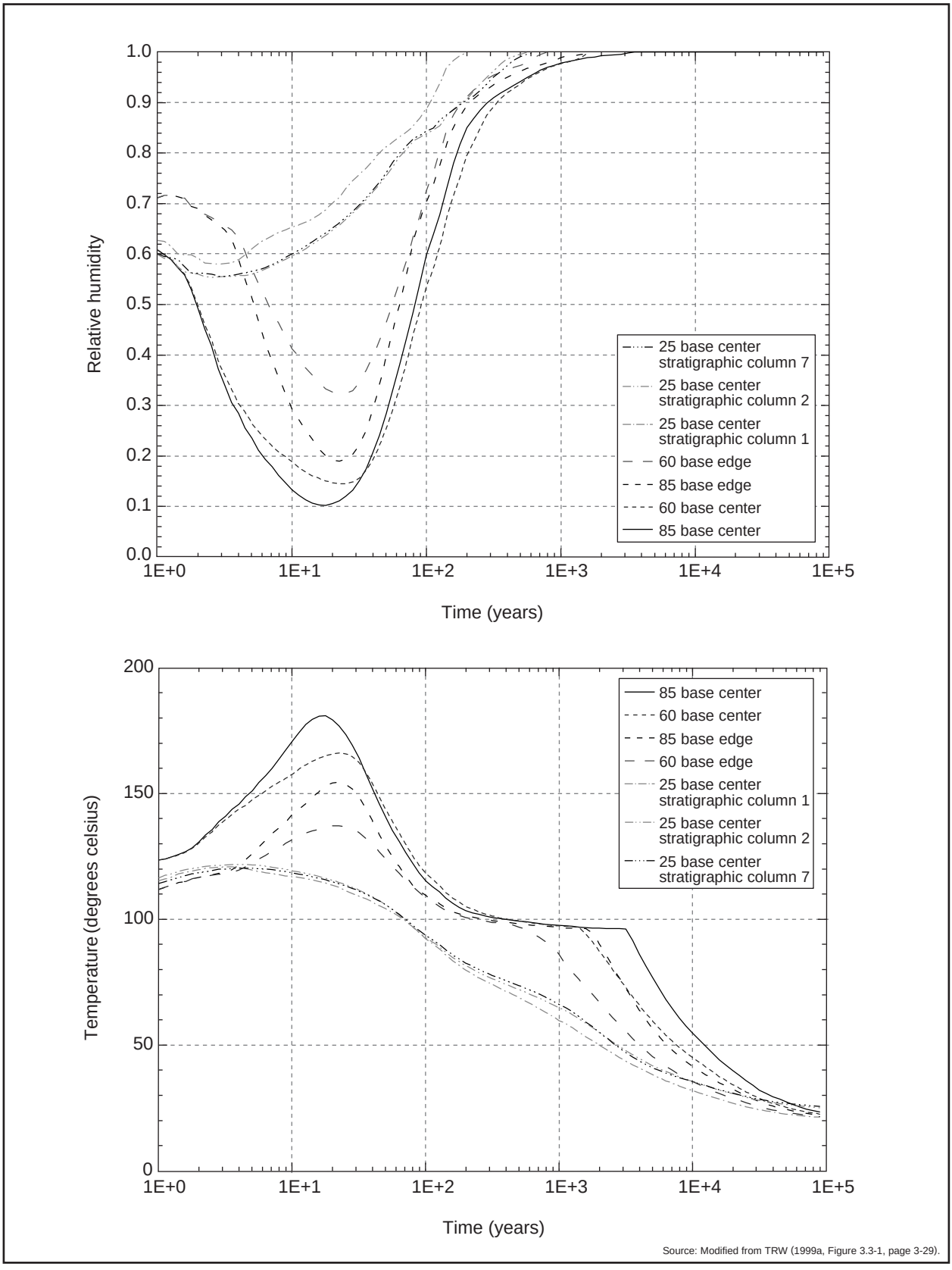

Source: Modified from TRW (1999a, Figure 3.3-1, page 3-29).

Figure I-15. WAPDEG input temperature and relative humidity histories for all thermal loads with Proposed Action inventory.

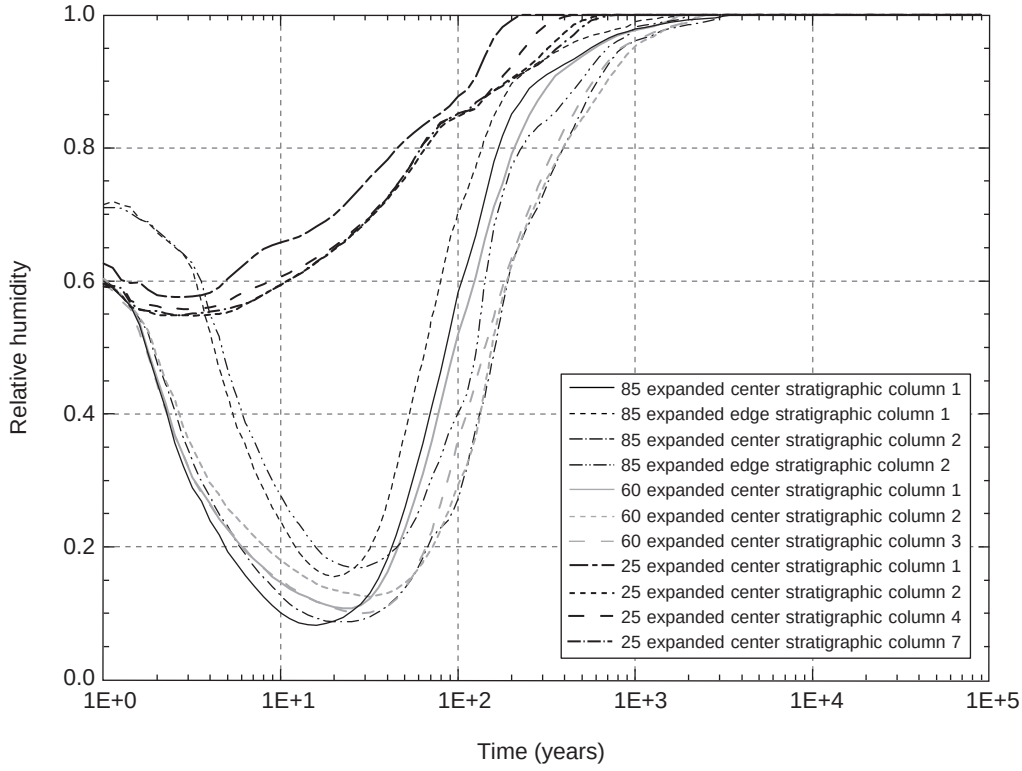

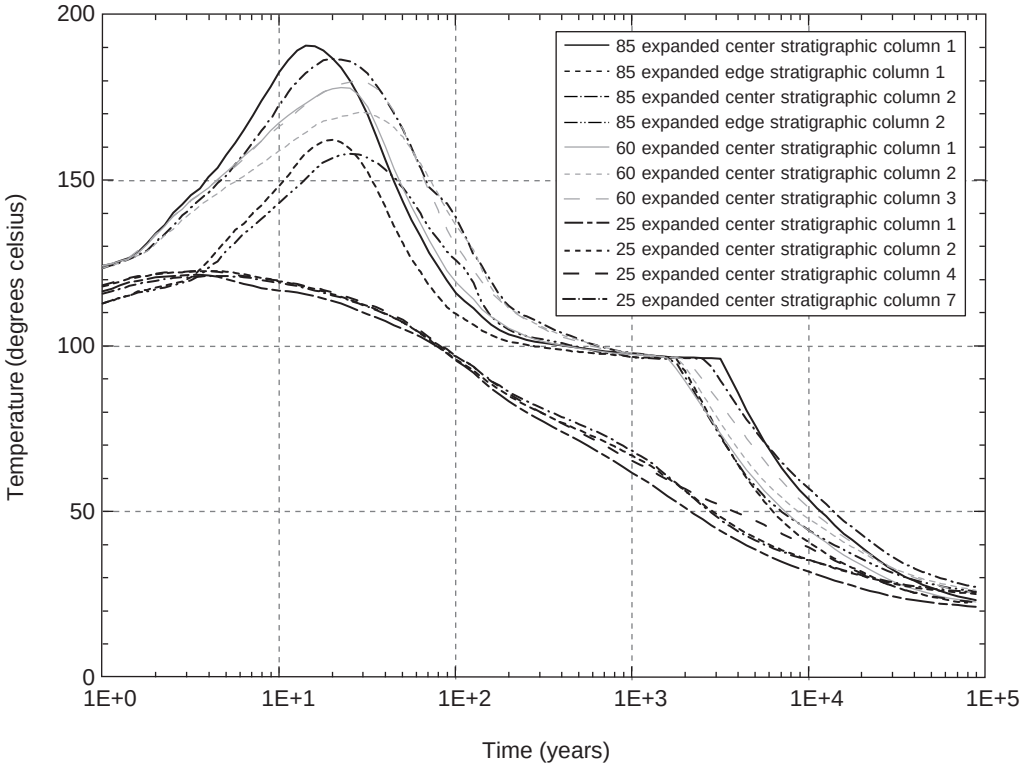

Source: Modified from TRW (1999a, Figure 3.3-2, page 3-30).

Figure I-16. WAPDEG input temperature and relative humidity histories for all thermal loads with Inventory Modules 1 and 2.

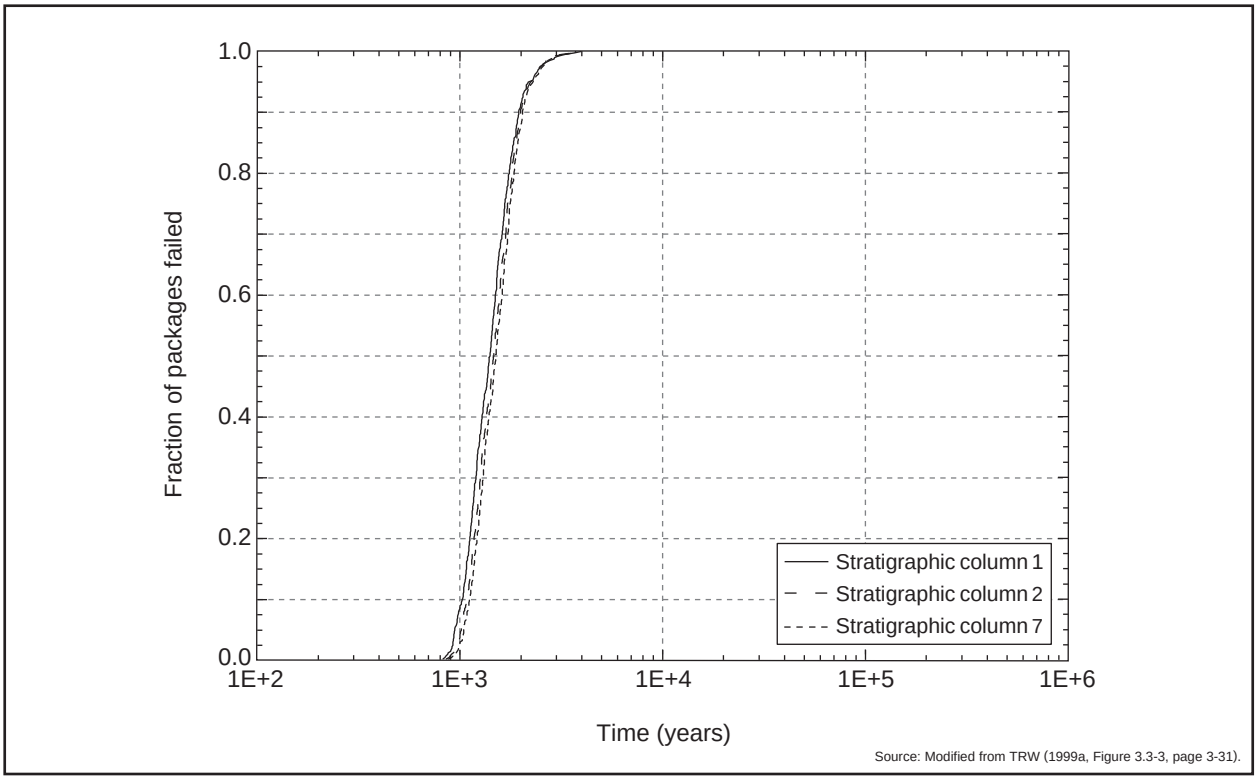

Figure I-17. Time to first breach of the corrosion-allowance material for low thermal load scenario, Proposed Action inventory, all three stratigraphic columns, always-dripping waste packages.

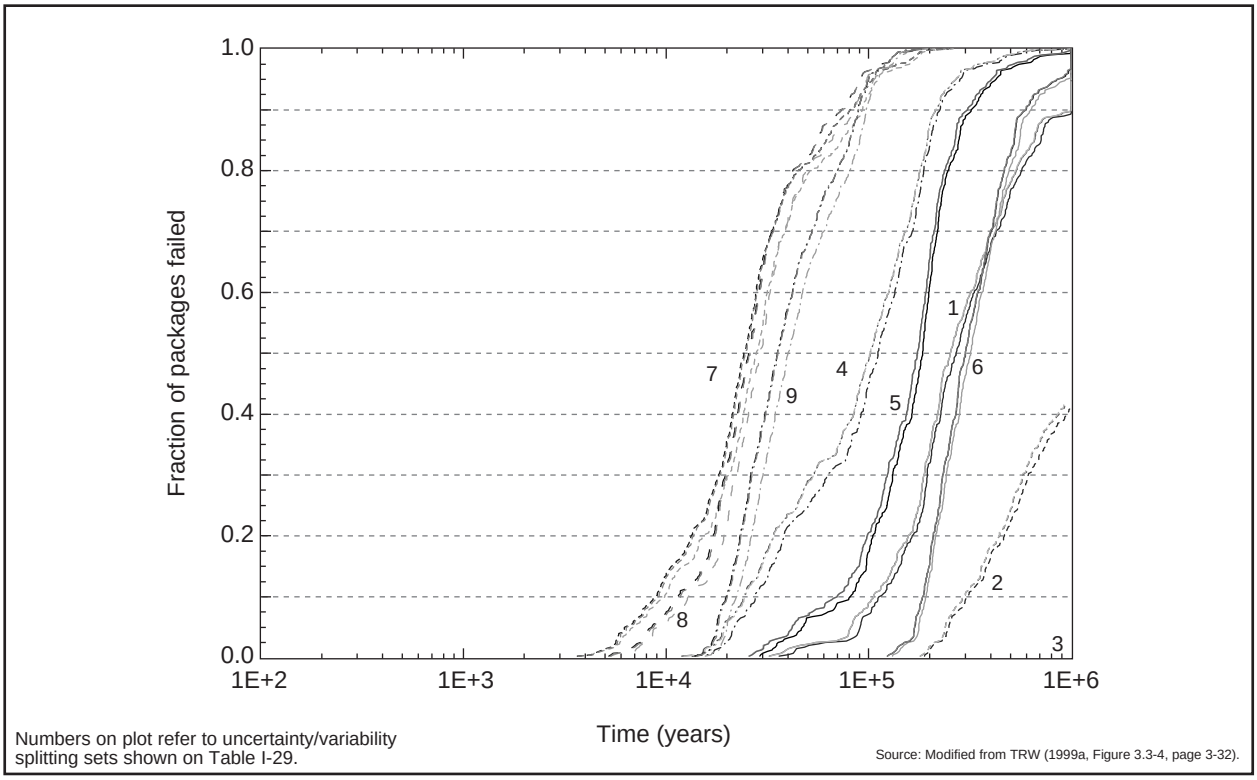

Figure I-18. Time to first breach of the corrosion-resistant material for low thermal load scenario, Proposed Action inventory, all three stratigraphic columns, always-dripping waste packages, and all nine uncertainty/variability splitting sets.

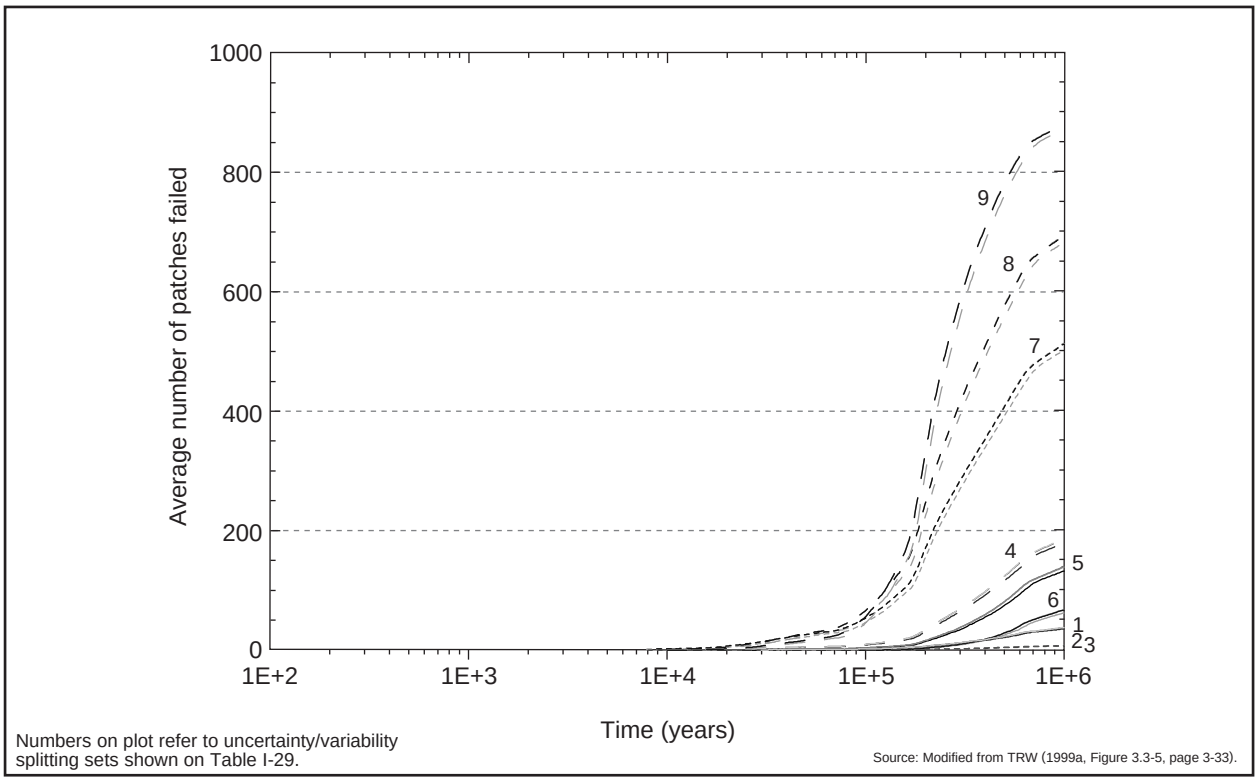

Figure I-19. Average number of patches failed per waste package as a function of time for low thermal load scenario, Proposed Action inventory, all three stratigraphic columns, always-dripping waste packages, and all nine uncertainty/variability splitting sets.

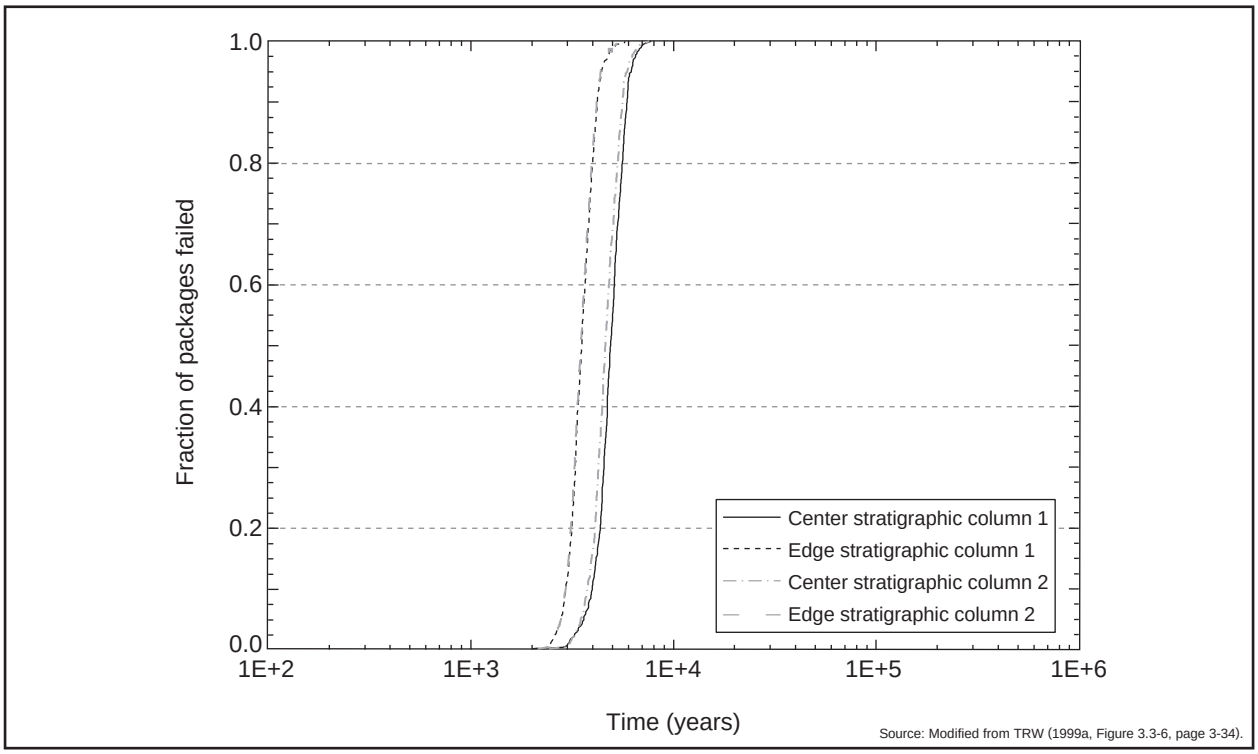

Figure I-20. Time to first breach of the corrosion-allowance material for high thermal load scenario, Inventory Modules 1 and 2, center and edge regions for both stratigraphic columns, always-dripping waste packages.

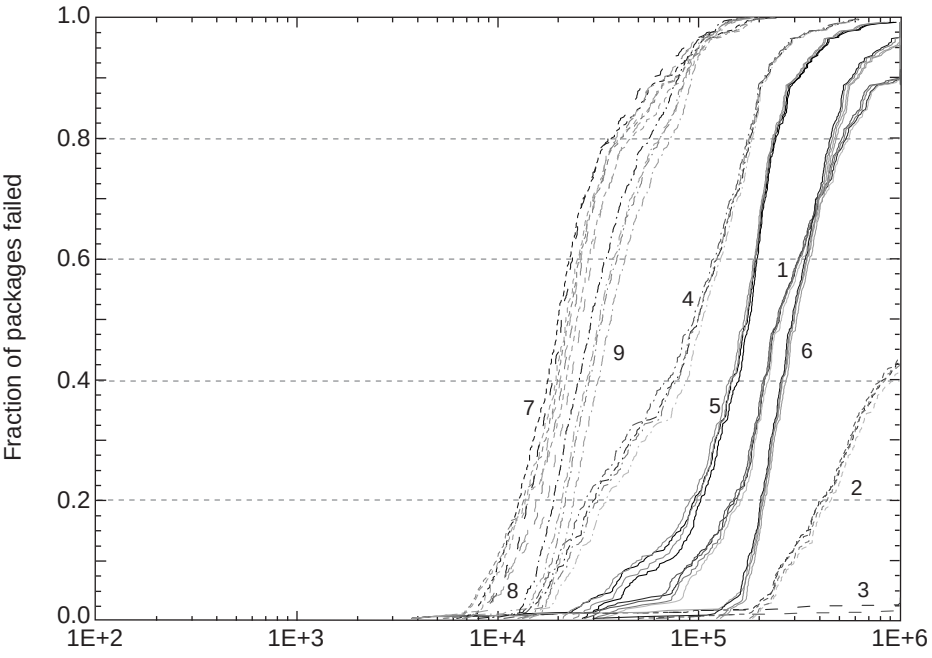

Numbers on plot refer to uncertainty/variability splitting sets shown on Table I-29.

Source: Modified from TRW (1999a, Figure 3.3-7, page 3-35).

Figure I-21. Time to first breach of the corrosion-resistant material for high thermal load scenario, Inventory Modules 1 and 2, center and edge regions for both stratigraphic columns, always-dripping waste packages, and all nine uncertainty/variability splitting sets.

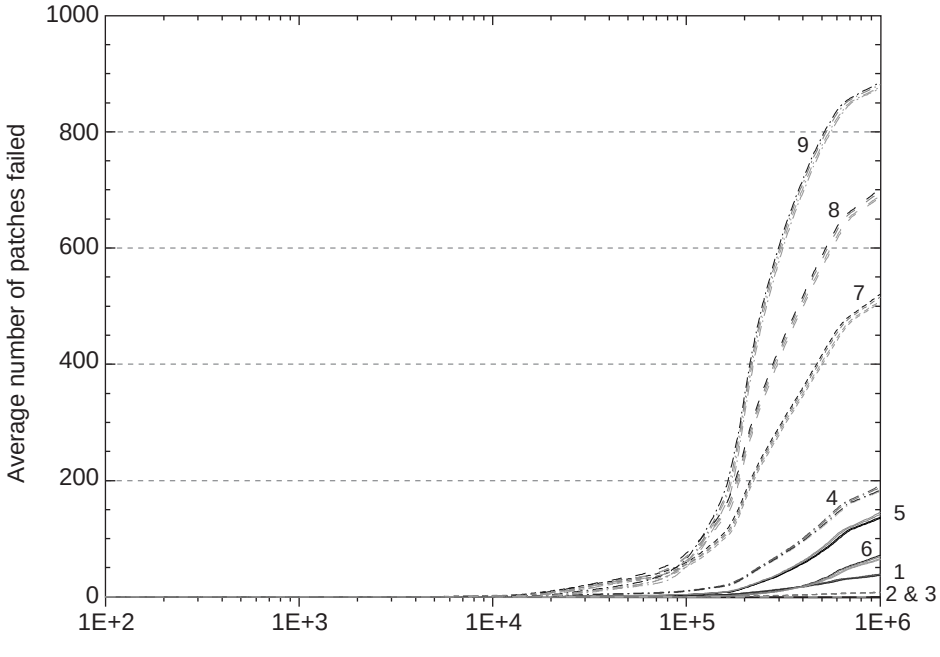

Numbers on plot refer to uncertainty/variability splitting sets shown on Table I-29.

Source: Modified from TRW (1999a, Figure 3.3-8, page 3-36).

Figure I-22. Average number of patches failed per package as a function of time for high thermal load scenario, Inventory Modules 1 and 2, center and edge regions for both stratigraphic columns, always-dripping waste packages, and all nine uncertainty/variability splitting sets.

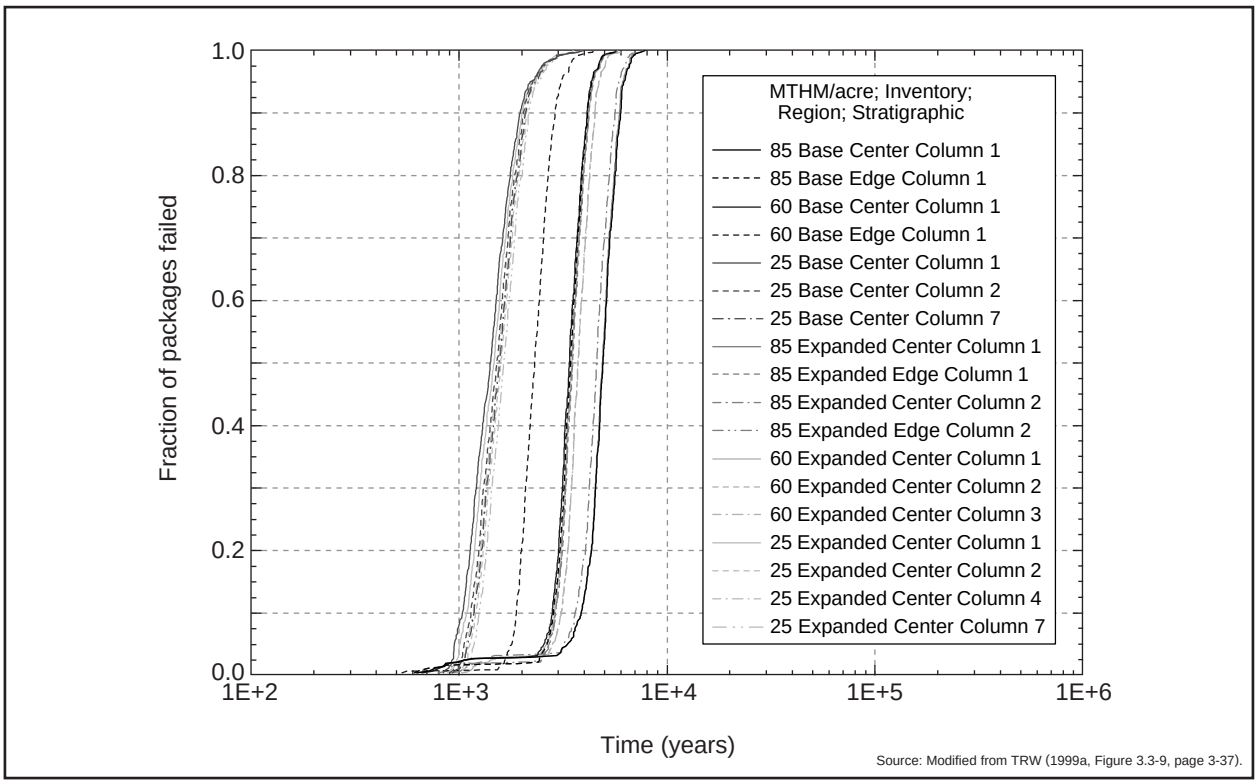

Figure I-23. Time to first breach of the corrosion-allowance material for all thermal loads and inventories, all regions, always-dripping waste packages, uncertainty/variability splitting set 5.

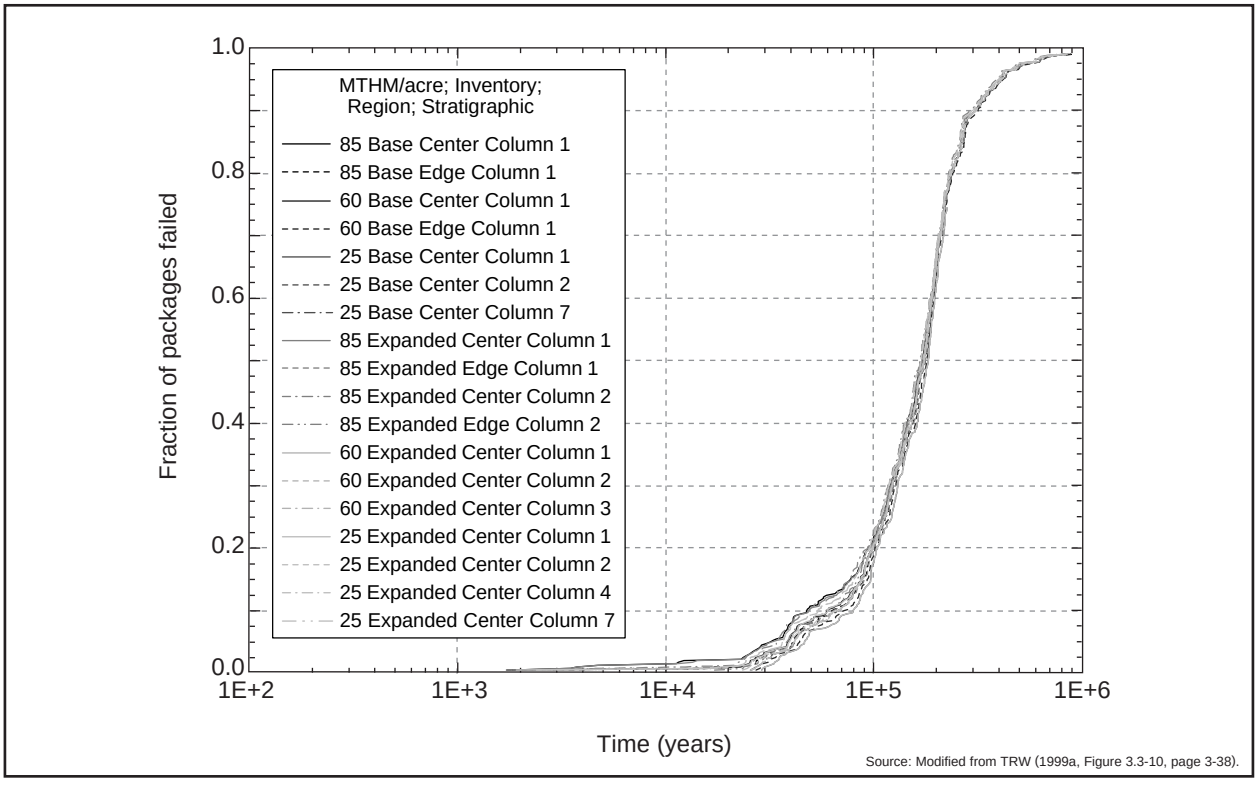

Figure I-24. Time to first breach of the corrosion-resistant material for all thermal loads and inventories, all regions, always-dripping waste packages, uncertainty/variability splitting set 5.

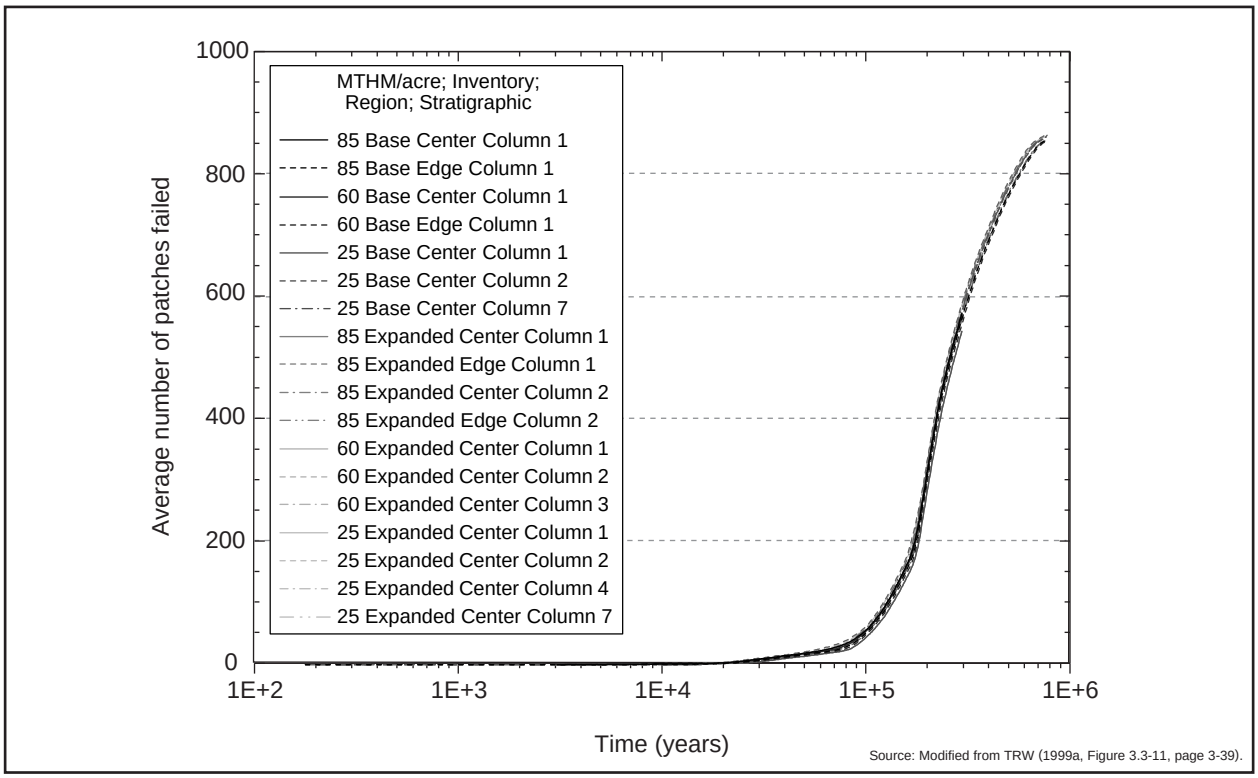

Figure I-25. Average number of patches failed per waste package as a function of time for all thermal loads and inventories, all regions, always-dripping waste packages, uncertainty/variability splitting set 9.

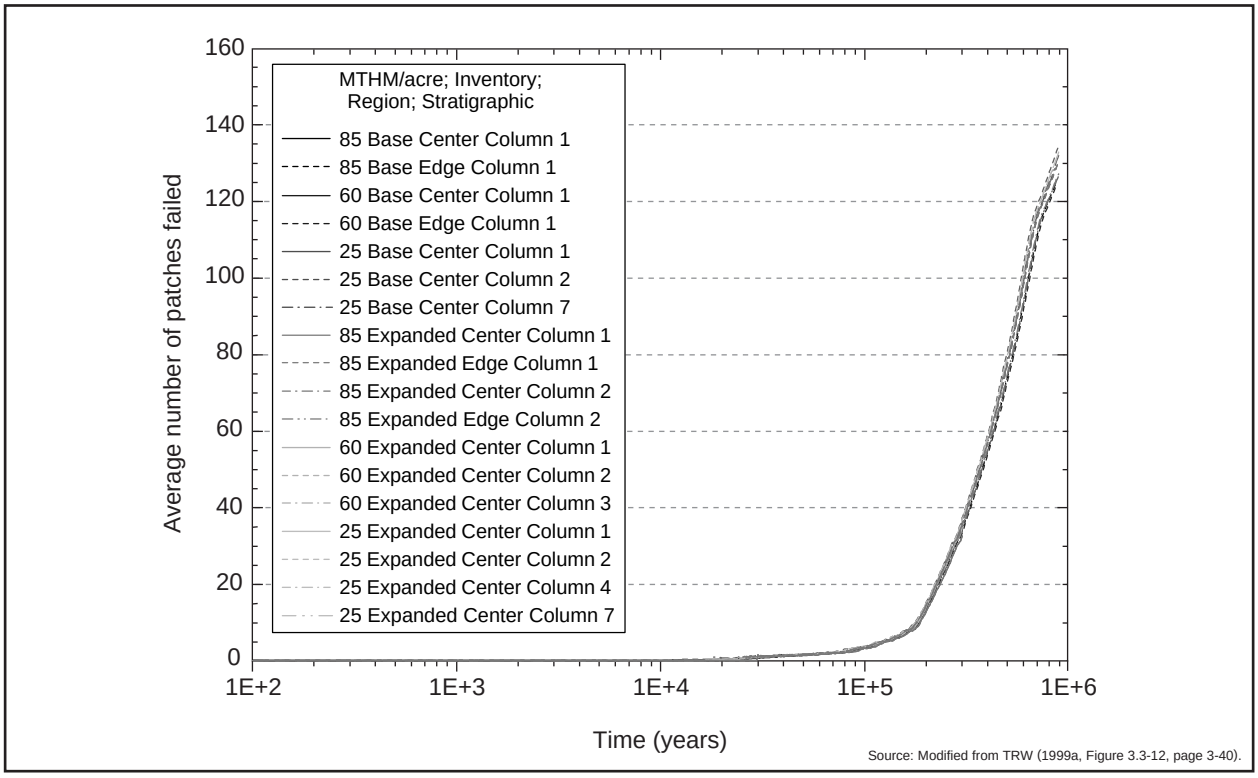

Figure I-26. Average number of patches failed per waste package as a function of time for all thermal loads and inventories, all regions, always-dripping waste packages, uncertainty/variability splitting set 5.

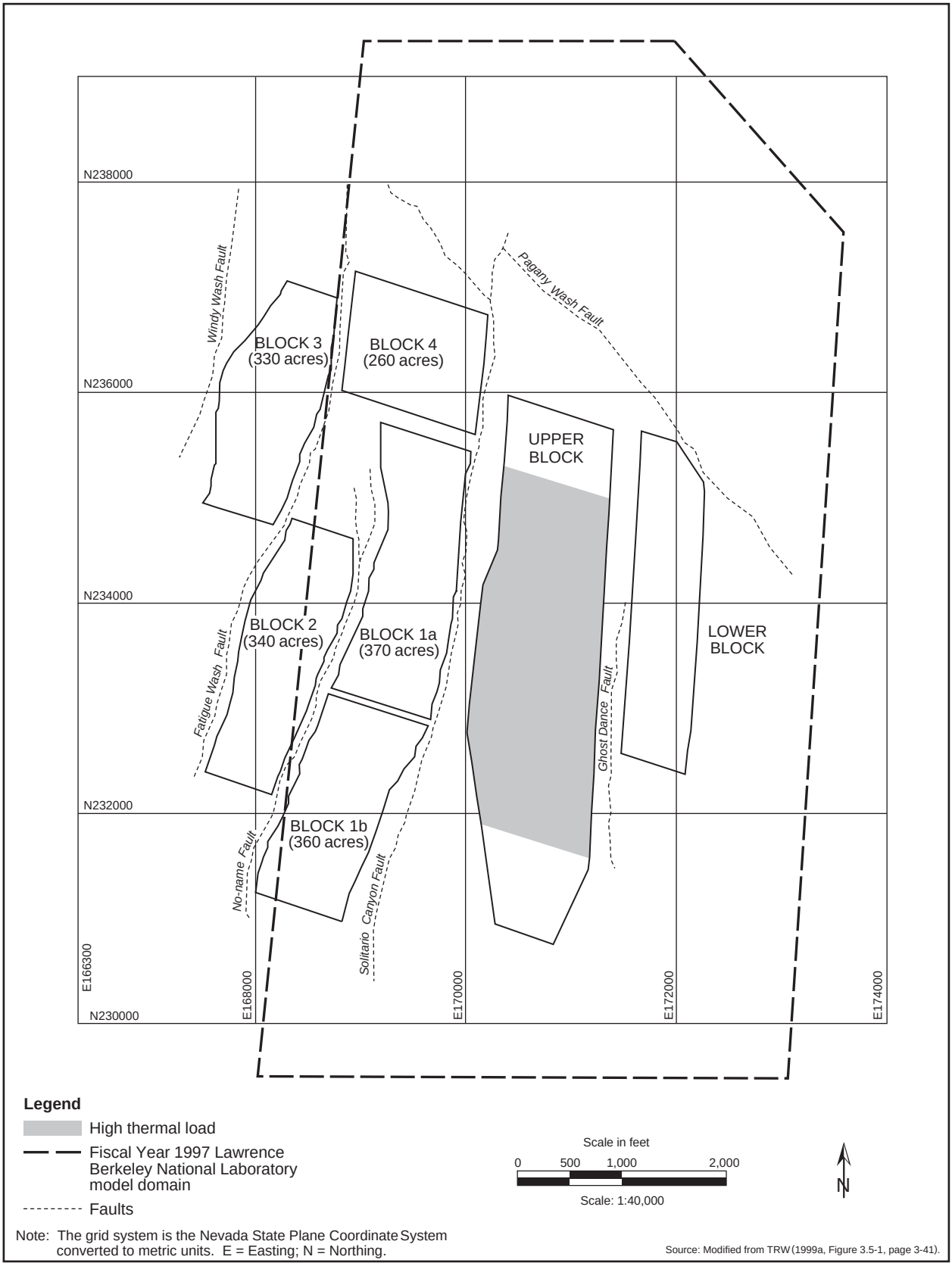

Figure I-27. Regions for performance assessment modeling, Option 1, high thermal load scenario, Proposed Action inventory.

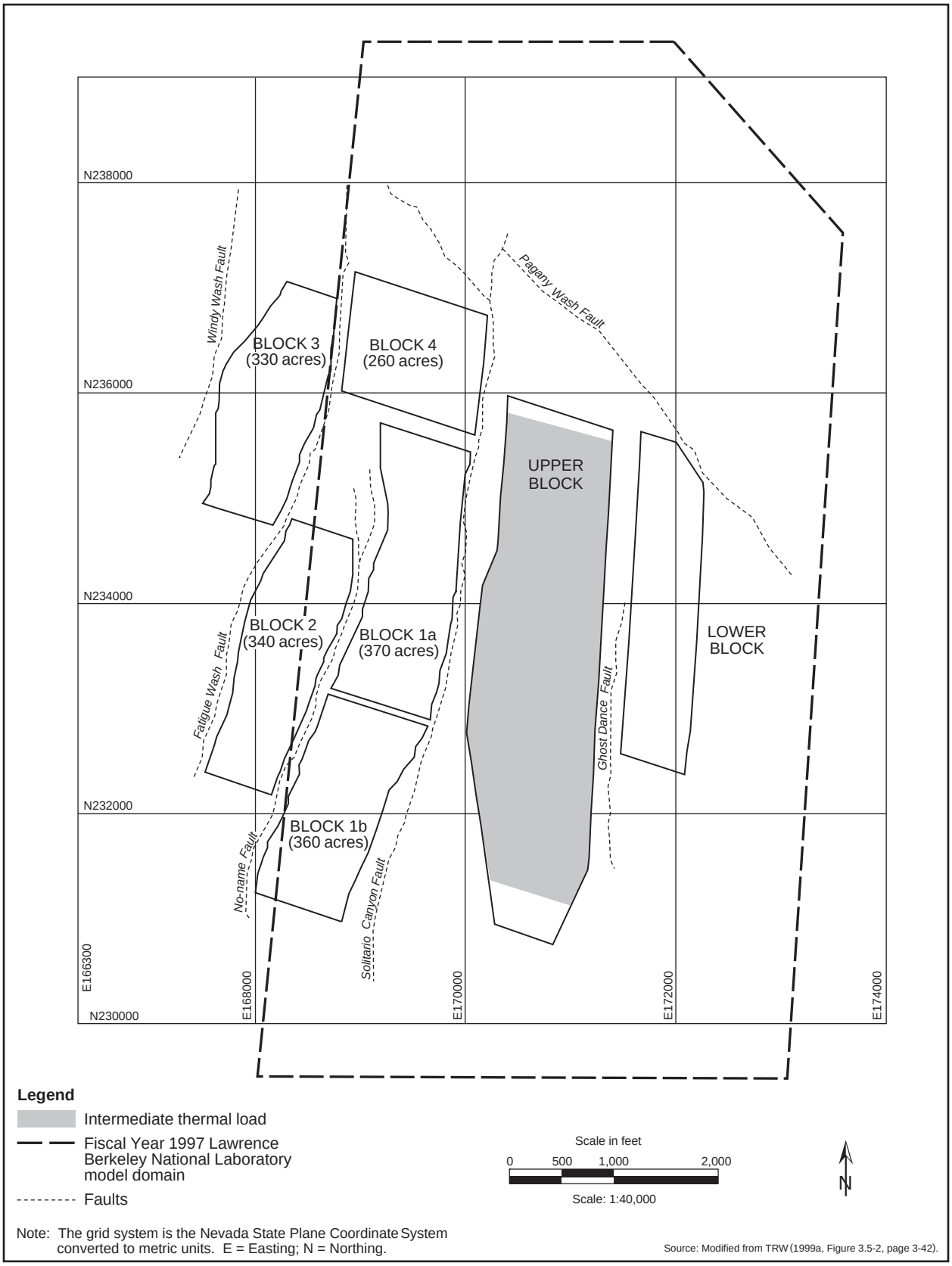

Figure I-28. Regions for performance assessment modeling, Option 2, intermediate thermal load scenario, Proposed Action inventory.

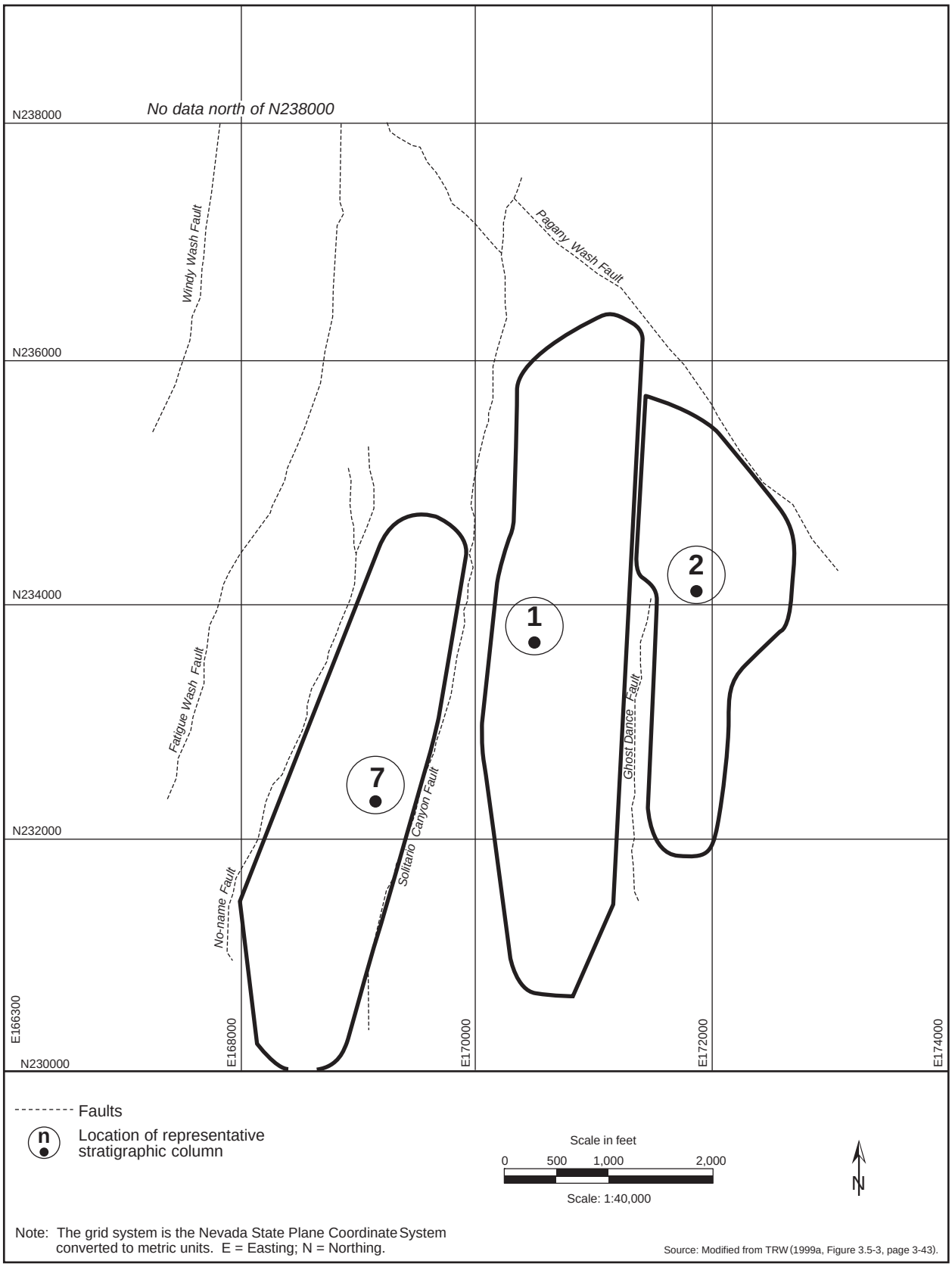

Figure I-29. Repository block areas for performance assessment modeling, Option 3, low thermal load scenario with Inventory Module 1, and intermediate thermal load scenario with Inventory Module 1 cases.

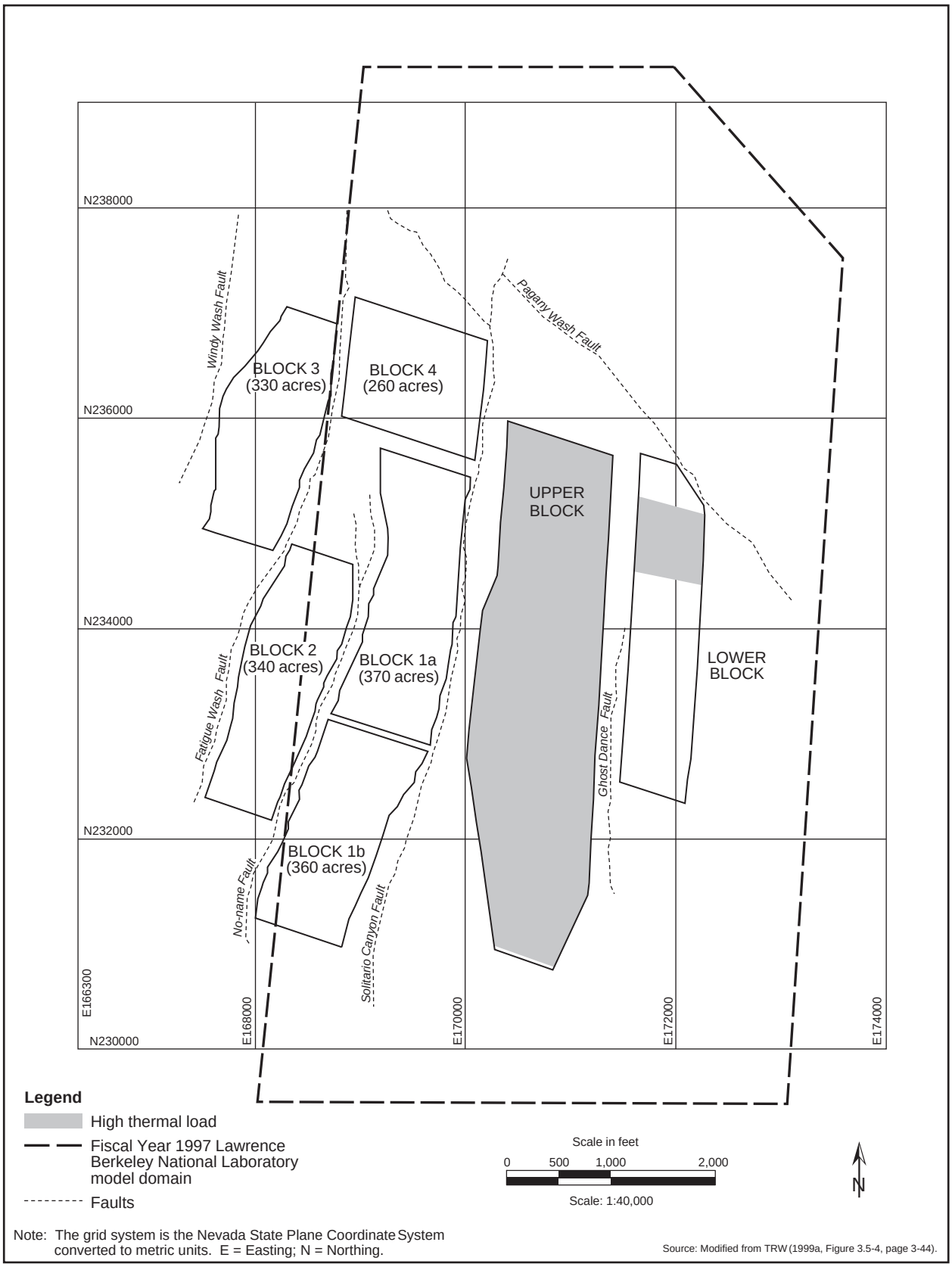

Figure I-30. Regions for performance assessment modeling, Option 4, high thermal load scenario, Proposed Action inventory.

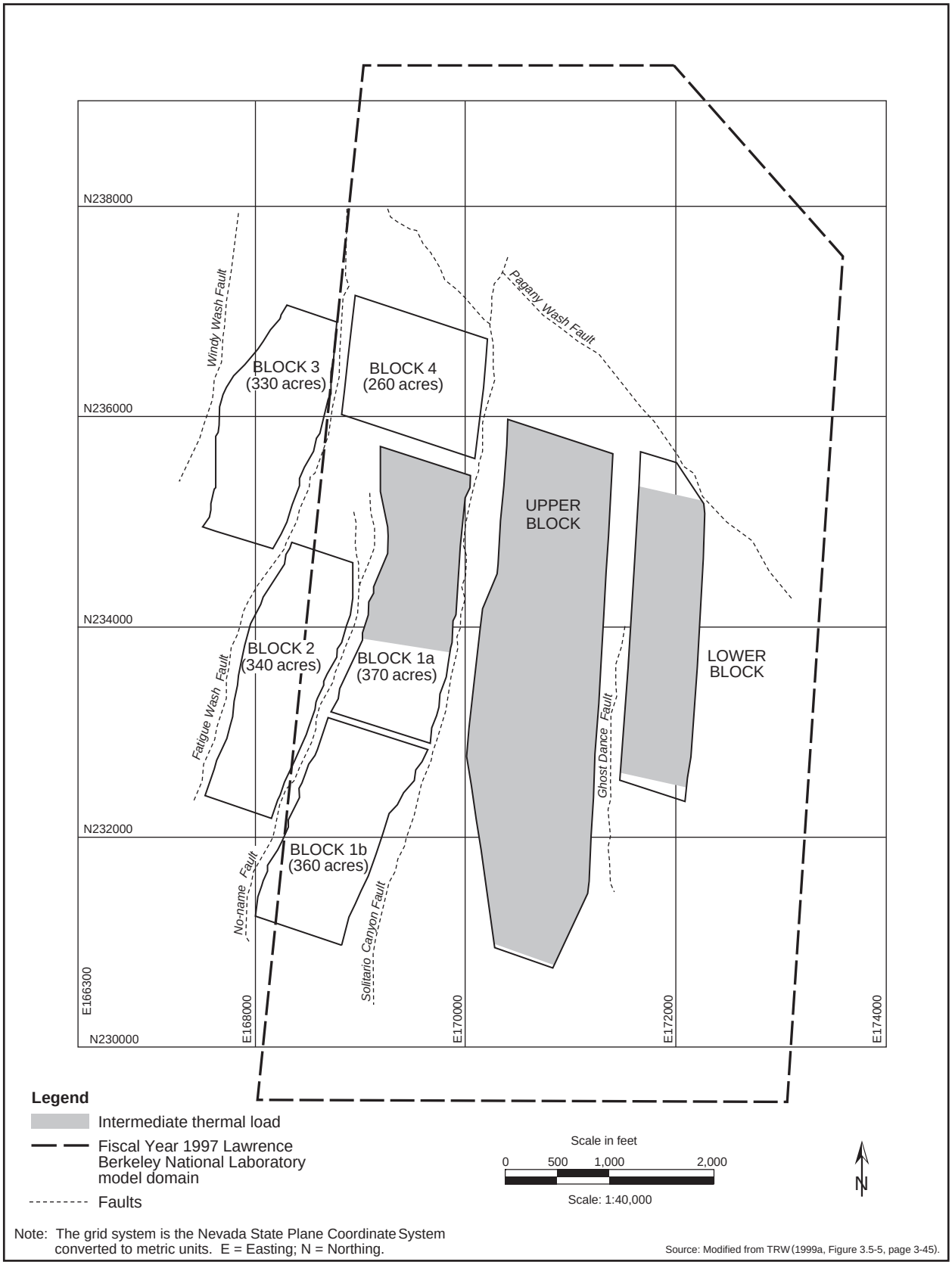

Figure I-31. Regions for performance assessment modeling, Option 5, intermediate thermal load scenario, Inventory Module 1.

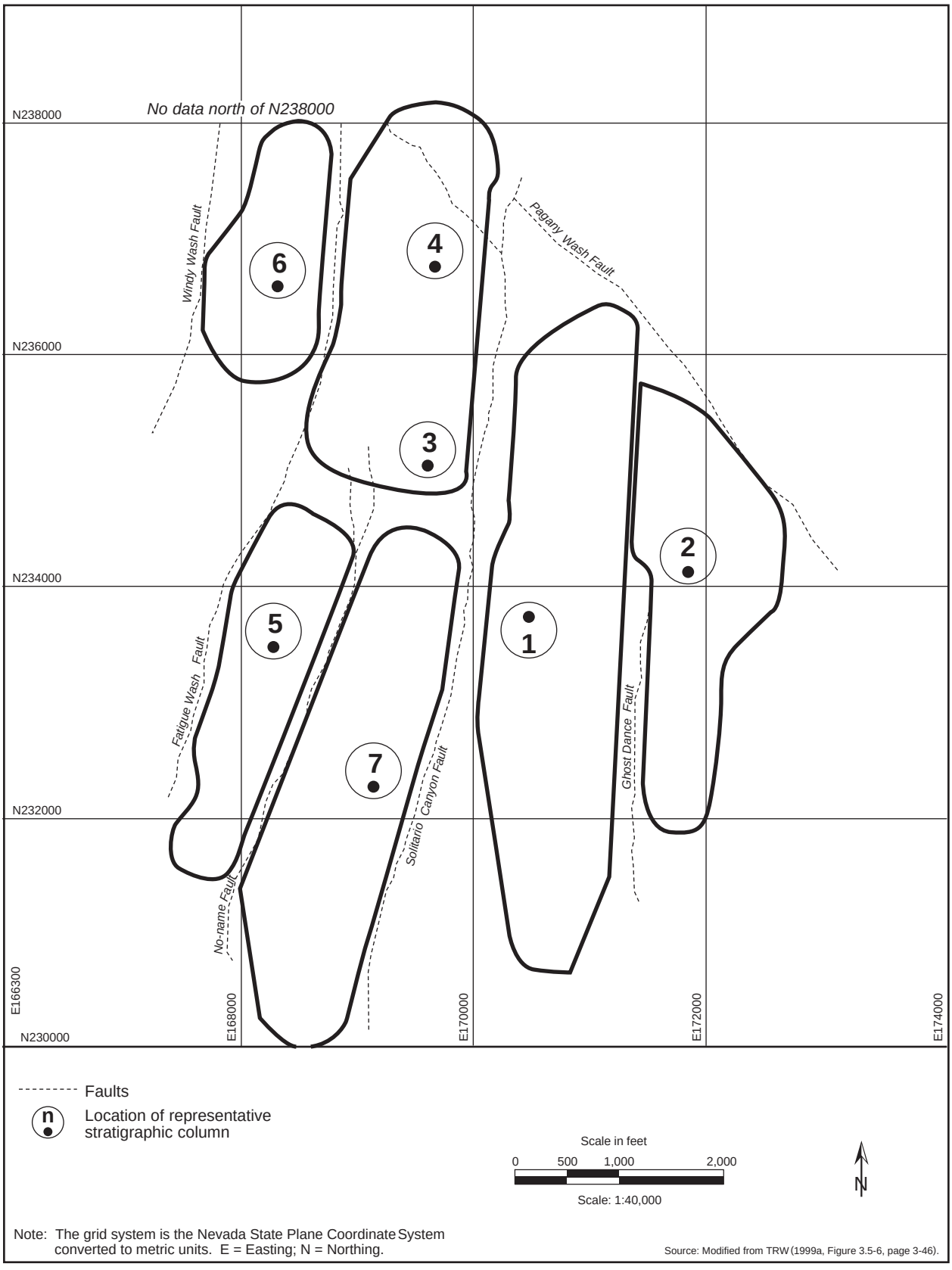

Figure I-32. Repository block areas for performance assessment modeling, Option 6, low thermal load scenario, Inventory Module 1.

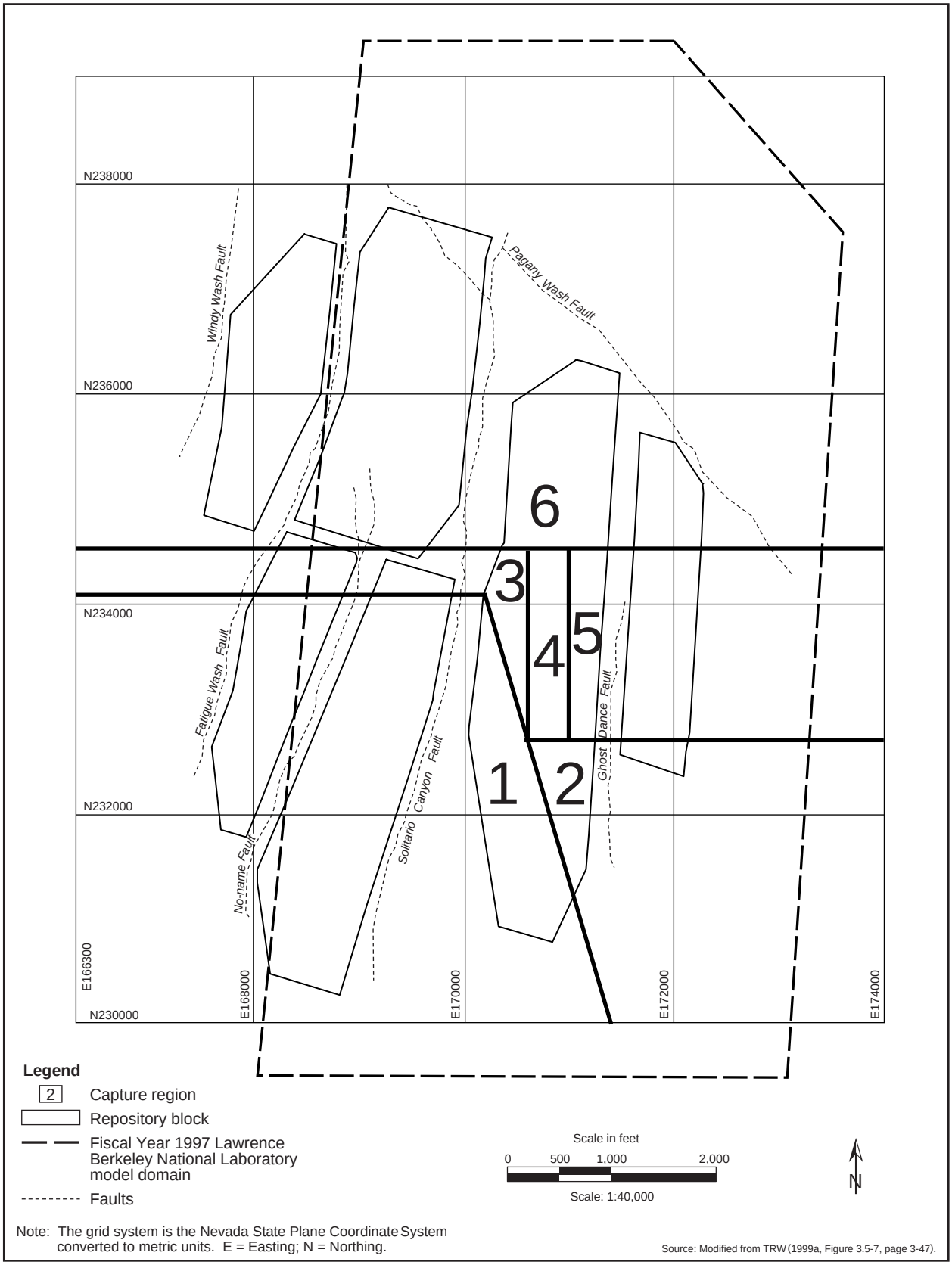

Figure I-33. Capture regions for high and intermediate thermal load scenarios with Proposed Action inventory.

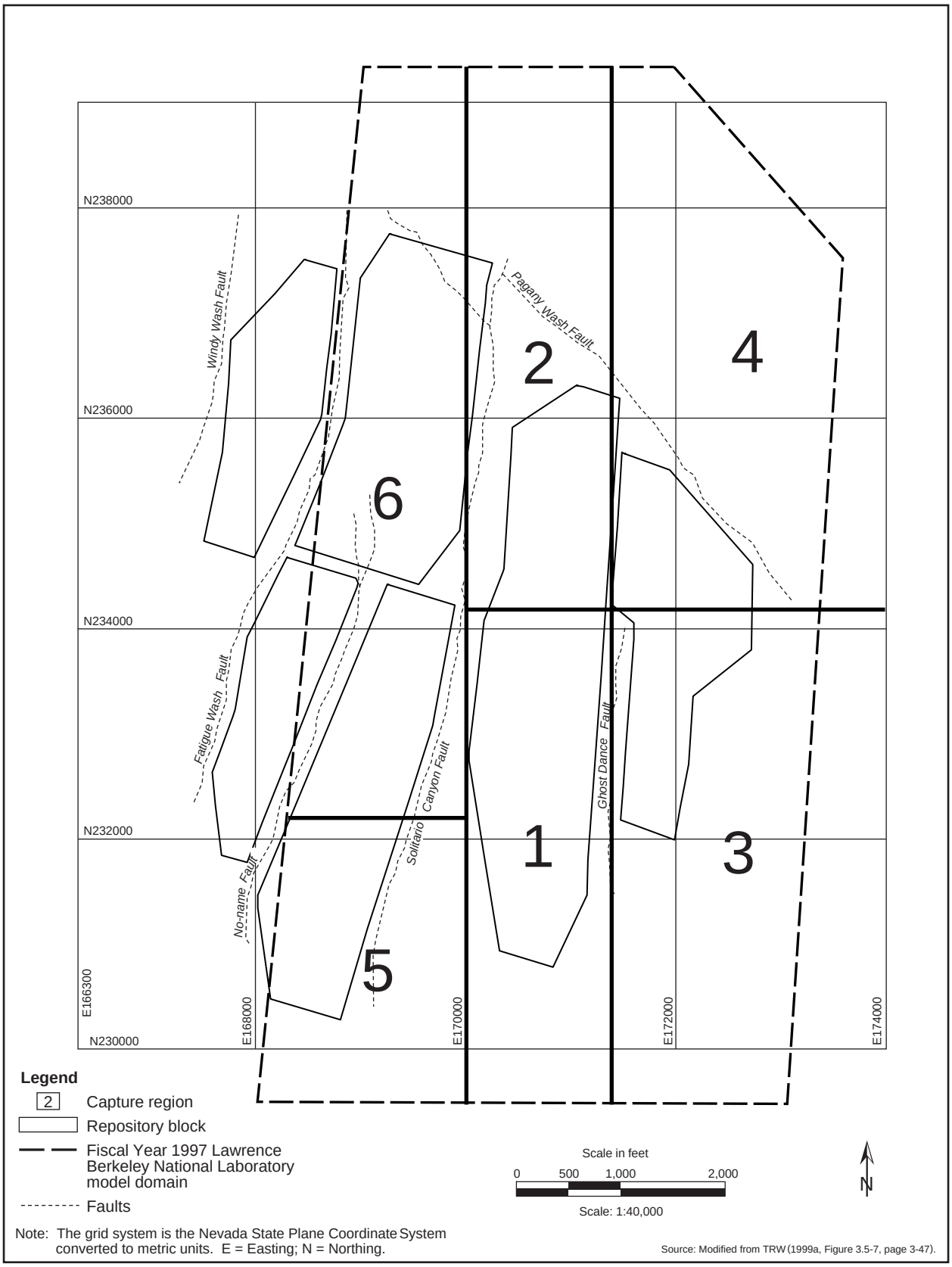

Figure I-34. Capture regions for low thermal load scenario with Proposed Action Inventory and low and intermediate thermal load scenarios with Inventory Modules 1 and 2.

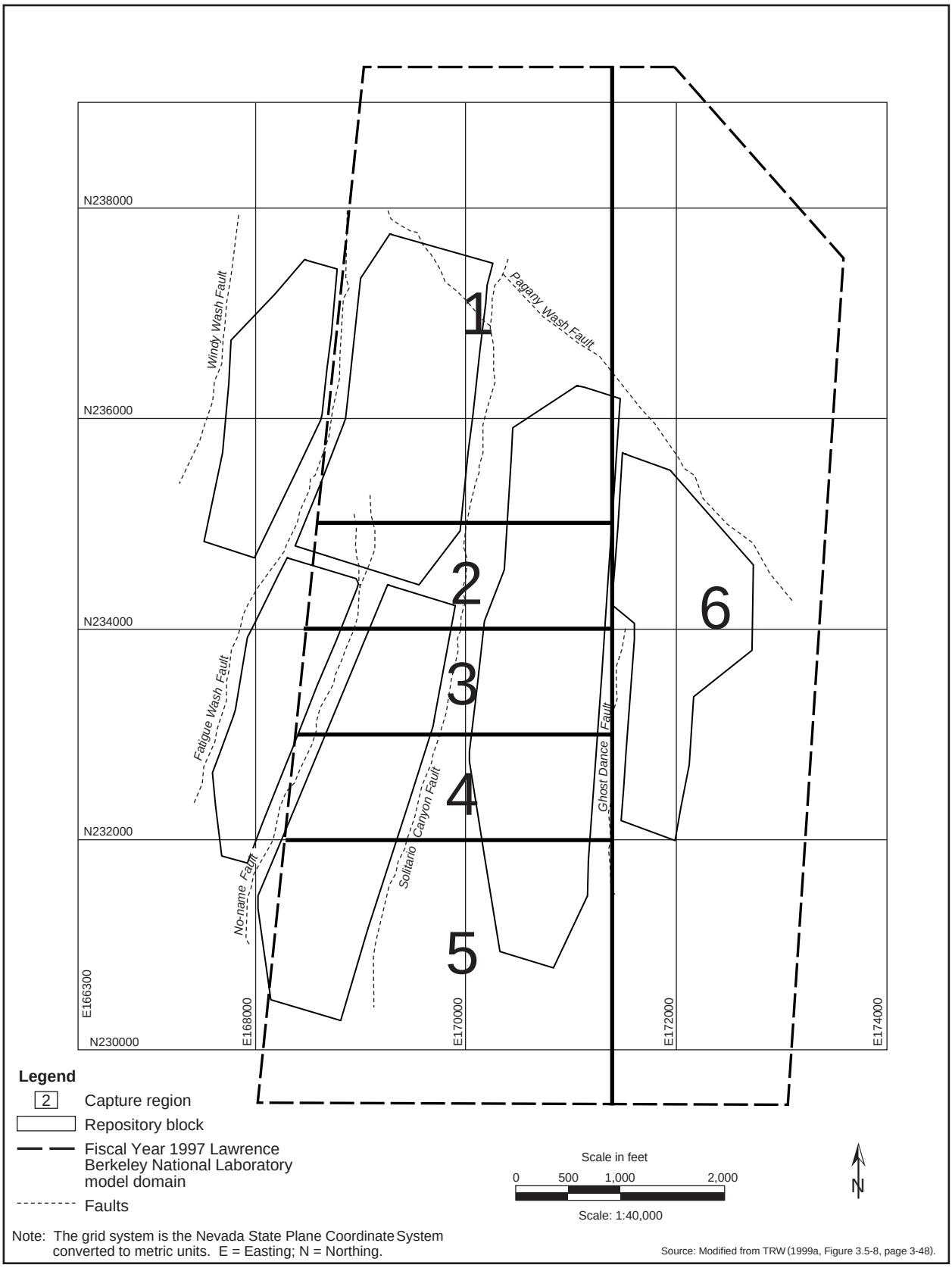

Figure I-35. Capture regions for high thermal load scenario with Inventory Modules 1 and 2.

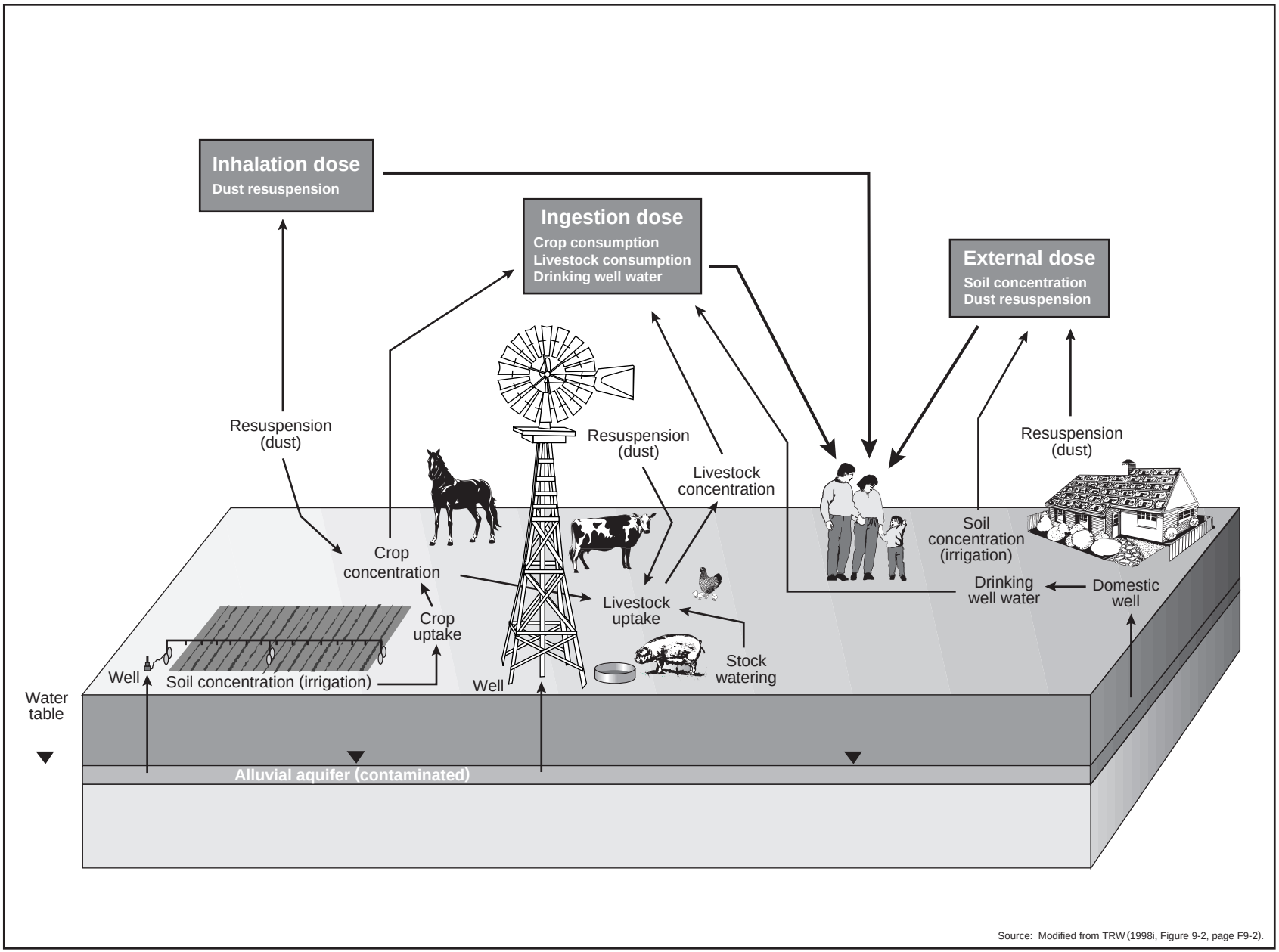

Figure I-36. Biosphere modeling components, including ingestion of contaminated food and water, inhalation of contaminated air, and exposure to direct external radiation.

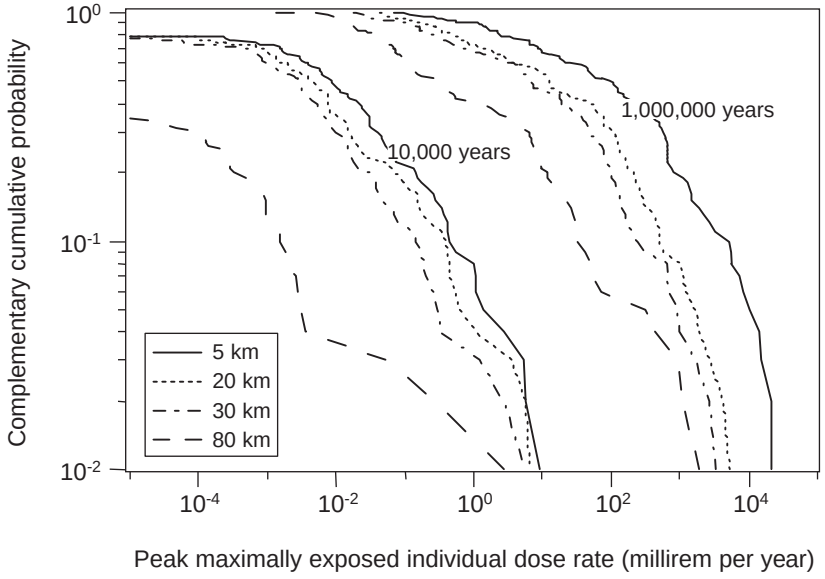

km = kilometer. To convert kilometers to miles, multiply by0.62137.

Figure I-37. Complementary cumulative distribution function of peak maximally exposed individual radiological dose rates during 10,000 and 1 million years following closure for high thermal load scenario with Proposed Action inventory (100 realizations, all pathways, all distances).

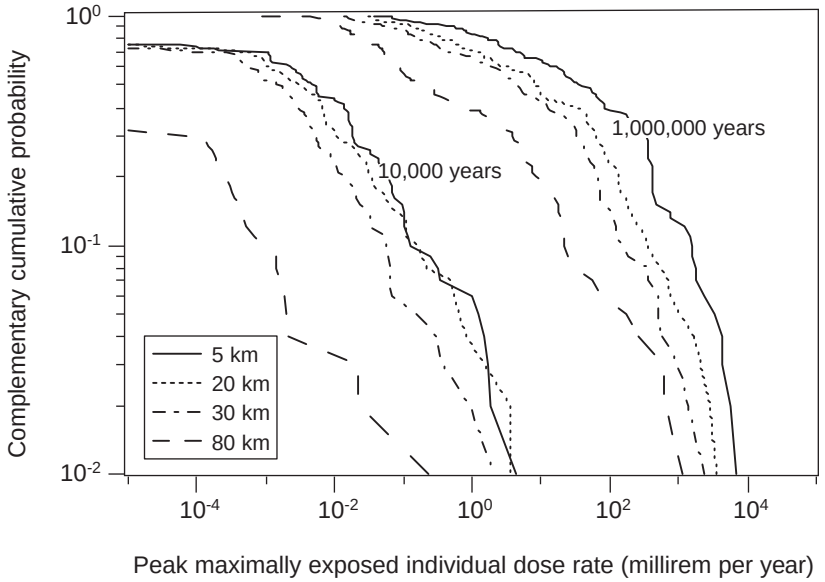

km = kilometer. To convert kilometers to miles, multiply by0.62137.

Figure I-38. Complementary cumulative distribution function of peak maximally exposed individual radiological dose rates during 10,000 and 1 million years following closure for intermediate thermal load scenario with Proposed Action inventory (100 realizations, all pathways, all distances).

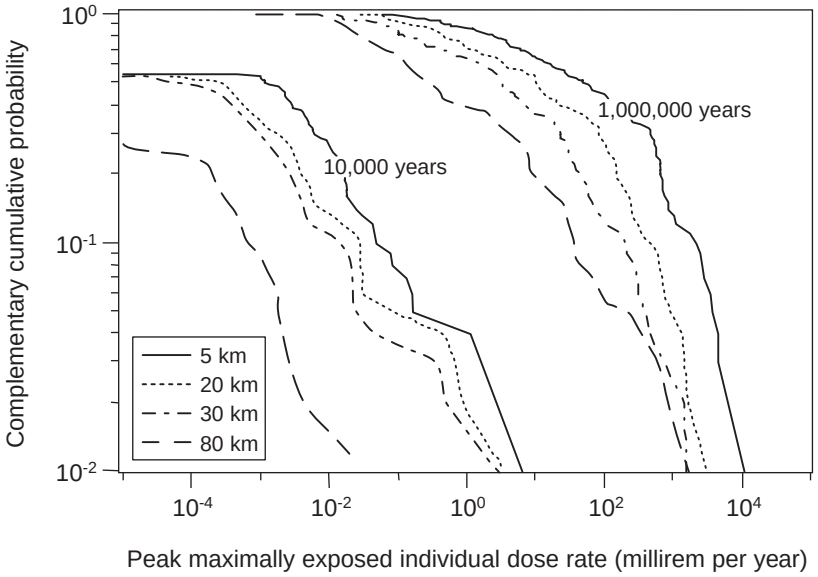

km = kilometer. To convert kilometers to miles, multiply by0.62137.

Figure I-39. Complementary cumulative distribution function of peak maximally exposed individual radiological dose rates during 10,000 and 1 million years following closure for low thermal load scenario with Proposed Action inventory (100 realizations, all pathways, all distances).

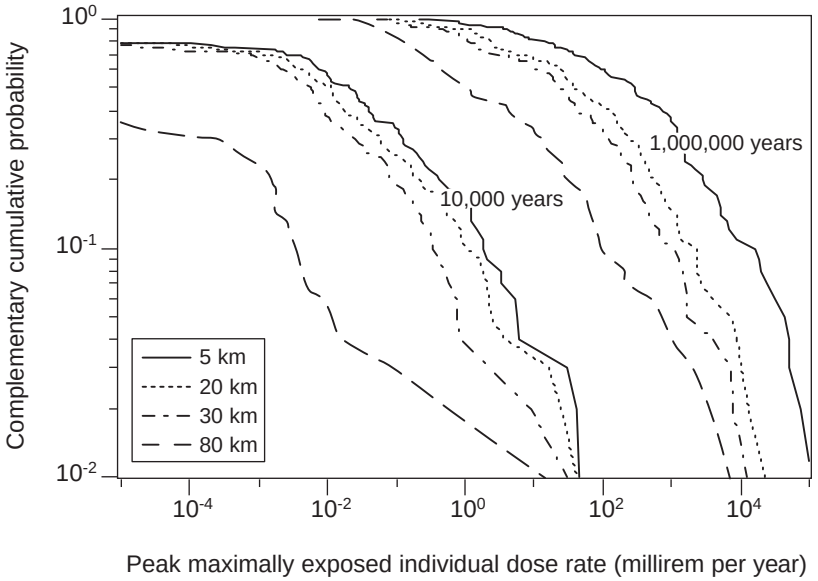

km = kilometer. To convert kilometers to miles, multiply by0.62137.

Figure I-40. Complementary cumulative distribution function of peak maximally exposed individual radiological dose rates during 10,000 and 1 million years following closure for high thermal load scenario with Inventory Module 1 (100 realizations, all pathways, all distances).

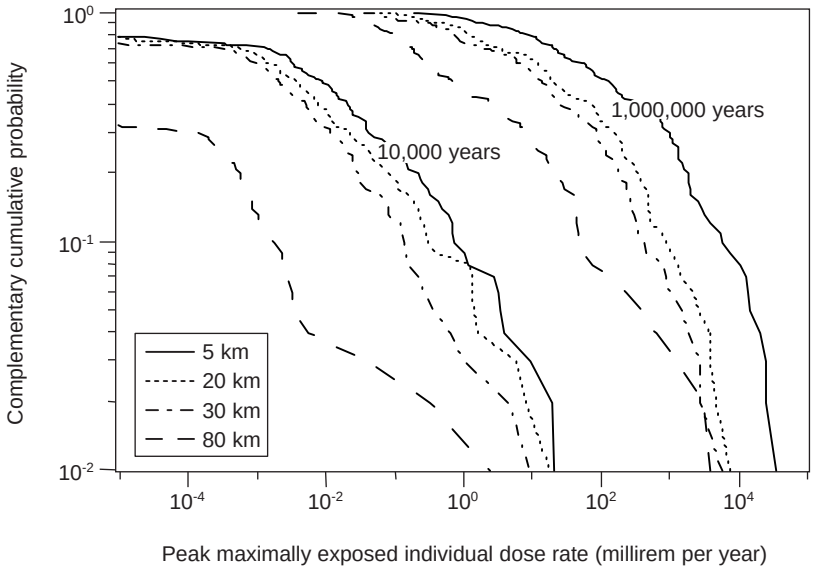

km = kilometer. To convert kilometers to miles, multiply by0.62137.

Figure I-41. Complementary cumulative distribution function of peak maximally exposed individual radiological dose rates during 10,000 and 1 million years following closure for intermediate thermal load scenario with Inventory Module 1 (100 realizations, all pathways, all distances).

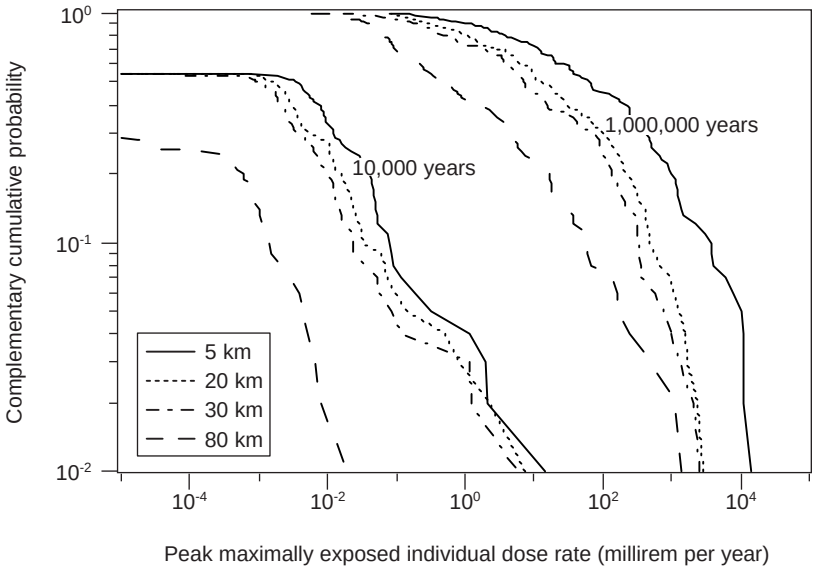

km = kilometer. To convert kilometers to miles, multiply by0.62137.

Figure I-42. Complementary cumulative distribution function of peak maximally exposed individual radiological dose rates during 10,000 and 1 million years following closure for low thermal load scenario with Inventory Module 1 (100 realizations, all pathways, all distances).

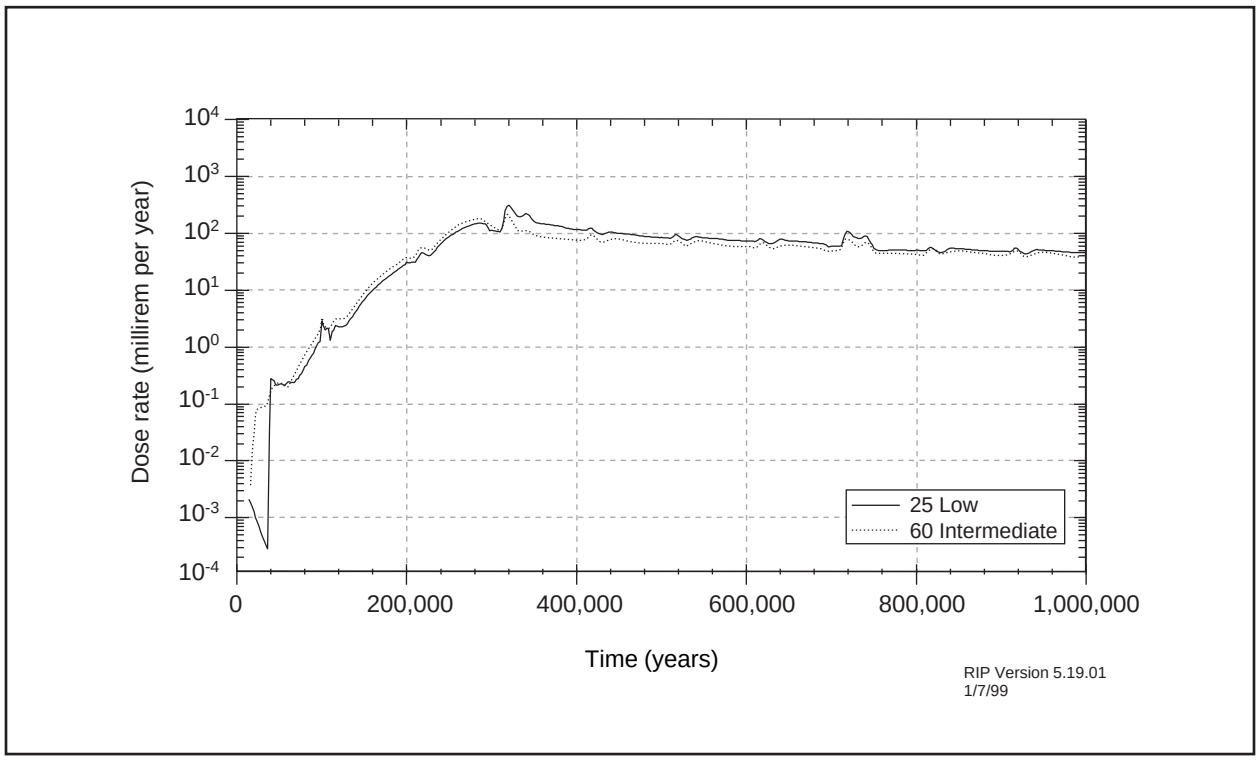

Figure I-43. Comparison of low and intermediate thermal load scenarios total radiological dose histories for the Proposed Action inventory 20 kilometers (12 miles) from the repository.

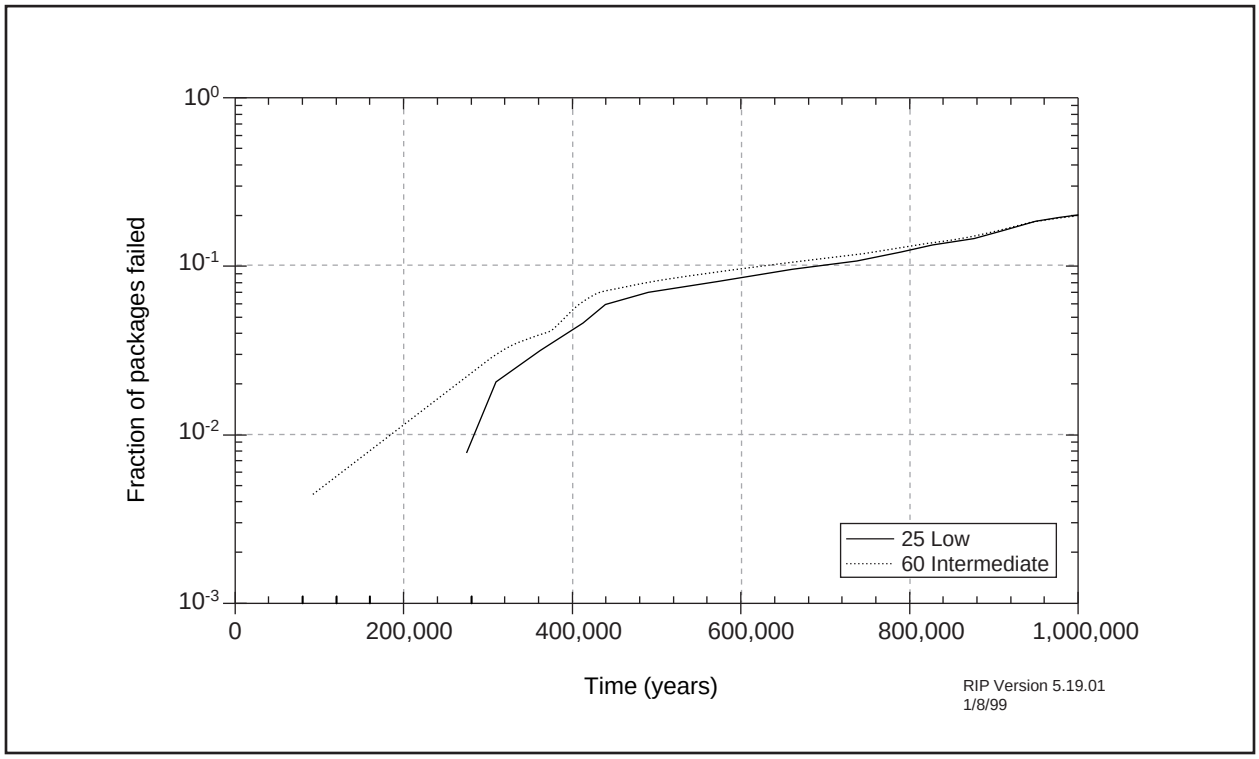

Figure I-44. Waste package failure curves for low and intermediate thermal load scenarios.

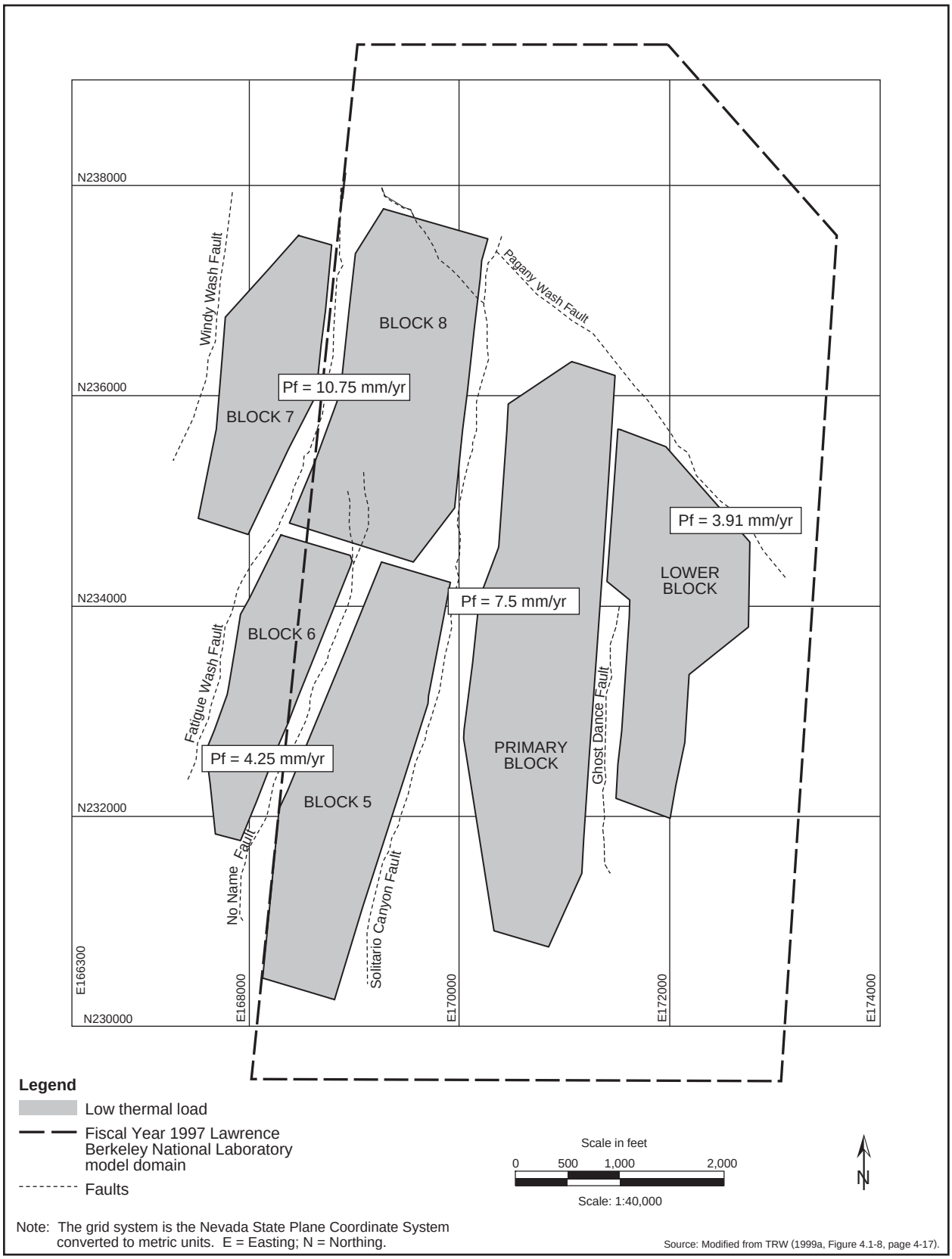

Figure I-45. Average percolation flux for repository blocks.

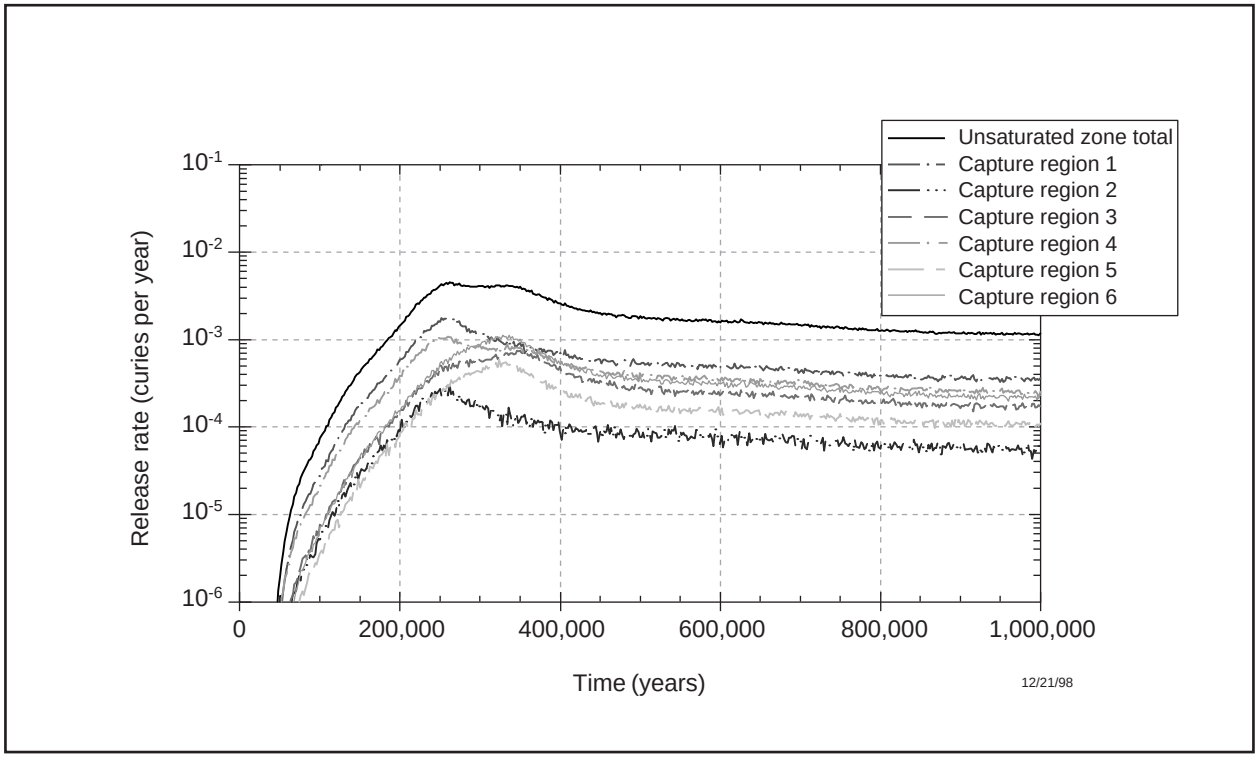

Figure I-46. Neptunium-237 release rate at the water table for fixed long-term average climate for low thermal load scenario during the first 1 million years following repository closure.

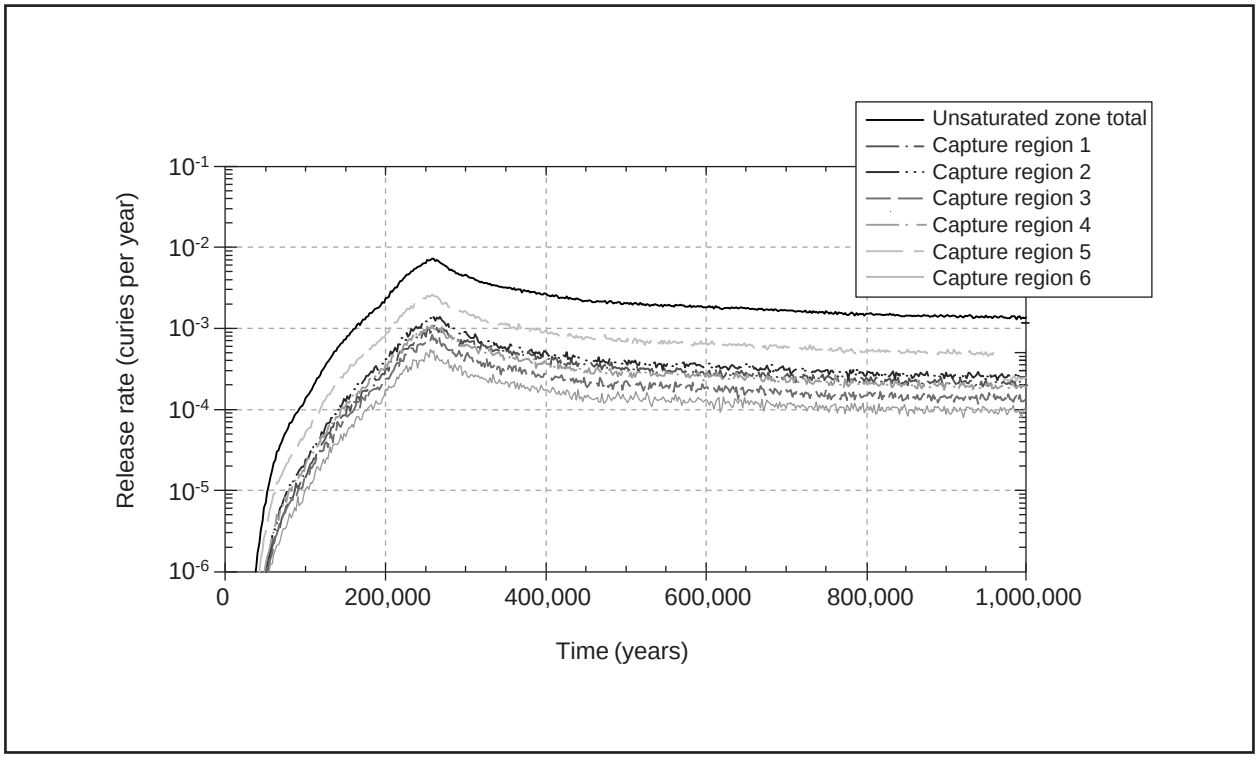

Figure I-47. Neptunium-237 release rate at the water table for fixed long-term average climate for intermediate thermal load scenario during the first 1 million years following repository closure.

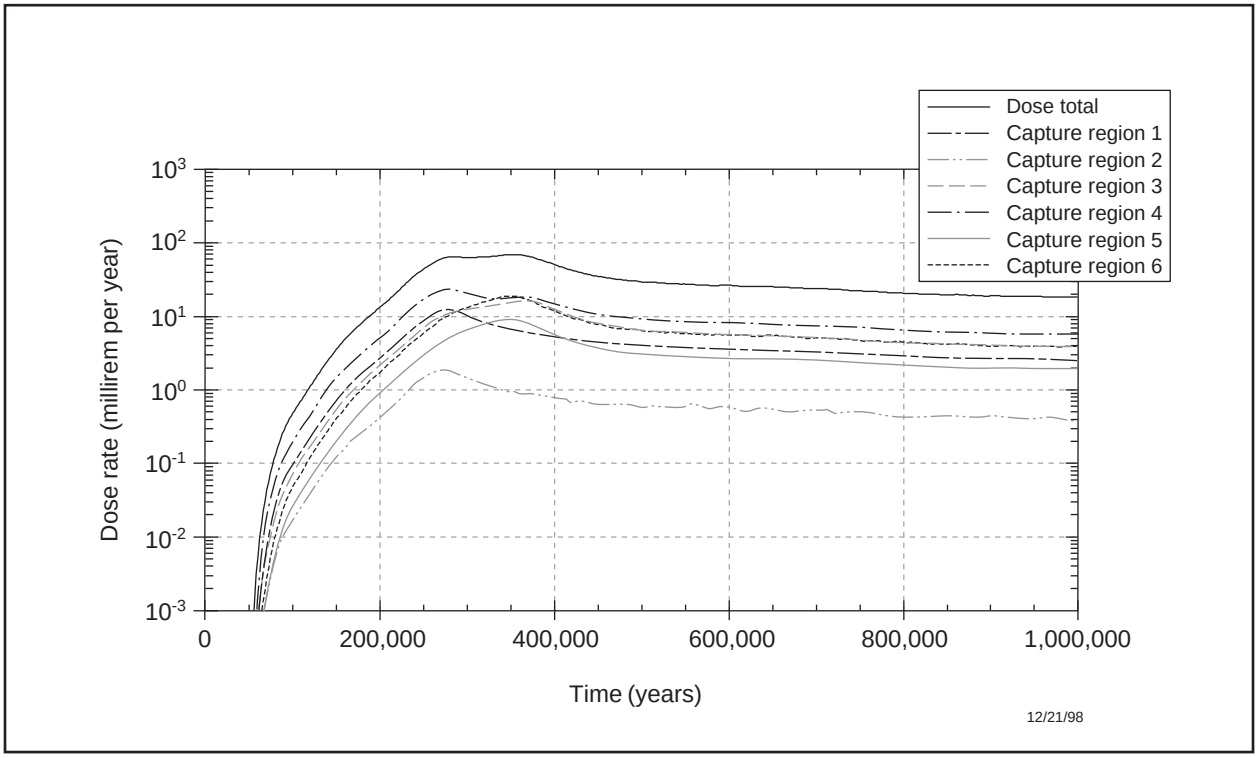

Figure I-48. Neptunium-237 release rate at the end of the saturated zone for fixed long-term average climate for low thermal load scenario during the first 1 million years following repository closure.

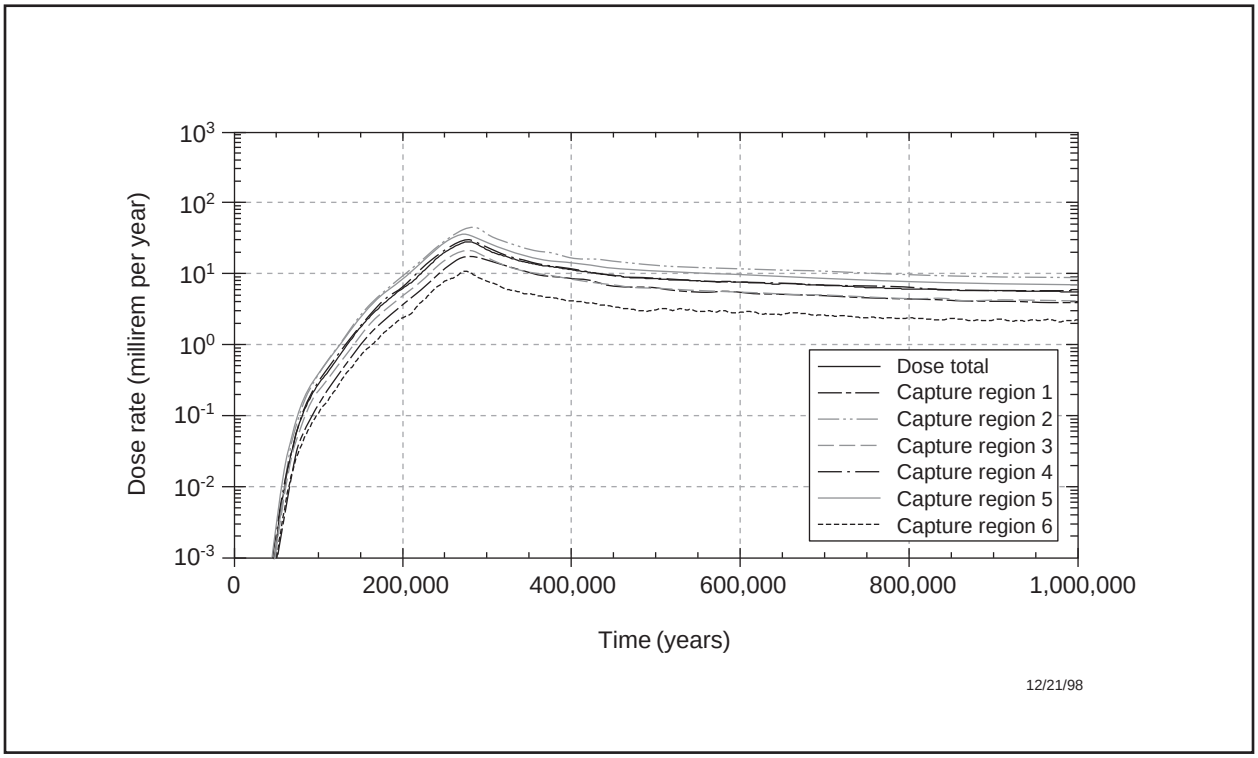

Figure I-49. Neptunium-237 release rate at the end of the saturated zone for fixed long-term average climate for intermediate thermal load scenario during the first 1 million years following repository closure.

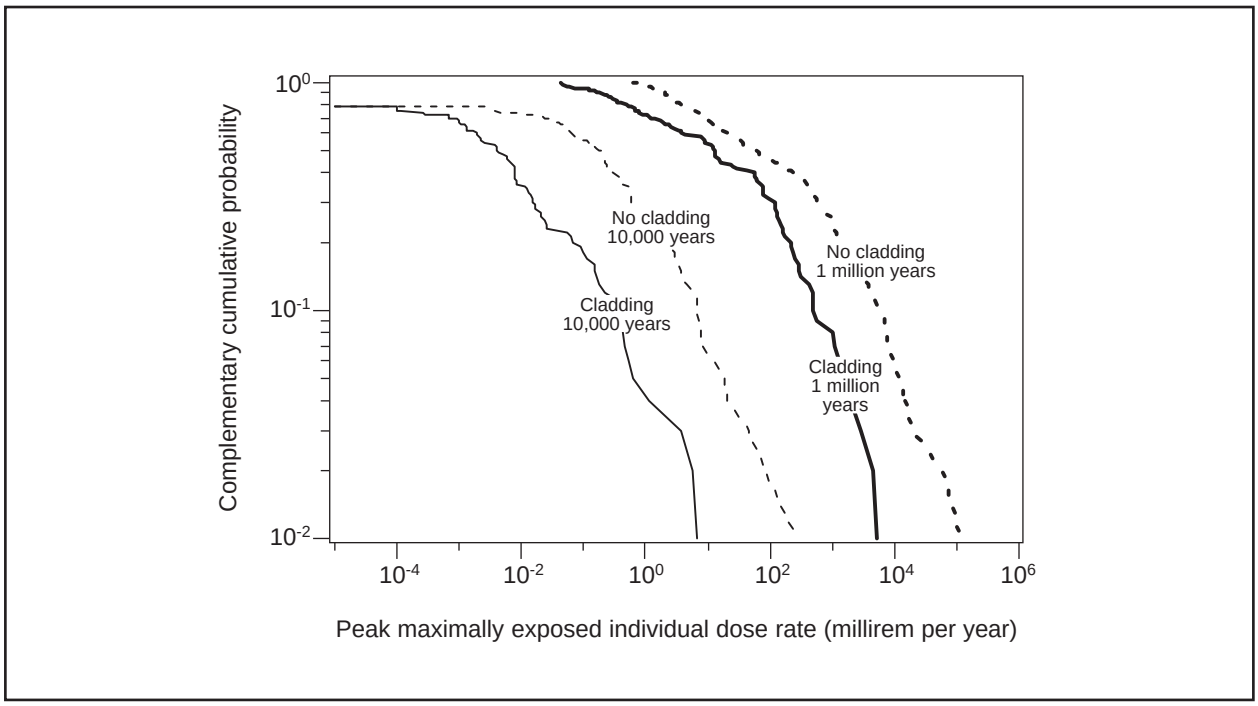

Figure I-50. Complementary cumulative distribution function of radiological doses with and without cladding for a maximally exposed individual at 20 kilometers (12 miles) under the Proposed Action 10,000 and 1 million years after repository closure.

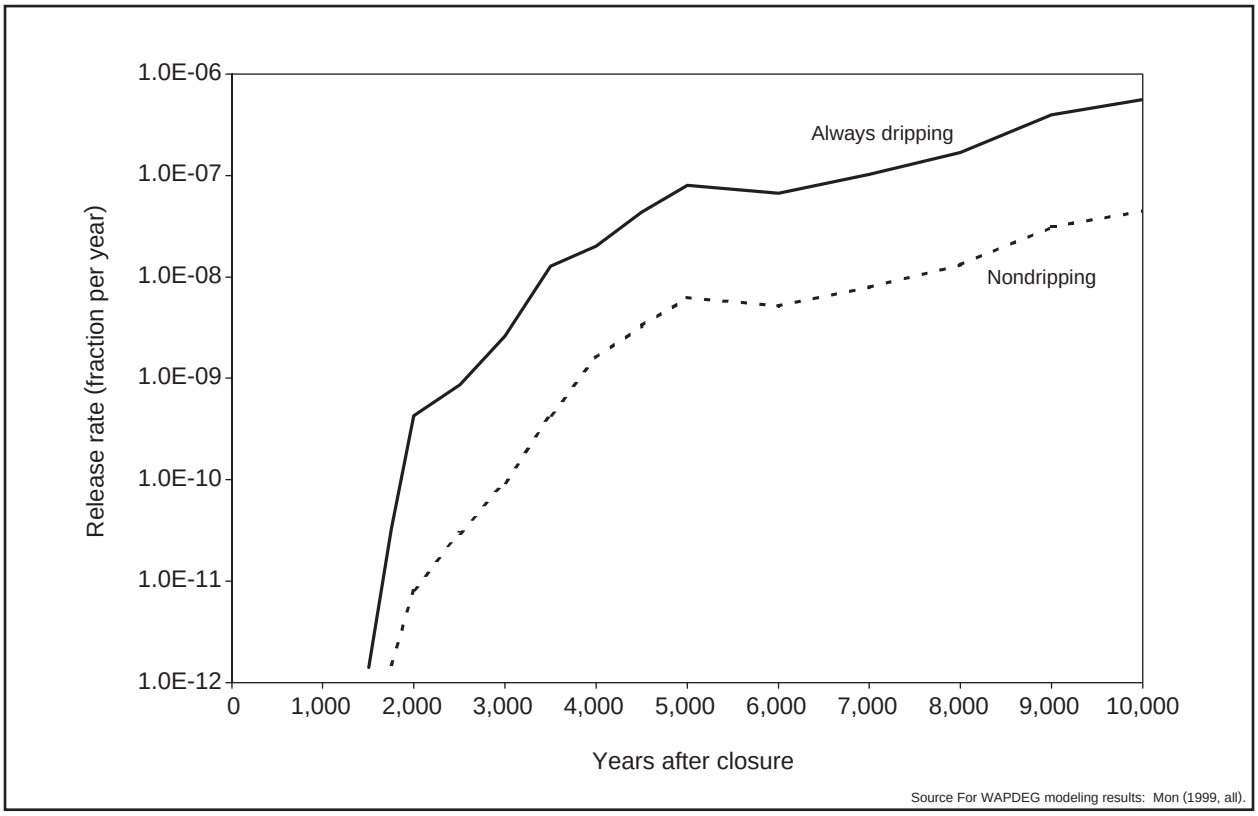

Figure I-51. Average fractional release rate of corrosion-resistant material (Alloy-22) for continually dripping and nondripping conditions computed from WAPDEG modeling results for 400 simulated waste packages.

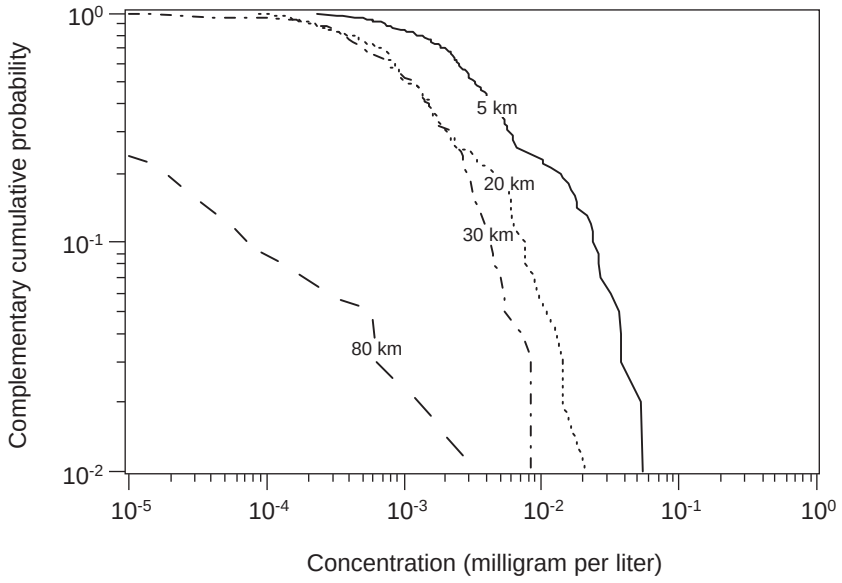

km = kilometer. To convert kilometers to miles, multiply by0.62137.

Figure I-52. Complementary cumulative distribution function of mean peak groundwater concentrations of chromium during 10,000 years following closure under high thermal load scenario with Proposed Action inventory.

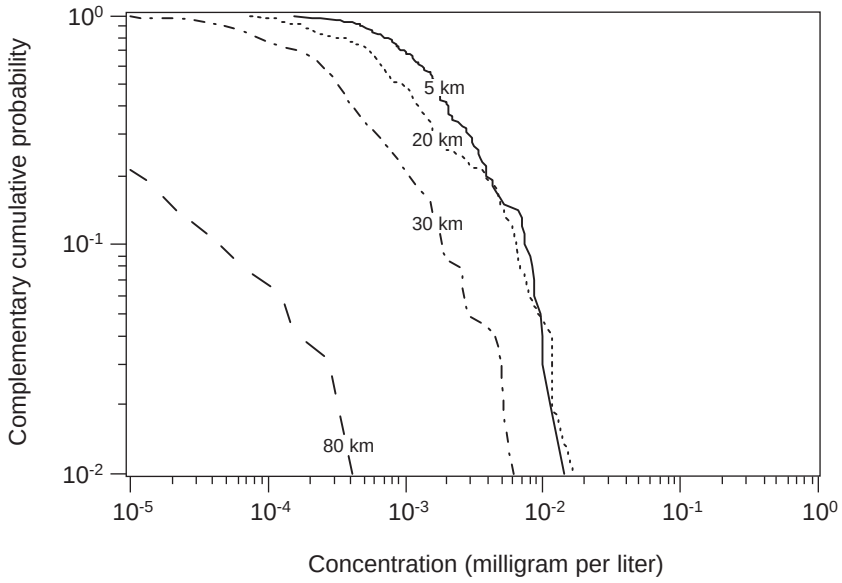

km = kilometer. To convert kilometers to miles, multiply by0.62137.

Figure I-53. Complementary cumulative distribution function of mean peak groundwater concentrations of chromium during 10,000 years following closure under intermediate thermal load scenario with Proposed Action inventory.

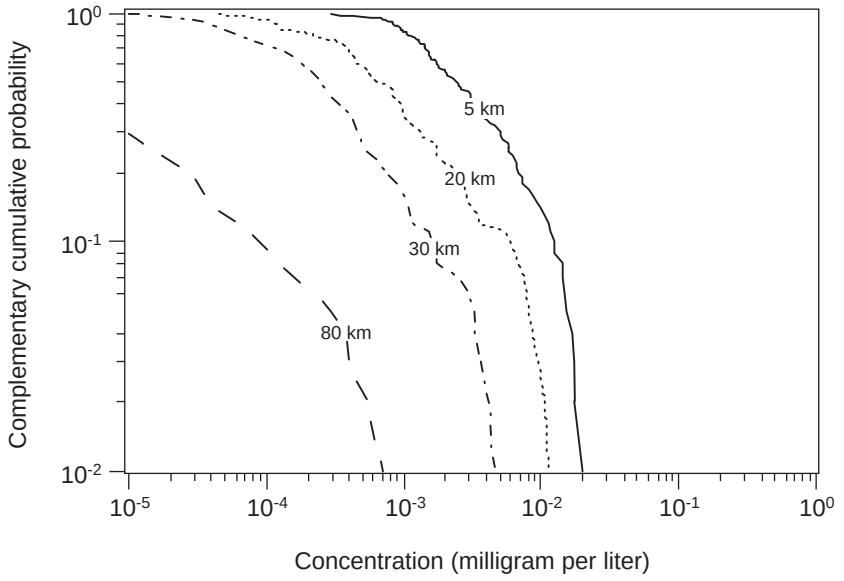

km = kilometer. To convert kilometers to miles, multiply by0.62137.

Figure I-54. Complementary cumulative distribution function of mean peak groundwater concentration of chromium during 10,000 years following closure under low thermal load scenario with Proposed Action inventory.

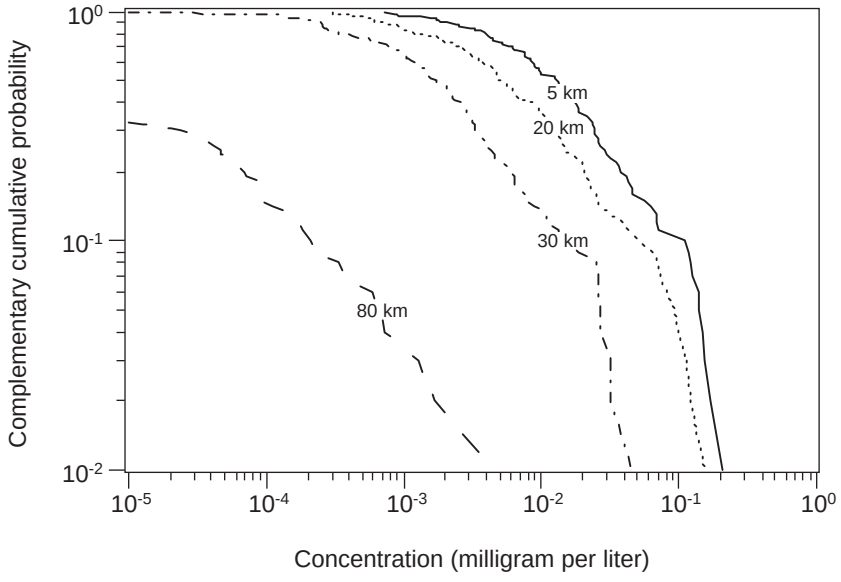

km = kilometer. To convert kilometers to miles, multiply by0.62137.

Figure I-55. Complementary cumulative distribution function of mean peak groundwater concentration of chromium during 10,000 years following closure under high thermal load scenario with Inventory Module 1.

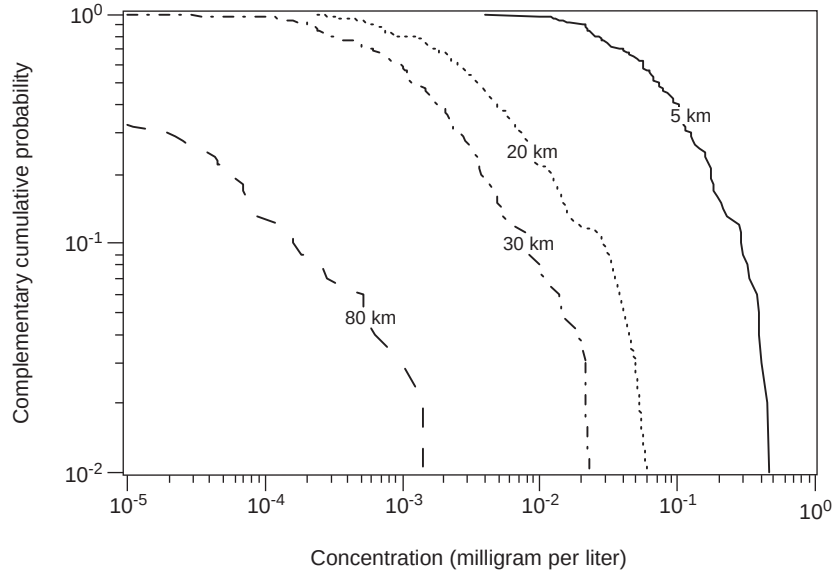

km = kilometer. To convert kilometers to miles, multiply by0.62137.

Figure I-56. Complementary cumulative distribution function of mean peak groundwater concentration of chromium during 10,000 years following closure under intermediate thermal load scenario with Inventory Module 1.

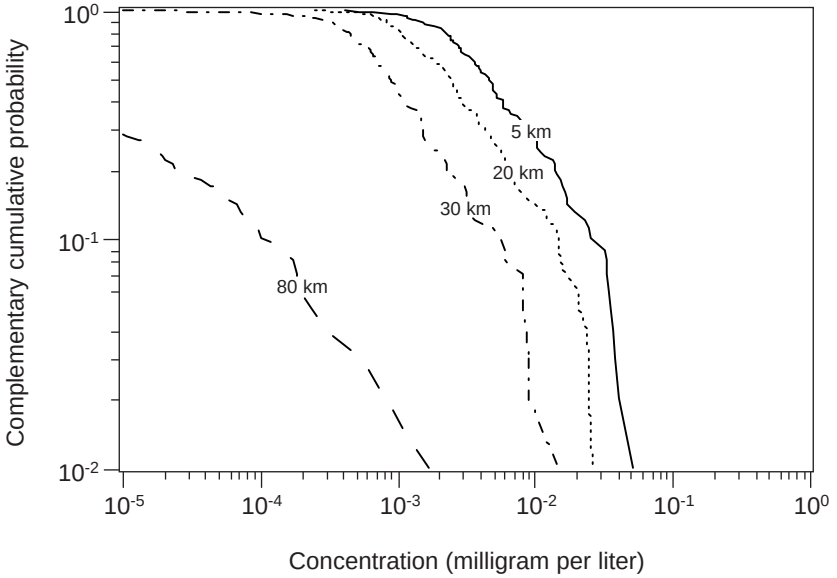

km = kilometer. To convert kilometers to miles, multiply by0.62137.

Figure I-57. Complementary cumulative distribution function of mean peak groundwater concentration of chromium during 10,000 years following closure under low thermal load scenario with Inventory Module 1.

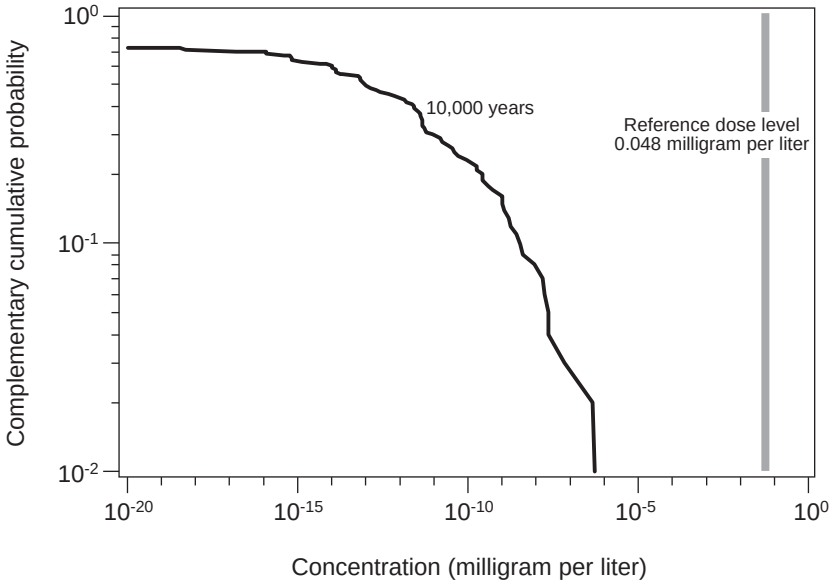

Figure I-58. Complementary cumulative distribution function of mean peak groundwater concentration of elemental uranium in water at 5 kilometers (3 miles) during 10,000 years following closure under high thermal load scenario with Proposed Action inventory.

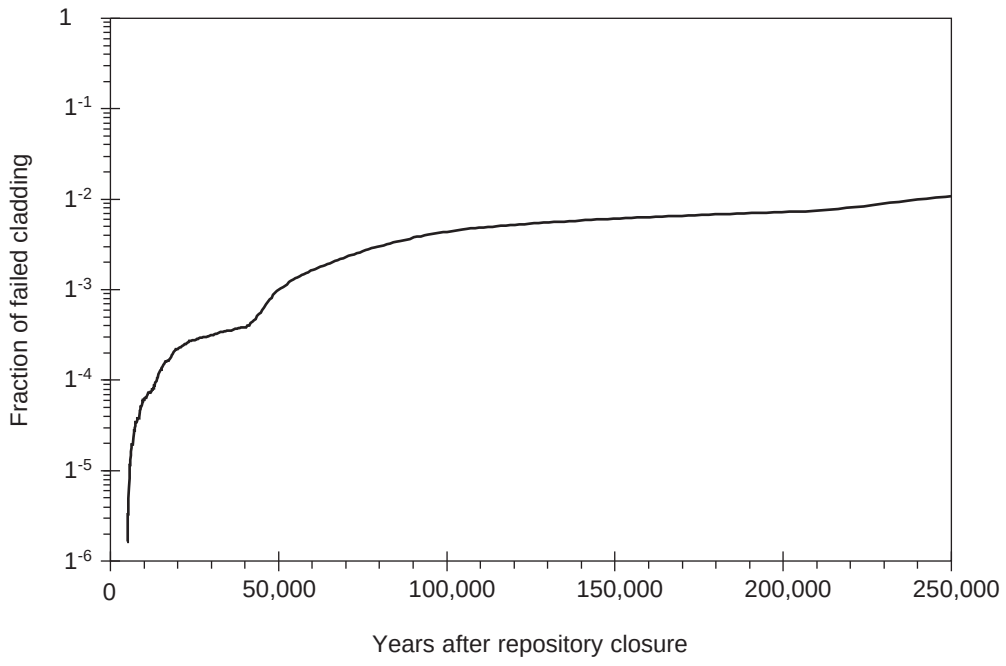

Figure I-59. Fraction (patch area) of cladding that would fail using a zirconium-alloy corrosion rate equal to 1.0 percent of that of Alloy-22.

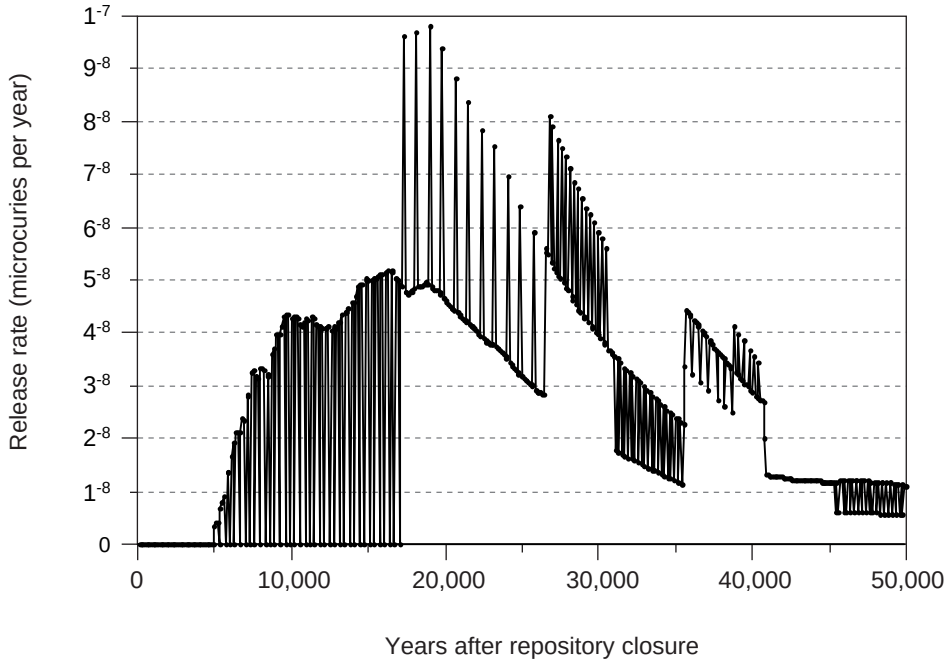

Figure I-60. Release rate of carbon-14 from the repository to the ground surface.

REFERENCES

ASTM 1994 — ASTM (American Society for Testing and Materials), 1994, "Standard Specification for Low-Carbon Nickel-Molybdenum-Chromium, Low-Carbon Nickel-Chromium-Molybdenum, and Low-Carbon Nickel-Chromium-Molybdenum-Tungsten Alloy Rod," B574-94, Conshohocken, Pennsylvania. [243913]

Barnard et al. 1992 — Barnard, R. W., M. L. Wilson, H. A. Dockery, J. H. Gauthier, P. G. Kaplan, R. R. Eaton, F. W. Bingham, and T. H. Robey, 1992, *TSPA 1991: An Initial Total-System Performance Assessment for Yucca Mountain,* SAND91-2795, Sandia National Laboratories, Albuquerque, New Mexico. [NNA.19920630.0033]

Bodvarsson, Bandurraga, and Wu 1997 — Bodvarsson, G. S., T. M. Bandurraga, and Y. S. Wu, editors, 1997, *The Site-Scale Unsaturated Zone Model of Yucca Mountain, Nevada, for the Viability Assessment,* LBNL-40376, Lawrence Berkeley National Laboratory, Berkeley, California. [MOL.19971014.0232]

Croff 1980 — Croff, A. G., 1980, *ORIGEN2 – A Revised and Updated Version of the Oak Ridge Isotope Generation and Depletion Code,* ORNL-5621, Oak Ridge National Laboratory, Oak Ridge, Tennessee. [NNA.19910326.0094]

DOE 1992 — DOE (U.S. Department of Energy), 1992, *Characteristics of Potential Repository Wastes,* DOE/RW-0184-R1, Oak Ridge National Laboratory, Oak Ridge, Tennessee. [HQO.19920827.0001, Volume 1; HQO.19920827.0002, Volume 2; HQO.19920827.0003, Volume 3; HQO.19920827.0004, Volume 4]

DOE 1994 — DOE (U.S. Department of Energy), 1994, *Greater-Than-Class C Low-Level Radioactive Waste Characterization: Estimated Volumes, Radionuclide Activities, and Other Characteristics,* DOE/LLW-114, Revision 1, Idaho National Engineering Laboratory, Idaho Falls, Idaho. [231330]

DOE 1998a — DOE (U.S. Department of Energy), 1998a, *Viability Assessment of a Repository at Yucca Mountain,* DOE/RW-0508, Office of Civilian Radioactive Waste Management, Washington, D.C. [U.S. Government Printing Office, MOL.19981007.0027, Overview; MOL.19981007.0028, Volume 1; MOL.19981007.0029, Volume 2; MOL.19981007.0030, Volume 3; MOL.19981007.0031, Volume 4; MOL.19981007.0032, Volume 5]

DOE 1998b — DOE (U.S. Department of Energy), 1998b, *DOE Standard: Guide of Good Practices for Occupational Radiological Protection in Plutonium Facilities,* DOE-STD-1128-98, Office of Environment, Safety and Health, Washington, D.C. [243733]

Eckerman, Wolbarst, and Richardson 1988 — Eckerman, K. F., A. B. Wolbarst, and A. C. B. Richardson, 1988, *Limiting Values of Radionuclide Intake and Air Concentration and Dose Conversion Factors for Inhalation, Submersion, and Ingestion,* Federal Guidance Report No. 11, EPA-520/1-88-020, U.S. Environmental Protection Agency, Office of Radiation Programs, Oak Ridge National Laboratory, Oak Ridge, Tennessee. [203350]

EPA 1994	EPA (U.S. Environmental Protection Agency), 1994, *Health Effects Assessment Summary Tables: FY-1994 Annual*, EPA-540-R-94-020, Office of Solid Waste and Emergency Response, Office of Emergency Remedial Response, Office of Research and Development, Washington, D.C. [243734]
EPA 1998	EPA (U.S. Environmental Protection Agency), 1998, *Toxicological Review of Hexavalent Chromium (CAS No. 18540-29-9),* Washington, D.C. [243147]
EPA 1999	EPA (U.S. Environmental Protection Agency), 1999, "List of Substances on IRIS," http://www.epa.gov/iris/subst/index.html, Boron/0410.htm, Cadmium/0141.htm, Chromium III/0028.htm, Chromium IV/0144.htm, Manganese/0373.htm, Molybdenum/0425.htm, Nickel/0271.htm, Uranium/0421.htm, Vanadium/0125.htm, Zinc/0426.htm, June 10, Office of Research and Development, National Center for Environmental Assessment, Cincinnati, Ohio. [244100 to 244109]
Golder 1998	Golder Associates, Inc., 1998, *RIP Integrated Probabilistic Simulator for Environmental Systems: Theory Manual and User's Guide*, Redmond, Washington. [238560]
Harrar et al. 1990	Harrar, J. E., J. I. Carley, W. I. Isherwood, and E. Raber, 1990, *Report of the Committee to Review the Use of J-13 Well Water in Nevada Nuclear Waste Storage Investigations*, UCID-21867, Lawrence Livermore National Laboratory, Livermore, California. [209096]
IAEA 1994	IAEA (International Atomic Energy Agency), 1994, *Technical Reports Series No. 364, Handbook of Parameter Values for the Prediction of Radionuclide Transfer in Temperate Environments,* Vienna, Austria. [232035]
ICRP 1975	ICRP (International Commission on Radiological Protection), 1975, *Report of the Task Group on Reference Man; a report prepared by a task group of Committee 2 of the International Commission on Radiological Protection,* Publication 23, Pergamon Press, Oxford, Great Britain. [237218]
ICRP 1979	ICRP (International Commission on Radiological Protection), 1979, *Limits for Intakes of Radionuclides by Workers; a report of Committee 2 of the International Commission on Radiological Protection*, Publication 30, Pergamon Press, New York. [4939]
International Consultants 1997	International Consultants, Inc., 1997, *Health Effects Assessment Summary Tables: FY-1997 Update*, EPA-540-R-97-036, Dayton, Ohio. [243784]
Killough and Rohwer 1978	Killough, G. G., and P. S. Rohwer, 1978, "A New Look at the Dosimetry of ^{14}C Released to the Atmosphere as Carbon Dioxide," *Health Physics*, Volume 34, pp. 141-159, Pergamon Press, London, Great Britain. [243510]
LaPlante and Poor 1997	LaPlante, P. A., and K. Poor, 1997, *Information and Analyses to Support Selection of Critical Groups and Reference Biospheres for Yucca Mountain Exposure Scenarios*, CNWRA97-009, The Center for Nuclear Waste Regulatory Analysis, San Antonio, Texas. [236454]

Leigh et al. 1993	Leigh, C.D., B. M. Thompson, J. E. Campbell, D. E. Longsine, R. A. Kennedy, and B. A. Napier, 1993, *User's Guide for GENII-S: A Code for Statistical and Deterministic Simulations of Radiation Doses to Humans from Radionuclides in the Environment,* SAND91-0561, Performance Assessment Department, Sandia National Laboratories, Albuquerque, New Mexico. [231133]
Leij, Scaggs, and van Genuchten 1991	Leij, L. J., T. H. Scaggs, and M. Th. Van Genuchten, 1991, "Analytical solutions for solute transport in three-dimensional semi-infinite porous media," *Water Resources Research,* Volume 27, Number 10, pp. 2719-2733. [238367]
Mon 1999	Mon, K. G., 1999, "Environmental Impact Statement - Chromium Model Inputs from WAPDEG Version 3.11," memorandum to W. Nichols (Jason Technologies Corporation), January 12, TRW Environmental Safety Systems Inc., Las Vegas, Nevada. [MOL.19990511.0387]
National Research Council 1995	National Research Council, 1995, *Technical Bases for Yucca Mountain Standards,* Committee on Technical Bases for Yucca Mountain Standards, Board on Radioactive Waste Management, Commission on Geosciences, Environment, and Resources, National Academy Press, Washington, D.C. [217588]
NCRP 1993	NCRP (National Council on Radiation Protection and Measurements), 1993, *Limitation of Exposure to Ionizing Radiation: Recommendations of the National Council on Radiation Protection and Measurements,* Report No. 116, Bethesda, Maryland. [207090]
Nitao 1998	Nitao, J. J., 1998, *Reference Manual for the NUFT Flow and Transport Code, Version 2.0,* Lawrence Livermore National Laboratory, Livermore, California. [MOL.19980810.0391]
Oversby 1987	Oversby, V. M., 1987, "Spent fuel as a waste form: data needs to allow long-term performance assessment under repository disposal conditions," *Scientific Basis for Nuclear Waste Management: symposium held December 1-4, 1986,* J. K. Bates and W. B. Seefeldt, editors, Volume 84, pp. 87-101, Materials Research Society, Pittsburgh, Pennsylvania. [243874]
Pruess 1991	Pruess, K., 1991, *TOUGH2-A: General Purpose Numerical Simulator for Multiphase Fluid and Heat Flow,* LBL-29400, Lawrence Berkeley Laboratory, Berkeley, California. [NNA.19940202.0088]
RamaRao, Ogintz, and Mishra 1998	RamaRao, B. S., J. B. Ogintz, and S. Mishra, 1998, "Alternative Approaches to Modeling Thermohydrologic Processes at Yucca Mountain," *Proceedings of 1998 International High Level Radioactive Waste Management Conference,* pp. 116-118, American Nuclear Society, La Grange Park, Illinois. [240685]
TRW 1995	TRW (TRW Environmental Safety Systems Inc.), 1995, *Total System Performance Assessment – 1995, An Evaluation of the Potential Yucca Mountain Repository,* B00000000-01717-2200-00136, Revision 01, Las Vegas, Nevada. [MOL.19960724.0188]

TRW 1997a — TRW (TRW Environmental Safety Systems Inc.), 1997a, *Waste Quantity, Mix and Throughput Study Report,* B00000000-01717-5705-00059, Revision 01, TRW, Las Vegas, Nevada. [MOL.19971210.0628]

TRW 1997b — TRW (TRW Environmental Safety Systems Inc.), 1997b, *Predecisional Document: Degraded Mode Criticality Analysis of Immobilized Plutonium Waste Forms in a Geologic Repository,* A00000000-01717-5705-00014, Revision 01, Las Vegas, Nevada. [MOL.19980422.0911]

TRW 1997c — TRW (TRW Environmental Safety Systems Inc.), 1997c, *Evaluation of the Potential for Deposition of Uranium/Plutonium from a Repository Waste Package,* BBA000000-01717-0200-00050, Revision 00, Las Vegas, Nevada. [MOL.19980216.0001]

TRW 1997d — TRW (TRW Environmental Safety Systems Inc.), 1997d, *ISM2.0: A 3-D Geologic Framework and Integrated Site Model of Yucca Mountain,* B00000000-01717-5700-00004, Revision 00, Las Vegas, Nevada. [MOL.19970625.0119]

TRW 1998a — TRW (TRW Environmental Safety Systems Inc.), 1998a, "Chapter 1: *Total System Performance Assessment – Viability Assessment (TSPA-VA) Analyses Technical Basis Document,* B00000000-01717-4301-00001, Revision 01, Las Vegas, Nevada. [MOL.19981008.0001]

TRW 1998b — TRW (TRW Environmental Safety Systems Inc.), 1998b, "Chapter 2: Unsaturated Zone Hydrology Model," *Total System Performance Assessment – Viability Assessment (TSPA-VA) Analyses Technical Basis Document,* B00000000-01717-4301-00002, Revision 01, Las Vegas, Nevada. [MOL.19981008.0002]

TRW 1998c — TRW (TRW Environmental Safety Systems Inc.), 1998c, "Chapter 3: Thermal Hydrology," *Total System Performance Assessment – Viability Assessment (TSPA-VA) Analyses Technical Basis Document,* B00000000-01717-4301-00003, Revision 01, Las Vegas, Nevada. [MOL.19981008.0003]

TRW 1998d — TRW (TRW Environmental Safety Systems Inc.), 1998d, "Chapter 4: Near-Field Geochemical Environmental," *Total System Performance Assessment – Viability Assessment (TSPA-VA) Analyses Technical Basis Document,* B00000000-01717-4301-00004, Revision 01, Las Vegas, Nevada. [MOL.19981008.0004]

TRW 1998e — TRW (TRW Environmental Safety Systems Inc.), 1998e, "Chapter 5: Waste Package Degradation Modeling Abstraction," *Total System Performance Assessment – Viability Assessment (TSPA-VA) Analyses Technical Basis Document,* B00000000-01717-4301-00005, Revision 01, Las Vegas, Nevada. [MOL.19981008.0005]

TRW 1998f — TRW (TRW Environmental Safety Systems Inc.), 1998f, "Chapter 6: Waste Form Degradation, Radionuclide Mobilization and Transport through the Engineered Barrier System," *Total System Performance Assessment – Viability Assessment (TSPA-VA) Analyses Technical Basis Document,* B00000000-01717-4301-00006, Revision 01, Las Vegas, Nevada. [MOL.19981008.0006]

TRW 1998g — TRW (TRW Environmental Safety Systems Inc.), 1998g, "Chapter 7: Unsaturated Zone Radionuclide Transport," *Total System Performance Assessment – Viability Assessment (TSPA-VA) Analyses Technical Basis Document,* B00000000-01717-4301-00007, Revision 01, Las Vegas, Nevada. [MOL.19981008.0007]

TRW 1998h — TRW (TRW Environmental Safety Systems Inc.), 1998h, "Chapter 8: Saturated Zone Flow Transport," *Total System Performance Assessment – Viability Assessment (TSPA-VA) Analyses Technical Basis Document,* B00000000-01717-4301-00008, Revision 01, Las Vegas, Nevada. [MOL.19981008.0008]

TRW 1998i — TRW (TRW Environmental Safety Systems Inc.), 1998i, "Chapter 9: *Total System Performance Assessment – Viability Assessment (TSPA-VA) Analyses Technical Basis Document,* B00000000-01717-4301-00009, Revision 01, Las Vegas, Nevada. [MOL.19981008.0009]

TRW 1998j — TRW (TRW Environmental Safety Systems Inc.), 1998j, "Chapter 10: *Total System Performance Assessment – Viability Assessment (TSPA-VA) Analyses Technical Basis Document,* B00000000-01717-4301-00010, Revision 01, Las Vegas, Nevada. [MOL.19981008.0010]

TRW 1998k — TRW (TRW Environmental Safety Systems Inc.), 1998k, "Chapter 11: *Total System Performance Assessment – Viability Assessment (TSPA-VA) Analyses Technical Basis Document,* B00000000-01717-4301-00011, Revision 01, Las Vegas, Nevada. [MOL.19981008.0011]

TRW 1998l — TRW (TRW Environmental Safety Systems Inc.), 1998l, *Software Routine Report for WAPDEG (Version 3.07),* 30048-M04-001, Revision 01, Las Vegas, Nevada. [MOL.19980715.0166]

TRW 1998m — TRW (TRW Environmental Safety Systems Inc.), 1998m, *Definition of the Radionuclide Inventory for the Commercial Spent Nuclear Fuel Used in the TSPA-VA Base Case,* B00000000-01717-0210-00017, Revision 00, Las Vegas, Nevada. [MOL.19980512.0106]

TRW 1998n — TRW (TRW Environmental Safety Systems Inc.), 1998n, *Total System Performance Assessment - Viability Assessment (TSPA-VA) Base Case,* B00000000-01717-0210-00011, Revision 01, Las Vegas, Nevada. [MOL.19981202.0279]

TRW 1998o — TRW (TRW Environmental Safety Systems Inc.), 1998o, *Definition of the Radionuclide Inventory for High Level Waste Used in the TSPA-VA Base Case,* B00000000-01717-0210-00019, Revision 00, Las Vegas, Nevada. [MOL.19980518.0197]

TRW 1999a — TRW (TRW Environmental Safety Systems Inc.), 1999a, *EIS Performance-Assessment Analyses for Disposal of Commercial and DOE Waste Inventories at Yucca Mountain,* B00000000-01717-5705-00128, Revision 00, Las Vegas, Nevada. [MOL.19990615.0207]

TRW 1999b — TRW (TRW Environmental Safety Systems Inc.), 1999b, *Waste Package Final Update to EIS Engineering File,* BBA000000-01717-5705-00019, Revision 01, Las Vegas, Nevada. [MOL.19990330.0530]

TRW 1999c	TRW (TRW Environmental Safety Systems Inc.), 1999c, *Engineering File – Subsurface Repository*, BCA000000-01717-5705-00005, Revision 02 with DCN1, Las Vegas, Nevada. [MOL.19990622.0202, document; MOL.19990621.0157, DCN1]
TRW 1999d	TRW (TRW Environmental Safety Systems Inc.), 1999d, *Environmental Baseline File for Meteorology and Air Quality*, B00000000-01717-5705-00126, Revision 00, Las Vegas, Nevada. [MOL.19990302.0186]
Wescott et al. 1995	Wescott, R. G., M. P. Lee, N. A. Eisenberg, T. J. McCartin, and R. G. Baca, editors, 1995, *NRC Iterative Performance Assessment Phase 2, Development of Capabilities for Review of a Performance Assessment for a High-Level Waste Repository*, NUREG-1464, Office of Nuclear Material Safety and Safeguards and Office of Nuclear Regulatory Research, U.S. Nuclear Regulatory Commission, Washington, D.C., and Center for Nuclear Waste Regulatory Analyses, San Antonio, Texas. [221527]
Wilson et al. 1994	Wilson, M. L., J. H. Gauthier, R. W. Barnard, G. E. Barr, H. A. Dockery, E. Dunn, R. R. Eaton, D. C. Guerin, N. Lu, M. J. Martinez, R. Nilson, C. A. Rautman, T. H. Robey, B. Ross, E. E. Ryder, A. R. Schenker, S. A. Shannon, L. H. Skinner, W. G. Halsey, J. D. Gansemer, L. C. Lewis, A. D. Lamont, I. R. Triay, A. Meijer, and D. E. Morris, 1994, *Total-System Performance Assessment for Yucca Mountain – SNL Second Iteration (TSPA-1993), Volume 2*, Sandia National Laboratories, Albuquerque, New Mexico. [NNA.19940112.0123]
Wolery 1992	Wolery, T. J., 1992, *EQ3NR, A Computer Program for Geochemical Aqueous Speciation-Solubility Calculations: Theoretical Manual, User's Guide, and Related Documentation (Version 7.0)*, UCRL-MA-110662 PT III, Lawrence Livermore National Laboratory, Livermore, California. [205154]
Wolery and Daveler 1992	Wolery, T. J., and S. A. Daveler, 1992, *EQ6, A Computer Program for Reaction Path Modeling of Aqueous Geochemical Systems: Theoretical Manual, User's Guide, and Related Documentation (Version 7.0)*, UCRL-MA-110662 PT IV, Lawrence Livermore National Laboratory, Livermore, California. [MOL.19980701.0459]
Zyvoloski et al. 1995	Zyvoloski, G. A., B. A. Robinson, Z. V. Dash, and L. L. Trease, 1995, *Users Manual for the FEHM Application*, LA-UR-94-3788, Revision 1, Los Alamos National Laboratory, Los Alamos, New Mexico. [222338]